

Evaluation of Corrosion and Wear of Non-Skid Deck Surfaces in Marine Environments

by Amy Lockwood

A Thesis

Submitted to the Faculty

of the

WORCESTER POLYTECHNIC INSTITUTE

In partial fulfillment of the requirements for the

Degree of Master of Science

in Mechanical Engineering

By

April 2010

APPROVED:

Dr. Richard D. Sisson Jr., Advisor

Dr. Christopher A. Brown, Thesis Committee Member

Dr. Satya S. Shivkumar, Thesis Committee Member

Dr. James D. Van de Ven, ME Graduate Committee Representative

Abstract

The annual cost of corrosion in the United States Navy and Coast Guard is in excess of \$2.7 billion dollars. The salt water environment provides a ripe surrounding for rapid corrosion and deterioration of ship decking, which requires frequent and expensive maintenance. Decks of ships are susceptible to corrosion and wear, but must also maintain a non-slip surface in a constantly wet environment. Few options for non-skid deck materials are currently approved for use by the Navy and require frequent and expensive maintenance or replacement. A new material known as Laser Deposited Non-Skid, currently used in industrial flooring applications, shows potential for serving as a more durable non-skid material with extended service life and greater resistance to corrosion. The purpose of this research is to investigate the feasibility of Laser Deposited Non-Skid in decks of ships and to compare the corrosion, wear and cost data with existing deck materials.

Sample plates of A36 and A572 steel and 5086 and 5456 marine grade aluminum alloy were coated with selected non-skid materials and subjected to laboratory salt fog testing and corrosion in environmental conditions in the Caribbean Sea. Wear behavior among non-skid materials was evaluated through wear cycles, measurement of coefficient of friction, and surface characterization. Salt fog testing was more corrosive than the actual operational environment in all cases and the Laser Deposited Non-Skid samples had the best resistance to wear and corrosion. The Peel and Stick Non-Skid demonstrated corrosion by undercutting while the Traditional Non-Skid corroded through the material. The relative area did not correlate well with friction or wear mass loss. Aluminum Laser Deposited Non-Skid appears suitable for use as a deck material on small boats. More research is needed to evaluate maintenance issues and possible stress cracking associated with the Laser Deposited Non-Skid on steel decks.

Keywords Non-skid, corrosion, wear, friction, surface metrology

Acknowledgements

I would like to thank my advisor Professor Sisson for his support and encouragement of my topic, his availability for impromptu meetings despite a busy schedule, and his practical advice, both professional and personal. I thank the members of my thesis committee: Professor Christopher Brown, Professor Satya Shivkumar, and Professor James Van de Ven for their time and assistance throughout this process. I appreciate the assistance from Brendan Powers and Professor Brown with the generous use of the equipment and software in the Surface Metrology Lab. Also thank you to Barbara Edilberti for her support and helping me navigate registration and thesis requirements.

Thank you to my employer, the United States Coast Guard, for providing financial support for my education and research. Mark Dust introduced me to the topic of non-skid corrosion issues and provided tremendous guidance with starting my thesis. The crews of USCGC SPENCER, USCGC KODIAK ISLAND, and MAT Key West provided valuable support to my project. Thank you to Andy Ross at Ross Technology and Dave Zilber at 3M Corporation for providing information and materials.

I am very grateful to Matt Kelly and Charlie Tricou of The Penn State Applied Research Lab. I would not have been able to complete this thesis on time without the use of their lab. I am especially grateful to Matt for his time, assistance, and technical knowledge of non-skid issues.

Finally I would like to thank my husband Scott for his assistance with transporting my steel samples, printing posters, and generally for his understanding and patience while listening to me talk about the exciting topic of rust. I would also like to thank my 1 year old daughter Emma who has provided me with endless hours of entertainment and distraction from my thesis and constantly reminded me of what is more important.

Table of Contents

Abstract.....	i
Acknowledgements.....	ii
List of Figures.....	vi
List of Tables.....	vii
Nomenclature.....	viii
1 Introduction.....	1
1.1 Need.....	1
1.2 Objectives.....	2
2 Background.....	3
2.1 Types of Non-Skid.....	3
2.1.1 Traditional Non-Skid.....	3
2.1.2 “Peel and Stick” Non-Skid.....	4
2.1.3 Laser Deposited Non-Skid.....	4
2.2 Corrosion.....	5
2.3 Steel and Aluminum Characteristics.....	9
2.4 Wear.....	10
2.5 Friction.....	10
2.6 Surface Metrology.....	11
3 Methodology.....	14
3.1 Sample Preparation.....	14
3.1.1 .1 Types of Non-Skid.....	16
3.2 Corrosion Testing.....	17
3.2.1 Salt Fog.....	17
3.2.2 Environmental.....	18
3.2.3 Corrosion Analysis.....	19
3.3 Wear Testing.....	20

3.4 Coefficient of Friction Measurement.....	22
3.5 Surface Characterization.....	23
3.5.1 Surface Analysis	25
3.6 Cost Analysis	25
4 Results and Discussion	26
4.1 Corrosion.....	26
4.1.1 Salt Fog Testing.....	28
4.1.2 Environmental.....	29
4.2 Wear	30
4.3 Friction.....	31
4.4 Surface Feature Characterization.....	32
4.4.1 Area-scale Analysis	34
4.4.2 Discrimination of Samples.....	35
4.4.3 Functional Correlations.....	36
4.5 Cost Metrics	36
5 Conclusions and Recommendations	39
5.1 Conclusions.....	39
5.2 Recommendations.....	39
5.3 Future Work	40
6 References.....	41
Appendix 1: Images of Samples Before and After Corrosion	44
Appendix 2: Corrosion Image Analysis.....	50
Appendix 3: Corrosion Mass Loss and Corrosion Rates	57
Appendix 4: Images of Samples Before and After Wear	60
Appendix 5: Wear Mass Loss Calculations and Data.....	64

Appendix 6: Coefficient of Friction Measurements	65
Appendix 7: Surface Characterization Method and Images	74
Appendix 8: Cost Analysis Data.....	90

List of Figures

Figure 1: Traditional Non-Skid.....	4
Figure 2: Peel and Stick Non-Skid.....	4
Figure 3: Laser Deposited Non-Skid	5
Figure 4: Electromotive Force (Emf) Series	6
Figure 5: Corrosion of Iron.....	7
Figure 6: Pourbaix Diagrams for Iron and Aluminum.....	8
Figure 7: Tilted Plane Method of Measuring COF.....	10
Figure 8: Plot of Friction Against Roughness for Copper on Copper	13
Figure 9: Schematic of Materials.....	15
Figure 10: Experimental Procedure Flowchart.....	16
Figure 11: Salt Fog Testing Chamber at Ross Technology	18
Figure 12: Frame for Samples and 110' Patrol Boat	18
Figure 13: Wear Testing Apparatus.....	20
Figure 14: COF Measuring Apparatus.....	23
Figure 15: UBM Laser Scanning Profiler and Olympus LEXT 4000 confocal microscope in the Surface Metrology Lab	24
Figure 16: TNS A36 Sample post corrosion testing, 1000 Hours of salt fog chamber and 864 hours on USCGC KODIAK ISLAND	26
Figure 17: Corrosion rates of samples corroding in a salt fog test chamber to samples corroding onboard the USCGC KODIAK ISLAND	27
Figure 18: Mass changes of steel samples in the salt fog test chamber	29
Figure 19: Mass changes of steel samples onboard CGC KODIAK ISLAND.	30
Figure 20: LDN A572 screenshot from Olympus measurement and imported into Mountains™ with high point identified	33
Figure 21: LDN A572 zoomed on highest area and basic roughness parameters	33
Figure 22: Mean relative area as a function of scale for selected non-skid materials.	35
Figure 23: MSR-scale plot from F-test of significance analysis with 99% confidence	36
Figure 24: Correlation coefficient, R^2 , for the correlations between relative area and friction.....	37
Figure 25: Correlation coefficient, R^2 , for the correlation between relative area and mass loss....	37

List of Tables

Table 1: Composition and Tensile Requirements of Steel	9
Table 2: Composition and Tensile Requirements of Aluminum	9
Table 3: Summary of Roughness Parameters	12
Table 4: Test Matrix	17
Table 5: Olympus 4100 Confocal Microscope Characteristics	24
Table 6: Percentage of area corroded for each steel sample in the salt fog test chamber compared to the sample onboard the CGC KODIAK ISLAND.....	28
Table 7: Summary of Wear and COF Measurements	31
Table 8: Summary of Selected Pre and Post Wear Roughness Parameters	34
Table 9: Summary of non-skid characteristics	38

Nomenclature

ARL	Pennsylvania State Applied Research Laboratory
ASTM	American Society for Testing and Materials
CAD	Computer Aided Drafting
CGC	Coast Guard Cutter
CNC	Computer Numerical Control
COF	Coefficient of Friction
Emf	Electromotive Force
FOD	Foreign Object Damage
KI	USCGC KODIAK ISLAND
LDN	Laser Deposited Non-Skid
MIL-PRF	Military Performance Specification
PNS	Peel and Stick Non-Skid (3M Safety Walk 700 Series™ or equivalent)
SFT	Salt Fog Testing
SML	Surface Metrology Lab
TNS	Traditional Non-Skid (Ameron Amercoat 138™ Epoxy Non-Skid or equivalent)
USCG	United States Coast Guard
WPI	Worcester Polytechnic Institute

1 Introduction

The annual cost of corrosion to the United States Coast Guard is approximately \$300 million dollars, which includes the cost of preventing corrosion and repairing damage caused by corrosion in small boats, cutters (boats greater than 65 feet), aircraft, and infrastructure (Herzberg 2008). Approximately 35% of the annual maintenance budget of Coast Guard cutters is spent on issues related to corrosion (Linton 2009). The annual cost of corrosion on Navy ships alone is over \$2.4 billion and deck coverings account for approximately 5% of those corrosion costs (Herzberg, et al. 2006). Decks of naval vessels are extremely susceptible to corrosion due to the routine exposure to seawater combined with the continuous foot traffic, impacts, and scraping inherent in the nature of work conducted on the decks. Non-skid or non-slip flooring surfaces are necessary in many work environments for purposes of safety and maneuverability. Such flooring is typically found in commercial and industrial areas where slip hazards exist due to wet environments, but they are especially important in marine environments particularly on boats and ships at sea. A durable non-slip surface on the decks of ships is paramount to the safety of the crew being able to perform their duties in rough seas or inclement weather.

The performance specification MIL-PRF-24667 governs the acceptable use of the approved non-skid materials systems based on if the intended use is for a flight deck or weather deck. Most non-skid deck surfaces are typically replaced every 2-3 years with costs ranging from \$3.20 to \$6.10 per square foot, not including labor costs. The USCG is exploring a proposed alternative system known as Laser Deposited Non-Skid (LDN), which incorporates the non-slip system directly into the aluminum or steel deck material with laser deposition welding, thereby reducing or eliminating multiple steps for installation and a possible increase in overall service life.

1.1 Need

The overall annual cost of deck coverings ranks 5th in the list of corrosion related maintenance issues for the U.S. Navy and accounts for 5%, or \$135 million dollars of the annual cost of corrosion. An additional \$107 million dollars is spent annually on non-skid maintenance issues, typically related to wear and failure (Cherry 2007).

1.2 Objectives

The goal of this thesis is to explore the area of corrosion and wear of non-skid deck systems on vessels by adding to the current work in the field and evaluating the feasibility of an alternate non-skid deck system with the purpose of extending deck service life and decreasing overall maintenance costs. The USCG sponsored an investigation into the feasibility of using LDN on as a viable material on decks of boats and cutters.

- Objective 1: To determine the extent of corrosion on LDN in comparison to existing non-skid materials.
- Objective 2: To determine the extent of wear and retention of non-slip characteristics on LDN in comparison to existing non-skid materials.
- Objective 3: Make recommendations with respect to cost based on the results of corrosion and wear testing.

To accomplish these objectives, an experimental investigation was conducted and three sample sets of selected non-skid materials were created. The first sample set was allowed to corrode in a salt fog testing chamber, the second sample set was allowed to corrode in the actual marine environment onboard a 110' cutter, the USCGC KODIAK ISLAND in the Caribbean Sea, and finally the third sample set was subjected to wear testing and coefficient of friction measurement. For objective 1, the first and second sample sets were compared. For objective 2, coefficient of friction was measured and the non-skid surfaces were characterized before and after wear. To accomplish objective 3, a basic cost analysis was completed and compared with the results of objectives 1 and 2.

2 Background

2.1 Types of Non-Skid

Non-skid materials are simply deck coverings with non-slip characteristics that must be corrosive resistant, wear and skid resistant, non-flammable, and easily maintained while retaining an attractive appearance. The coverings are applied to weather decks and flight decks of air capable ships. The military performance specification MIL-PRF-24667 governs the required characteristics and acceptable use of the materials. Requirements and characteristics specified by the military spec are numerous and include the following considerations: material composition, toxicity, coefficient of friction, impact resistance, adhesion, flashpoint, resistance to solvents, light, fire, wear, corrosion, and weight.

The primary approved non-skid materials currently used on USCG vessels is a “Traditional Non-Skid” used on cutters and a slip resistant sheet material known as a “Peel and Stick” coarse adhesive tape, used smaller boats, but is also approved for use on cutter weather decks. The traditional non-skid is a two part epoxy system generally installed by experienced contractors and it is the only material approved for flight decks, which are inspected for yearly during annual training periods. The Peel and Stick material is not approved for flight decks and may be installed by the ship’s crew with minimal tools.

2.1.1 Traditional Non-Skid

Coast Guard cutters must conform to MIL-PRF-24667, Type 1, and Composition G. Type 1 indicates a high durability rollable system, and Composition G specifies that the system is approved for general use, including helicopter flight decks, but not for aircraft carrier landings. The non-skid system requires an epoxy primer such as Ameron Amercoat 137 and then the 2 part epoxy non-skid is applied. The non-skid material consists of an abrasive material of Nepheline Syenite and Aluminum Oxide in an epoxy. The material is applied with a roller. Installation requires a proper surface preparation of a 2 to 6 millimeter surface profile. The material is approved for use on steel decks.

It has required service life of 12 months, but the decks are generally re-surfaced every 2-3 years at a cost of \$3.20 per square foot, not including labor costs. Successful installation is highly weather dependent and labor intensive. One of the problems associated with non-skid failures is Foreign Object Debris (FOD) on flight decks. Before flight operations, members of a ship's crew must walk over the flight deck and pick up any FOD so that it is not sucked into a helicopter's engine. The majority of FOD is small pieces of non-skid material.



Figure 1: Traditional Non-Skid, Wear (left), Corrosion (middle), Failure (right)
from: (Dust, 2008)

2.1.2 “Peel and Stick” Non-Skid

Approved for use in 2009, the material consists of abrasive particles (aluminum oxide or silicon carbide) embedded into a polymer backing with the reverse side coated with a pressure sensitive adhesive. The product generally used is 3M Safetywalk 700 Series. The recommended service life is approximately 3 years. The cost to replace the decking on a 110 foot patrol boat is \$15,302 or \$6.10 per square foot. The base cost of the material is \$4.50 per square foot, with higher prices for ship specific kits with pieces cut to fit the unique curvature and areas of the deck. It may be applied to a steel or aluminum deck.



Figure 2: Peel and Stick Non-Skid, 110' Patrol Boat (left), Edge Failure (right)
from: (Dust, 2007)

2.1.3 Laser Deposited Non-Skid

Ross Technology Incorporated has developed a slip-resistant flooring product known as Algrip™. Ross specializes in providing Algrip™ safety floor plates for use in industrial environments, such as stair treads, platforms, and walkways in food processing plants, oil rigs, and other facilities. The Algrip™ flooring product is manufactured by using a patented CNC laser deposition process that essentially welds beads of alloy material onto a plate of carbon steel, stainless steel, or aluminum.

The USCG is currently investigating the use of this LDN for use on their 41 foot Utility Boat (aluminum deck) instead of the “peel and stick” material currently used. The USCG is interested in determining if it is feasible for use on other platforms.

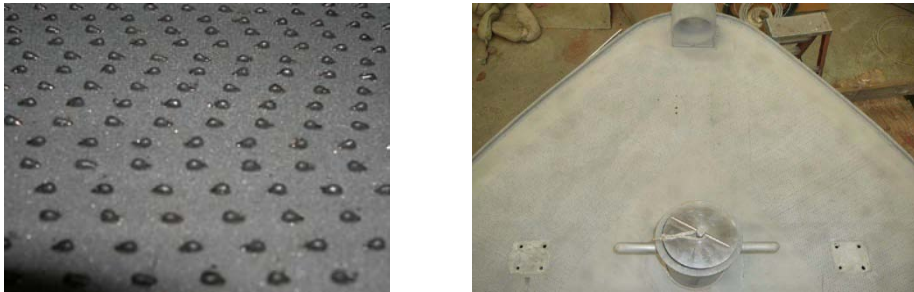


Figure 3: Laser Deposited Non-Skid, Steel with LDN (left), LDN on 41' UTB (right)
from: (Dust 2007 & 2008)

2.2 Corrosion

Corrosion is an electrochemical reaction between a material, generally metal, and the environment that causes deterioration to the material and its properties (Baboian 1995). Generally people picture rust when they think of corrosion. Rust is a corrosion product of ferrous alloys and consists of hydrated iron oxides and is generally red or orange in color.

Aqueous or wet corrosion is the primary problem with corrosion of ship decks and the typical type of corrosion observed on steel decks is a uniform attack on the surface, with occasional pitting. The Electromotive Series (Emf) is a tabular representation of the standard potentials for metals. The more noble or cathodic materials are at one end of the table and the more active or

anodic materials are at the other end. Corrosion takes place at the anode, so more active materials corrode preferentially to more noble materials, which is known as galvanic corrosion between two dissimilar metals. The further away the two metals are from each other on the Emf Series, the greater potential voltage (Revie and Uhlig 2008).

TABLE 3.2. Electromotive Force (Emf) Series

Electrode Reaction	Standard Potential, ϕ° , in volts at 25 °C
$\text{Au}^{3+} + 3e^- = \text{Au}$	1.50
$\text{Pt}^{2+} + 2e^- = \text{Pt}$	-1.2
$\text{Pd}^{2+} + 2e^- = \text{Pd}$	0.987
$\text{Hg}^{2+} + 2e^- = \text{Hg}$	0.854
$\text{Ag}^+ + e^- = \text{Ag}$	0.800
$\text{Hg}_2^{2+} + 2e^- = 2\text{Hg}$	0.789
$\text{Cu}^+ + e^- = \text{Cu}$	0.521
$\text{Cu}^{2+} + 2e^- = \text{Cu}$	0.342
$2\text{H}^+ + 2e^- = \text{H}_2$	0.000
$\text{Pb}^{2+} + 2e^- = \text{Pb}$	-0.126
$\text{Sn}^{2+} + 2e^- = \text{Sn}$	-0.136
$\text{Mo}^{3+} + 3e^- = \text{Mo}$	-0.2
$\text{Ni}^{2+} + 2e^- = \text{Ni}$	-0.250
$\text{Co}^{2+} + 2e^- = \text{Co}$	-0.277
$\text{Tl}^+ + e^- = \text{Tl}$	-0.336
$\text{In}^{3+} + 3e^- = \text{In}$	-0.342
$\text{Cd}^{2+} + 2e^- = \text{Cd}$	-0.403
$\text{Fe}^{2+} + 2e^- = \text{Fe}$	-0.440
$\text{Ga}^{3+} + 3e^- = \text{Ga}$	-0.53
$\text{Cr}^{3+} + 3e^- = \text{Cr}$	-0.74
$\text{Zn}^{2+} + 2e^- = \text{Zn}$	-0.763
$\text{Cr}^{2+} + 2e^- = \text{Cr}$	-0.91
$\text{Nb}^{3+} + 3e^- = \text{Nb}$	-1.1
$\text{Mn}^{2+} + 2e^- = \text{Mn}$	-1.18
$\text{Zr}^{4+} + 4e^- = \text{Zr}$	-1.53
$\text{Ti}^{2+} + 2e^- = \text{Ti}$	-1.63
$\text{Al}^{3+} + 3e^- = \text{Al}$	-1.66
$\text{Hf}^{4+} + 4e^- = \text{Hf}$	-1.70
$\text{U}^{3+} + 3e^- = \text{U}$	-1.80
$\text{Be}^{2+} + 2e^- = \text{Be}$	-1.85
$\text{Mg}^{2+} + 2e^- = \text{Mg}$	-2.37
$\text{Na}^+ + e^- = \text{Na}$	-2.71
$\text{Ca}^{2+} + 2e^- = \text{Ca}$	-2.87
$\text{K}^+ + e^- = \text{K}$	-2.93
$\text{Li}^+ + e^- = \text{Li}$	-3.05

Figure 4: Electromotive Force (Emf) Series from: (Revie and Uhlig 2008)

Four things must exist for corrosion to occur:

- Anode
 $\text{Fe}^{2+} + 2e^- \rightarrow \text{Fe}$
- Cathode
 $\text{O}_2 + 2\text{H}_2\text{O} + 4e^- \rightarrow 4\text{OH}^-$
- Electrolyte
Seawater
- Completed circuit
One metal with different potential

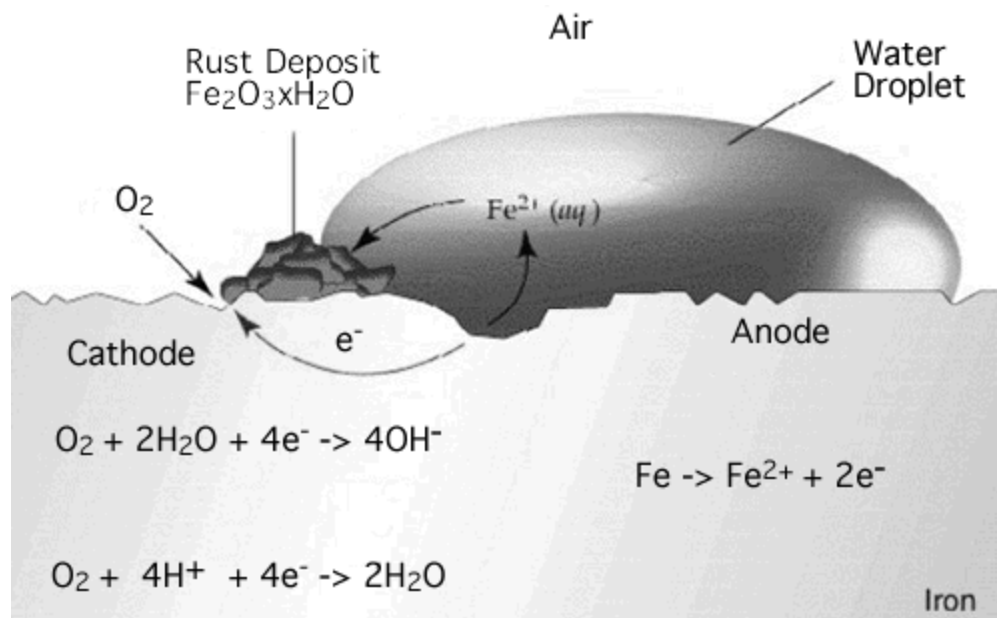
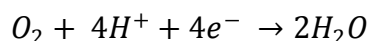


Figure 5: Corrosion of Iron
from: <http://www.splung.com/contents/sid/3/page/batteries>

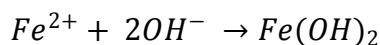
The following reaction also occurs:



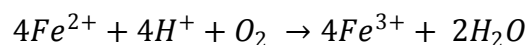
The electrons are consumed by hydrogen ions from water and dissolved oxygen to produce water.

Rust forms when the hydrogen ions are consumed and as the iron corrodes, the pH in the water rises. Hydroxide ions (OH^-) form as the hydrogen ion concentration falls and react with the iron to produce rust (<http://corrosion-doctors.org/Experiments/rust-chemistry.htm>).

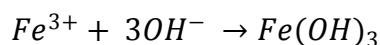
The OH^- react with the iron(II) ions to produce insoluble iron(II) hydroxides:



The iron(II) ions also react with hydrogen ions and oxygen to produce iron(III) ions:



The iron(III) ions react with hydroxide ions to produce hydrated iron(III) oxides (also known as iron(III) hydroxides):



Corrosion rates may not be determined from the Emf Series, and are influenced by many factors including temperature, humidity, pH, composition of the material, composition of the corrosion product, and type of corrosion. Varied environmental factors obviously make it difficult to predict corrosion rates. Pourbaix diagrams are useful for determining if a material will corrode under a certain condition. These diagrams show areas of the material which are thermodynamically stable over a range of pH and electrochemical potential. Seawater has a pH range of 7.5 to 8.4. By looking at the Pourbaix diagrams below for iron in water and aluminum in water, the regions of metal stability and regions of corrosion may be seen given the standard potentials of iron and aluminum (-0.44 and -1.66 respectively, Figure 4). In the range of seawater, it can be seen that iron will corrode, but aluminum will not (Kramer 2008).

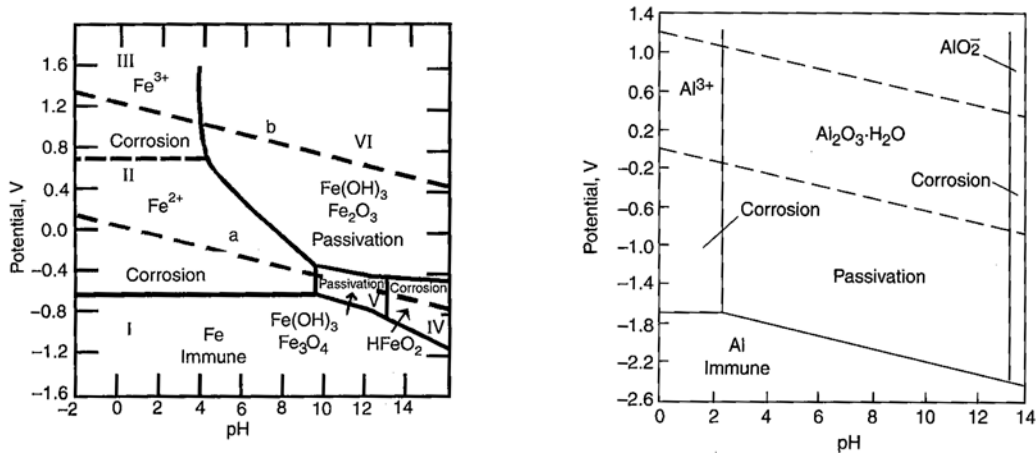


Figure 6: Pourbaix Diagrams for Iron in Water (left) and Aluminum in Water (right) from: (Kramer 2003)

So according to the Emf Series, aluminum is more active than iron; so why does it show less signs of corrosion? Aluminum is an active metal and corrodes by quickly forming a thin layer of aluminum oxide, which is “instantly self-renewing” and protects the aluminum from further corrosion. Contrary to rust on steel, the aluminum oxide is chemically bound to the surface and does not flake off like rust (Perryman 2007). Aluminum corrosion is typically a victim of galvanic corrosion rather than general uniform attack corrosion, evident through pitting. Characteristics of marine grade aluminums will be discussed in the methodology section.

Corrosion analysis has relied on visual means and is largely subjective. ASTM Standard D610 outlines a method for evaluating rust based on assigning a degree of rust on a scale of 1 to 10

after the corrosion product has been removed. Another metric for quantifying rust is weight loss (or gain) measurement. In addition to weight measurements, visual imaging software will be utilized to quantify corrosion.

2.3 Steel and Aluminum Characteristics

Steel is an iron and carbon based alloy and the A36 and A572 are structural steel commonly used in shipbuilding and bridges. Marine grade aluminum is a wrought alloy of the 5xxx series and have a high resistance to corrosion which makes them appropriate for use as boat materials for use in seawater (Skillingsberg 2004). The deposited “bumps” on the LDN are matched to the material of the base metal – the bumps of the aluminum substrate are composed of aluminum and the bumps on the steel substrate are composed of predominately iron with some nickel and chromium. The ASTM composition and tensile requirements of each of the materials (one quarter inch plates) are summarized in the tables below.

Table 1: Composition and Tensile Requirements of Steel
from: ASTM Standards A36 and A572

Steel Plate	C max	Mn max	P max	S max	Si max	Cu min	Yield Point, min (ksi)	Tensile Strength, min (ksi)
ASTM A36	0.25	---	0.04	0.05	0.40	0.20	36	58-80
ASTM A572, Gr 50	0.23	1.35	0.04	0.05	0.40	---	50	65

Table 2: Composition and Tensile Requirements of Aluminum
from: ASTM Standard B928

Aluminum Plate	Si	Fe	Cu	Mn	Mg	Cr	Zn	Ti	Other Elements (total)	Yield Point, min (ksi)	Tensile Strength, min (ksi)
5086, H116	0.40	0.50	0.10	0.20 - 0.70	3.5 - 4.5	0.05 - 0.25	0.25	0.15	0.15	28	40
5456, H116	0.25	0.40	0.10	0.50 - 1.0	4.7 - 5.5	0.05 - 0.20	0.25	0.20	0.15	33	46

2.4 Wear

In general, wear can be characterized as progressive damage to a surface. Although wear is described in terms of damage, it is not always an unintended consequence, since polishing is also a type of wear. Wear evaluation should also not be limited to investigating removal of material, because this is not the only result of wear. The main concern in engineering design is the adverse effects and unintended consequences of wear that limit the life of parts, devices, and products (Bayer 2004). Types of wear are described as follows:

- Loss of material from a surface (scratch, gouges)
- Movement of material without loss of mass (plastic deformation)
- Damage to a surface that does not involve loss of mass or dimensional changes (cracks)

General types of wear include adhesive wear, abrasive wear, and corrosive wear. Wear and friction are not material properties, but rather a systems response and depend on contact conditions such as material and counterpart material, contact pressure, and real area of contact (Kato 2002). The research in this thesis focuses on abrasive wear in order to gain a better understanding of durability characteristics.

2.5 Friction

A topic closely related to wear is friction. Friction can be defined as the force that opposes motion between two contacting materials. It is not strictly a property of material, but a system response and it must be determined empirically (Bayer 2004). Friction is generally described by the Coefficient of Friction (COF), μ :

$$\mu = \frac{F_f}{N} \text{ or } \mu = \tan \phi$$

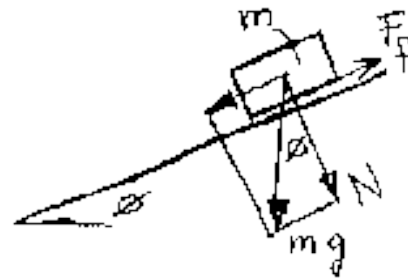


Figure 7: Tilted Plane Method of Measuring COF
from: <http://www.tribology-abc.com/abc/friction.html>

Where:

μ is the coefficient of friction

F_f is the friction force

N is the normal force pressing the two surfaces together

Type of friction should also be distinguished. Static coefficient of friction (μ_s) is the friction force that must be overcome to initiate sliding while dynamic or kinetic coefficient of friction (μ_k) is the friction force in order to continue sliding (Bayer 2004).

2.6 Surface Metrology

Surface metrology is defined as the measurement and analysis of surface geometry or surface textures, commonly described in terms of roughness. The primary objective is to characterize measured surface features in order to discriminate the textures and establish functional correlations. Surfaces cover everything and can be defined as locally continuous regions with a high gradient of physical properties – the extremity of a medium (Brown, spring 2010).

Measuring and quantifying surfaces is possible by contact and non-contact methods. A common contact method is to use profilometer with a stylus tip that is moved across a surface while the roughness measurement output is recorded on a chart. This method is limited by the shape, size, and material of the probe and can also result in surface damage (Rabinowicz 1995). While several techniques exist, another common non-contact technique is measuring the surface with a triangulation sensor or optical microscope, either interferometric or confocal. Scanning laser profiler and laser triangulation sensors determine position of a target by measuring reflected light from the surface. Interferometric microscopes use wave interference have better vertical resolution while confocal microscopes use focal depth and have better lateral resolution. Textures are characterized by statistical parameters and denoted with R for profile measurements or S for surface measurement (Brown, spring 2010). In surface metrology, two dimensional measurements are represented as $z = z(x)$, where z is the height and a function of x and three dimensional measurements are represented as $z = z(x,y)$, where z is the height and is a

function of x and y (the spacial directions). Typical surface parameters are summarized below in table 3.

Table 3: Summary of Roughness Parameters
 from: http://en.wikipedia.org/wiki/Surface_metrology and (Brown, spring 2010)

Parameter	Name	Description	Type	Formula
S_a	Arithmetic Mean Height	Mean of the absolute values of the profile heights measured from a mean line averaged over the profile	Amplitude	$S_a = \frac{1}{n} \sum_{i=1}^n y_i $
S_q, S_{RMS}	Root Mean Squared	Root Mean Squared Height - Standard deviation of heights	Amplitude	$S_{RMS} = \sqrt{\frac{1}{n} \sum_{i=1}^n y_i^2}$
S_v	Maximum Valley Depth	Maximum depth of the profile below the mean line with the sampling length	Amplitude	$S_v = \min y_i$
S_p	Maximum Peak Height	Maximum height of the profile above the mean line within the sampling length	Amplitude	$S_p = \max y_i$
S_z	Maximum Profile Height	Maximum peak to valley height of the profile	Amplitude	$S_z = S_p + S_v$
S_{sk}	Skewness	Symmetry of the profile about the mean line	Amplitude	$S_{sk} = \frac{1}{nR_q^3} \sum_{i=1}^n y_i^3$
S_{ku}	Kurtosis	Measure of the sharpness of the profile	Hybrid	$R_{ku} = \frac{1}{nR_q^4} \sum_{i=1}^n y_i^4$

Scale is an influential factor in terms of measuring surfaces. The basis of scale importance is the difference between the apparent and real areas of contact on a surface. For example, road pavement should be rough on the scale of the tire tread, but smooth on the scale of the vehicle in order to maximize a smooth ride while maintaining friction between the tires and the road (Brown, spring 2010). In the same sense, non-skid surfaces should be rough on the scale of the sole of a shoe or landing gear of a helicopter, but smooth to the scale of a person or a helicopter.

It should be noted that the real area of contact changes as wear takes place. Contact occurs at discrete locations called junctions. As surface asperities are worn down during wear and deformation occurs, the junction area increases. The number of junctions formed is influenced by the surface roughness and the degree of penetration of one surface on the other, which is a

function of the normal force pushing the surfaces together (Bayer 2004). Therefore friction should be an important factor in surface roughness since it directly affects the real area of contact of surfaces due to the changes in contact area. Rabinowicz showed that for unlubricated copper on copper, the friction was high in smooth regions because of the high area of contact, while with rough surfaces the friction is high because of asperities hitting on lifting over each other. In between the friction is minimized and could be independent of roughness (Rabinowicz 1995). The research presented will explore relationships among friction, wear, and roughness in non-skid materials by characterizing the surfaces to discriminate the textures and establish functional correlations.

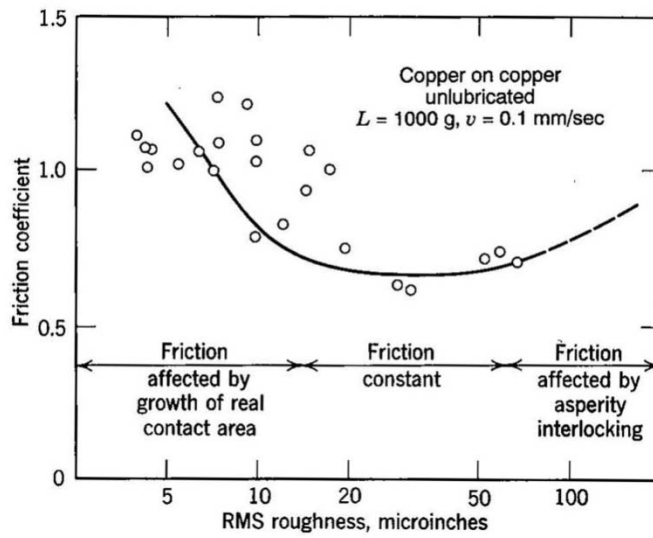


Figure 8: Plot of Friction Against Roughness from: (Rabinowicz 1995)

3 Methodology

3.1 Sample Preparation

The USCG purchased materials from Ross Technology and provided the materials listed below. All metal samples were shipped as 12" x 12", quarter inch thick plates. The raw materials were used as the substrate for non-skid materials. A schematic of the materials layout is shown below in figure 9 and the experimental procedure flowchart is shown in figure 10 and test matrix is shown in table 4.

- Aluminum 5416, H116
 - 1 plate uncoated (no non-skid applied)
 - 1 plate with LDN non-skid
- Aluminum 5086, H116
 - 1 plate uncoated (no non-skid applied)
 - 1 plate with LDN non-skid
- Mild Steel, ASTM A36
 - 1 plate uncoated (no non-skid)
 - 1 plate with LDN non-skid, unpainted
 - 1 plate with LDN non-skid, painted
- Low Alloy High Strength Steel, ASTM A572, Grade 50
 - 1 plate uncoated (no non-skid)
 - 1 plate with LDN non-skid, unpainted
 - 1 plate with LDN non-skid, painted

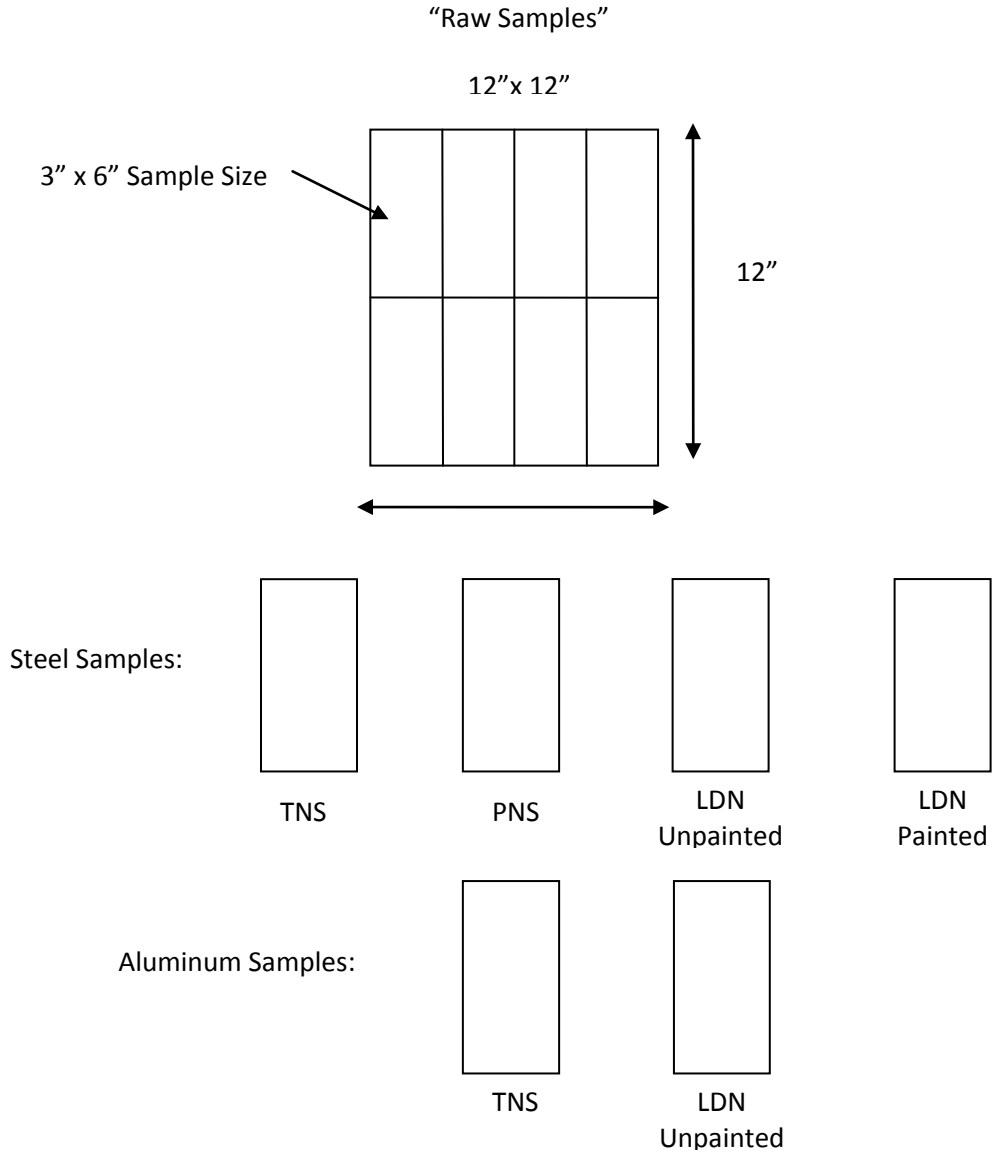


Figure 9: Schematic of Materials

All of the plates were cut into 3" x 6" samples at Vangy Tools in Worcester, MA by means of water jetting. After cutting, the uncoated samples were coated with non-skid materials. The steel samples were coated with TNS and PNS while the aluminum samples were coated with PNS since TNS is approved by the Navy for use on steel decks. The painted LDN samples were painted at Ross Technology with Ameron PSX 700, an engineered siloxane coating that may be applied to steel with no primer. The recommended application is 3-7 millimeters dry film thickness.

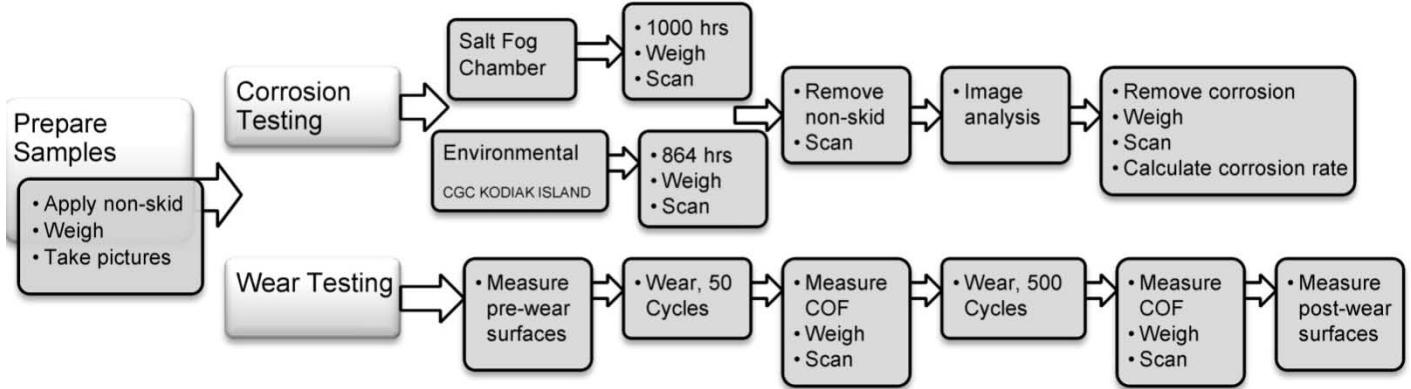


Figure 10: Experimental Procedure Flowchart

3.1.1 Non-Skid Application

Dave Zilber, Naval Programs Manager for Government Markets at 3M Corporation, provided a sheet of the Peel and Stick non-skid, 3M Safety Walk, Course Tread 770 (gray). The sheet was cut with scissors into 2 ½” x 5 ½” pieces and with rounded corners so the non-stick could be installed with a ¼” border. The pieces of PNS were installed on uncoated aluminum and steel samples using a rubber mallet and roller. The edges were sealed with 3M 902 Safety Walk Edge Sealing Compound. The edges and back of the steel samples were painted with Rust-Oleum™ Rusty Metal Primer.

The uncoated steel samples were taken aboard USCGC SPENCER and with help from the Deck Department, the steel samples were sanded with 60 grit sandpaper to give the surface a profile, cleaned with a wet rag, and then they were primed with 2 coats of Ameron Amerecote 236 Oxide Red Primer. Two days later the samples were coated with TNS - Ameron Amerecote 138G Type I/II, Composition G, in dark gray using a paint roller.

Table 4: Test Matrix

Material	Non-Skid Type	Type of Test		
		Salt Fog Chamber	Environmental: CGC KODIAK ISLAND	Wear
Steel: A 36	LDN, Unpainted	X	X	
	LDN, Painted	X	X	X
	PNS	X	X	X
	TNS	X	X	X
Steel: A572, Gr. 50	LDN, Unpainted	X	X	
	LDN, Painted	X	X	X
	PNS	X	X	X
	TNS	X	X	X
Aluminum: 5086, H116	LDN	X	X	X
	PNS	X	X	X
Aluminum: 5456, H116	LDN	X	X	X
	PNS	X	X	X

3.2 Corrosion Testing

Once the samples were coated with non-skid materials, the steel samples were scribed to expose the underlying steel using a Dremel™ rotary tool with a 1 ¼” fiber reinforced cut-off wheel attachment. The specimen should be scribed in such a manner that the scribe is lengthwise when positioned in the salt fog test cabinet (ASTM D1654). Since the intended orientation of the samples were unknown for the salt fog test cabinet and the location of placement on the Coast Guard cutter was not yet determined, the samples were scribed lengthwise on both axis. All samples were photographed and weighed prior to corrosion testing. Photographs showing the samples before and after corrosion testing are contained in Appendix 1.

3.2.1 Salt Fog Testing

On January 11, 2010, the 12 test samples were taken to Ross Technology in Leola, Pennsylvania for salt fog corrosion testing in a salt fog spray apparatus in accordance with ASTM B 117. The samples were placed in a Harshaw Environmental Chamber and subjected to 1000 continuous hours of corrosion testing in a 100% humidity environment at 35°C (95°F) with a fine spray of 10% sodium chloride solution to replicate seawater.

3.2.2 Environmental Testing



Figure 11: Salt Fog Testing Chamber at Ross Technology. Harshaw Environmental Chamber, Model 22, 3 Phase, 240 Volts, 60 Hz, 13 Amps. Made by Harshaw Chemical Co., Cleveland, Ohio.

On February 5, 2010 a set of 12 samples were taken to Key West, Florida for placement on CGC KODIAK ISLAND, a 110 foot patrol boat. Wood frames were built to hold the samples in order to prevent galvanic couples when attaching the samples to the ship. The wood frames were attached on the bow of the ship under the grating system that supports the 25 mm machine gun. The samples were placed in an area that receives ample amounts of sun and seawater. The samples remained onboard for the duration of a patrol in the Caribbean Sea for 36 days (864 hours).



Figure 12: Frame for Samples (above) and 110' Patrol Boat (right) from:
<http://reference.findtarget.com/search/List%20of%20United%20States%20Coast%20Guard%20cutters>



3.2.3 Corrosion Analysis

One set of samples were received from CGC KODIAK ISLAND on March 15, 2010 and the other set of samples were picked up from Ross Technology March 17th. All samples were weighed and scanned with a color scanner at 600 dpi. The samples were taken to the Pennsylvania State University Applied Research Laboratory (ARL) on March 17, 2010 for analysis using Clemex™ Vision PE image analysis software to quantify the corrosion of each sample. Prior to analyzing the degree of corrosion, the non-skid material was removed from each corrosion sample by placing the samples in a bath of Dichloromethane (Methylene Chloride), a solvent used for paint stripping. After sitting overnight, the non-skid material was scraped off using a plastic paint scraper, rinsed with acetone, and wiped off. With the non-skid material removed, the corroded areas of the sample were exposed. The samples were again scanned with a color scanner at 600 dpi. The image of the corroded sample (with the non-skid removed) was imported using the Clemex™ software, bitplanes were created to capture corrosion based on the color specified, and the percentage of area corroded was extracted. The image analysis process is outlined in detail in Appendix 2.

The corrosion product was removed from all of the samples using Naval Jelly® rust dissolver which is a Phosphoric Acid based gel used for removing rust on steel. The samples were coated with the Naval Jelly® for 24 hours and then the corrosion product was removed with a paint scraper. Care was taken not to remove any base metal while removing the corrosion product (ASTM G1 2009). It should be noted that acid cleaning high strength steel can lead to hydrogen embrittlement and ultimately unexpected brittle failure. When a source of hydrogen (acid) is introduced to high strength steel and the steel is subjected to stress, then the steel is susceptible unpredictable failure (Sisson 2007). After the corrosion product was removed, the mass of each sample was recorded. The corrosion rates were calculated based on the following formula (Baboian 1995):

$$\text{Corrosion Rate} = \frac{(K \times W)}{(A \times T \times D)}$$

Where:

K is a constant: To obtain millimeters per year (mm/y), 8.76×10^4 is K

T is time in hours

A is total area of the sample in cm^2

W is the mass loss in g

D is the density in g/cm^3

The corrosion mass loss data and calculations corrosion rates are outlined in Appendix 3.

3.3 Wear Testing

Samples were taken to the Pennsylvania State University ARL for wear testing March 17 -19, 2010. The wear testing was completed using a cable abrasion tester built at the ARL in accordance with the Military Performance Specification 24667B, sections 4.5.4 and 4.5.2.1. The apparatus consists of a jig to hold the non-skid test panel and a 30 pound weighted carriage holding a steel rod. The carriage was moved in a reciprocating fashion over the long axis of the test panel. The steel wire abrading the surface was $\frac{1}{8}$ " diameter high carbon spring steel with a class 2 temper. The steel wire is the type of wire used in strands of the arresting cables used on US Navy aircraft carriers. The 500 cycle wear test is intended to replicate the amount of wear experienced on a Navy ship in operation over a 2 year period. All samples were weighed and photographed before and after wear and the pictures are contained in Appendix 4.

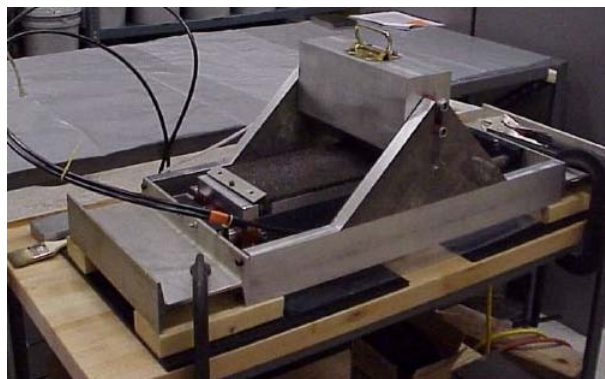


Figure 13: Wear Testing Apparatus
from: (Tricou and Kelly 2008)

The MIL-PRF-24667C outlines the following procedure for measuring wear of the non-skid samples:

- Measure the mass of each panel before application of the non-skid coating
- Abrade the sample for 50 cycles and weigh the sample, replace the wire
- Abrade the sample for an additional 450 cycles, replacing the wire every 150 cycles, and weigh the sample

The Navy specification considers the first 50 cycles of wear, the “break-in” period and the mass loss calculation takes into account the acceptable mass loss after the initial “break-in” period. The requirement is that the percent weight loss on wear of the coating system should not exceed 10 percent.

After completing the wear testing, the percent of determined mass loss should be calculated as follows:

$$\text{Percent mass loss} = \frac{100 \times (M2 - M3)}{(M2 - M1)}$$

Where:

M1 is the mass of the sample before applying the non-skid coating

M2 is the mass of the sample after 50 cycles

M3 is the mass of the sample at the end of the test

The test was conducted in accordance with the specification except the sample size was 3” x 6” instead of 6” x 12” as required. Also, the initial mass of the samples was not recorded prior to applying the non-skid material. It was not possible to weigh the individual LDN samples prior to the deposition of the LDN “bumps” onto the substrate. To overcome this oversight, the initial mass of the uncoated samples will be approximated by measuring the area and thickness and using the theoretical density of the material to calculate the initial mass. The images of all available wear samples were imported into AutoCAD (CAD) and a polyline was drawn around the sample to form a polygon. The area of the polygon was calculated in CAD and the “best” area for each sample was noted. The “best” area was selected because some scans did not fully capture the edges of the samples.

Using the area of each sample and the density of the material, the mass of the base material was calculated in the following manner:

$$Mass (M1) = \rho A t$$

Where:

M1 is the mass of the sample before applying the non-skid coating

ρ is the density of the base metal

A is the area of the sample

T is the thickness of the sample

The Excel file created to input the measurements and calculate the mass loss is contained in Appendix 5.

3.4 Coefficient of Friction Measurement

Samples were taken to the Pennsylvania State University ARL for COF measuring March 17 - 19, 2010. The COF measuring apparatus was built at the ARL in accordance with the Military Performance Specification 24667, sections 4.5.1. The apparatus consists of the following components:

- Force Gauge: “Transducer Techniques Load Cell” Brand, Model MLP-25
- Position Monitor: “Celesco” Brand, Model SP2-50
- Transverse Platform: “Parker Daedal” Model 404XR600MS-D2H2L2C2M3E1B1P1
- Data Acquisition Interfaces: “National Instruments” Models NIcDAQ-9172
- Interface Software: “CoF Tester” title, version 1.0.0, Creator: Eric Little



Figure 14: COF Measuring Apparatus
from: (Tricou and Kelly 2008)

The drag sled was a steel block 5.75 inches x 4 inches by 0.85 inch with a 0.75 inch edge radius. The bottom of the block was covered with a vulcanized neoprene rubber pad with a Durometer hardness of 57 and a thickness of $\frac{1}{2}$ inch. The total weight of the drag sled including the rubber pad and screw eye weighed 2.57 kg. The sled drag speed was 12 inches per minute.

The sled was placed rubber side down on the non-skid sample and connected to the force gauge. The sample was jogged out in such a manner that no tension was experienced while also minimizing the slack experienced in the connection. One measurement of static and dynamic COF was taken, the sample was turned 180 degrees and another measurement was taken. The average of the two measurements was recorded as the COF. Dry COF measurements were taken for all samples at the 50 cycle interval and at the completion of wear testing (500 cycles). Wet COF measurements were taken at the end of wear testing (500 Cycles). Screenshots of the COF measurements are in Appendix 6.

3.5 Surface Characterization

The surfaces of the non-skid samples were characterized before and after wear by taking surface roughness measurements in the WPI Surface Metrology Lab (SFL). The PNS non-skid surfaces were measured using the UBM Surface Scanning Laser Profiler by Solarius™ with a Keyence Brand LC-2100 Laser Displacement Meter and a Keyence LC-2210 Triangulation Sensor with a spot size of 10-100 μm and resolution of 0.2 μm . The measured areas were 1 cm x 1 cm, the sampling interval was 10 μm , and the measuring rate was 100 points/second.

The TNS and LDN non-skid samples were measured before and after wear using the Olympus LEXT OLS 4000 vertical scanning laser confocal microscope. Measurements were taken with the 20X lens using the stitching feature with 10 percent overlap to produce a measurement area of 1.8 mm x 1.8mm.

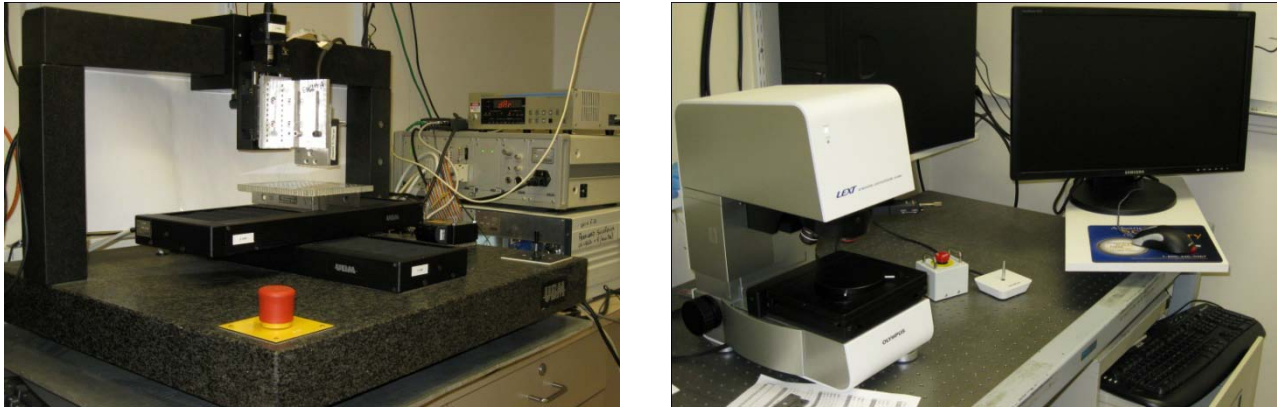


Figure 15: UBM Scanning Laser Profiler (left) and Olympus LEXT OLS 4000 confocal microscope in the Surface Metrology Lab

- Light Source: 405 nm semiconductor laser
- Optical zoom of 1x to 8x
- Scale resolution of 0.8 nm
- Display resolution of 1 nm

Table 5: Olympus 4100 confocal microscope characteristics.

Lens	Magnification	Field of View	Working Distance
5X	108x-864x	2,560-320 μm	20.0 mm
10X	216x-1,728x	1,280-160 μm	11.0 mm
20X	432x-3,456x	640-80 μm	1.0 mm
50X	1,080x-8,640x	256-32 μm	0.35 mm
100X	2,160x-17,280x	128-16 μm	0.35 mm

The peak to valley heights of the TNS and LDN non-skid samples were too large for use on the UBM and optical microscope, but since during wear, the areas of contact would be the limited to the peaks of the TNS and the “bumps” on the LDN. Therefore, a peak feature on each sample was identified and selected for measurement on the microscope. The feature on each sample was

circled with a permanent marker and the location was recorded by using a transparency to make a template of each sample and notate the location of the feature. The photographs of the surface features are contained in Appendix 7.

3.5.1 Surface Analysis

The acquired data was imported with MountainsMap® analysis software from Digital Surf and then imported into Surftract Sfrax© software to extract data, filter the data, and plot the results. Traditional roughness parameters were calculated for each sample and area-scale fractal analysis was performed for pre and post wear samples and plotted. The term fractal describes non-Euclidean geometry and scale-sensitive fractal analysis is based on the principle that the apparent area of a rough surface depends on the scale of observation (Berglund, et al. 2010). A discrimination analysis (F-test) was also performed with both filtered and unfiltered measurements. Next COF measurements were entered for selected samples and the data was analyzed to find a functional correlation between friction and relative area. The percentage of non-skid mass loss due to wear was also entered as a surface parameter and analyzed to find a functional correlation between mass loss and relative area. The method for extracting the data and characterizing the surface is described in detail in Appendix 7.

3.6 Cost Analysis

A basic cost analysis was performed by gathering actual cost data for the raw materials and comparing the cost of materials on the basis of cost per square foot. Type and cost of labor required for installing the non-skid materials was considered. Life cycle data was also gathered for TNS and PNS while the LDN was evaluated based on the results of the corrosion and wear testing data. Recommendations for non-skid use are made based on the cost and test results.

4 Results and Discussion

4.1 Corrosion

The salt fog chamber and environmental corrosion tests produced highly visual results – the level of corrosion among samples was easily seen without quantifying the results. The salt fog chamber corrosion samples were much more corroded than the set of samples placed on CGC KODIAK ISLAND. The result was expected since the salt fog chamber test was 136 hours longer and it maintained constant humidity and temperature while the daily temperature and humidity level varied while the cutter was underway. Images of the different corrosion tests are shown below in figure 16 for the TNS A36 sample; the differences in corrosion severity are evident.



Figure 16: TNS A36 sample post corrosion testing, 1000 hours of salt fog chamber (left) and 864 hours On USCGC KODIAK ISLAND

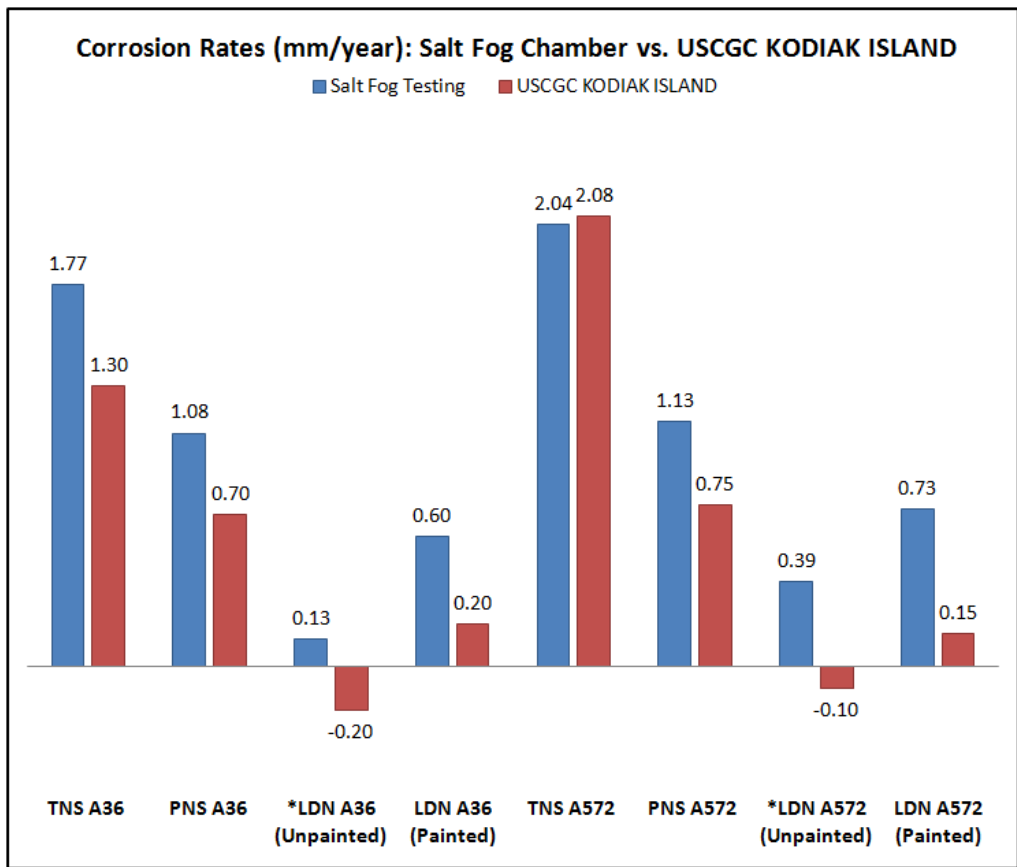


Figure 17: Corrosion rates of samples corroding in a salt fog test chamber to samples corroding onboard the USCGC KODIAK ISLAND.

Using the Clemex™ PE image analysis software, the percentage of area corroded was calculated for each sample. In the salt fog tests, the PNS experienced the highest percent of area corrosion, while onboard the cutter, the TNS was highest. In both test, the LDN had the lowest area percent of corrosion. The PNS corrosion seemed to experience “undercutting corrosion” due to water seeping in around the sealed edges while the TNS showed signs of “through corrosion” where water penetrated the non-skid material through small cracks in the coating. The large area percent corrosion of the TNS was surprising since this material is the predominant deck material on all large steel hulled ships in the USCG and Navy. The negative corrosion rates for the unpainted LDN steel samples are not a good indicator of the actual corrosion rate, rather the corrosion product was so thick that it could not be sufficiently removed and the ending mass was higher than the initial mass of the sample.

The percentages of area corroded are summarized in table 6 below. Depth of corrosion was not able to be evaluated, but the depth of corrosion into the scribe mark may be of interest in further

testing. The surface preparation and quality control of the non-skid material likely has a strong influence to the performance of the non-skid and its ability to resist corrosion and wear. The TNS was close to the expiration date and was stored in the forward peak of a ship and was subjected to thermal cycling over a period of 1-2 years. Some of the samples of base material had mill scale that was not removed prior to applying the non-skid material and some of the plates previously had LDN, but it had been ground off before being delivered. Improvements in non-skid performance are also expected when the material is applied by laborers experienced in the application of the specific type of non-skid.

Table 6: Percentage of area corroded for each steel sample in the salt fog test chamber compared to the sample onboard the CGC KODIAK ISLAND.

Material	Salt Fog Test, Percent Area Corroded	CGC KODIAK ISLAND, Percent Area Corroded
TNS A36	13.8	18.8
PNS A36	28.2	8.7
LDN A36 (Unpainted)	100	100
LDN A36 (Painted)	8.3	6.5
TNS A572	28.0	36.2
PNS A572	41.7	10.8
LDN A572 (Unpainted)	100	100
LDN A572 (Painted)	12.0	3.6

4.1.1 Salt Fog Testing

The salt fog chamber test results show that the salt fog testing chamber is more aggressive than the actual environment where the non-skid is used. It should be noted that ASTM B 117 calls for the use of a 5% salt water solution in the chamber and a solution of 10% sodium chloride was actually used. Daily temperature records were not provided. The mass changes of the samples in the test chamber are displayed in figure 18. The aluminum samples showed some staining from the corrosion product of the steel samples, but showed no mass change or noticeable corrosion. The aluminum samples visually showed only a loss of sheen.

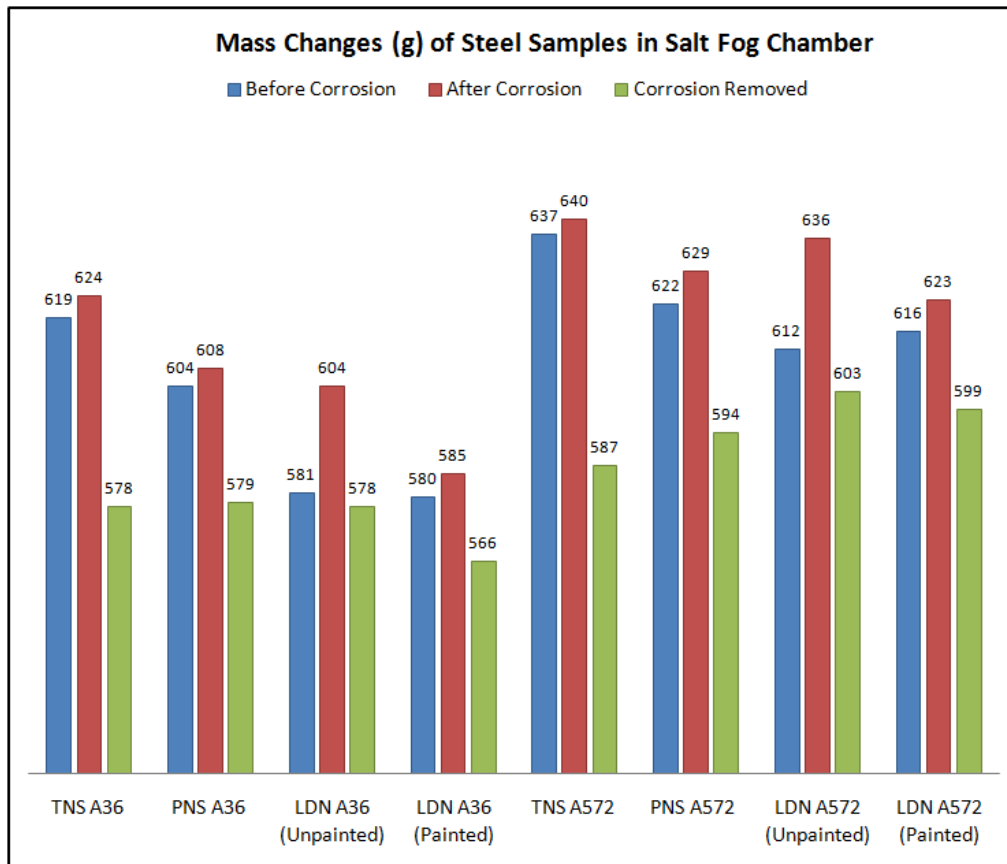


Figure 18: Mass changes of steel samples in the salt fog test chamber.

4.1.2 Environmental

The results of the corrosion test onboard the CGC KODIAK ISLAND were similar to the results of the salt fog test, but with less severity. The aluminum samples experienced no change in mass, no visible staining or corrosion, but only a loss of sheen. The steel non-skid samples experienced less corrosion, but color fade was evident due to the exposure to sun. After the test some of the samples had some green color likely due to brass shavings on the deck since the test samples were placed below the 25 mm machine gun. The mass changes of the samples in the test chamber are displayed in figure 19.

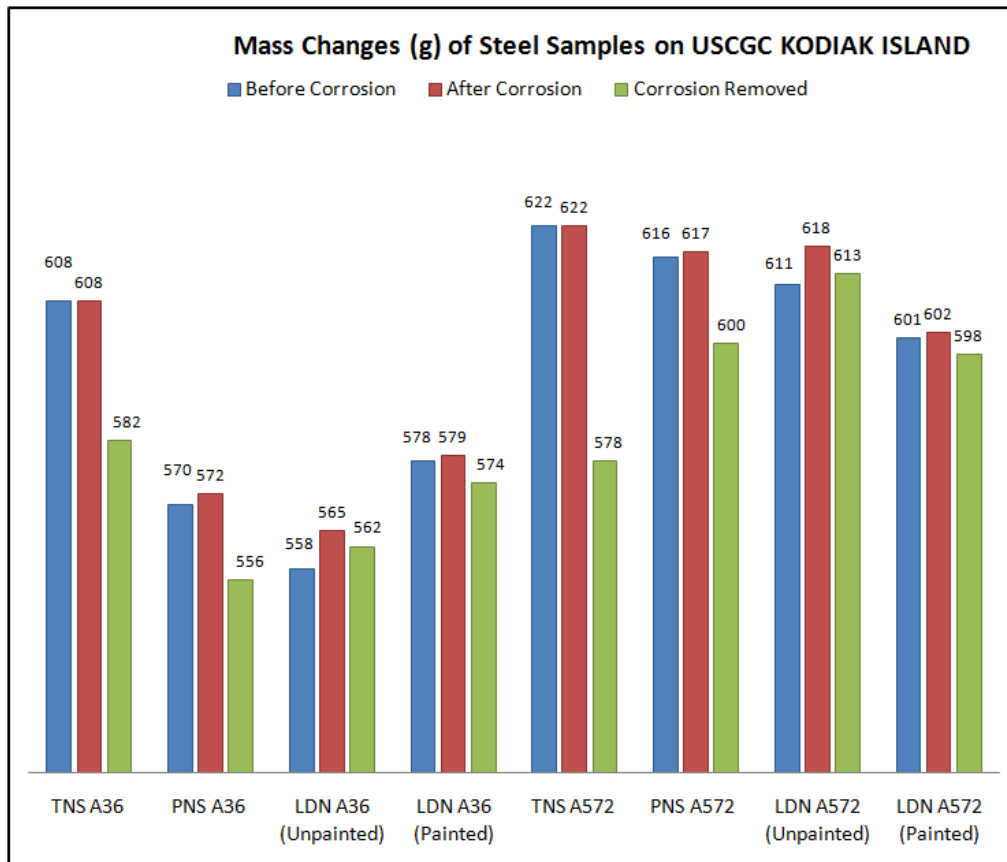


Figure 19: Mass changes of steel samples onboard CGC KODIAK ISLAND.

4.2 Wear

Wear tests were conducted with an initial 50 cycles as the “break-in” period, but the PNS non-skid surfaces were so severely worn that the surface was essentially pulled off of the metal substrate leaving only the sticky adhesive after approximately 20 to 30 cycles. The 500 cycle wear tests on the PNS samples were abandoned. The aluminum samples also showed severe signs of wear after 50 cycles, which was expected since hardened steel was interacting with aluminum. The plastic deformation is evident after 50 cycles, so the 500 cycle wear test was only conducted on the LDN 5086 sample and the “bumps” were worn off as the wear began to cause damage to the base metal. The percent of determined mass loss was calculated for the TNS and LDN steel samples in accordance with MIL-PRF-24667C. The TNS A36 and TNS A572 had a percent mass loss of 3.25 and 2.45 respectively. The LDN A36 and LDN A572 had a percent mass loss of 1.09 and 1.86 respectively. The requirement is for the percent mass loss to not exceed 10 percent. The TNS and LDN steel samples met this requirement. The LDN

aluminum 5086 had a percent mass loss of 56.44. The military specification does not include a separate test for aluminum decks.

4.3 Friction

Following each 50 cycle wear test and again following the 500 cycle wear test, the dry COF was measured for each sample. After the 50 cycle COF measurements were recorded, it was noticed that some of the adhesive on the PNS samples had contaminated the sled on the COF apparatus and contributed to higher than expected COF for most of the 50 cycle COF measurements. The contamination was not noticed in time to re-measure the 50 cycle COF because those samples had been worn to 500 cycles. The measurements were precise since they were repeatable for each sample and are included in this research, but the confidence in the trueness of the measurements is low. The samples highlighted in table 7 below are the samples affected by the adhesive contamination.

Table 7: Summary of Wear and Coefficient of Friction Measurements

Wear and COF Data						
Material	Pre-Wear Mass, 0 Cycles (g)	Mass After 50 Cycles (g)	COF, 50 Cycles	Mass, 500 Cycles (g)	COF, 500 Cycles (g)	***Wet COF, 500 Cycles
TNS A36	610	607	1.241	605	1.005	1.245
PNS A36	604	N/A	*N/A	*N/A	*N/A	*N/A
LDN A36 (Painted)	583	583	1.249	583	0.815	1.301
TNS A572	628	626	0.852	624	0.814	1.246
PNS A572	616	608	1.098	*N/A	*N/A	*N/A
LDN A572 (Painted)	608	607	0.978	606	0.924	1.282
PNS 5086	209	*N/A	*N/A	*N/A	*N/A	*N/A
LDN 5086	184	183	1.144	182	0.858	1.128
PNS 5456	208	199	1.105	*N/A	*N/A	*N/A
LDN 5456	201	200	0.905	**N/A	**N/A	**N/A

After noticing the contamination, the sled was replaced and “good” 500 cycle COF measurements were recorded. Wet COF measurements were also recorded following the 500 cycle wear test, but all of these values increased when it was expected they would decrease. The higher wet COF measurement could be due to the small size of the non-skid samples or old rubber which absorbed the water and created a “stickier” surface, although the source of the higher wet COF measurements is unknown. The confidence in the trueness of the wet COF measurements is also low.

4.4 Surface Feature Characterization

The focus of the surface characterization and analysis is on the TNS and LDN samples due to the glue contamination of the PNS samples and also because the wear was so excessive on the PNS samples that post-wear measurements were not possible. The intent of the surface characterization was to explore the area-scale fractal analysis, discriminate between materials, and find functional correlations associated with friction and mass loss.

Images taken on the Olympus confocal microscope were imported into Sfrax© to measure roughness parameters and area-scale fractal analysis. The TNS A36 sample was not saved properly, so that sample was omitted from the comparison. Comparisons among materials were observed for pre-wear and post-wear characteristics. The LDN A572 sample images and calculated roughness parameters are shown below in figures 20 and 21. The samples were at the upward limits the stand-off distance for the Olympus confocal microscope and care had to taken to prevent damaging the lens during the measurement process. The maximum peak to valley heights exceeded the working distances for the 50X and 100X lens, so measurements were limited to the 20X lens. The maximum vertical range of the triangulation sensor on the UBM Profiler was $\pm 3\text{mm}$, so only the PNS was able to be measured with the UBM Scanning Laser Profiler.

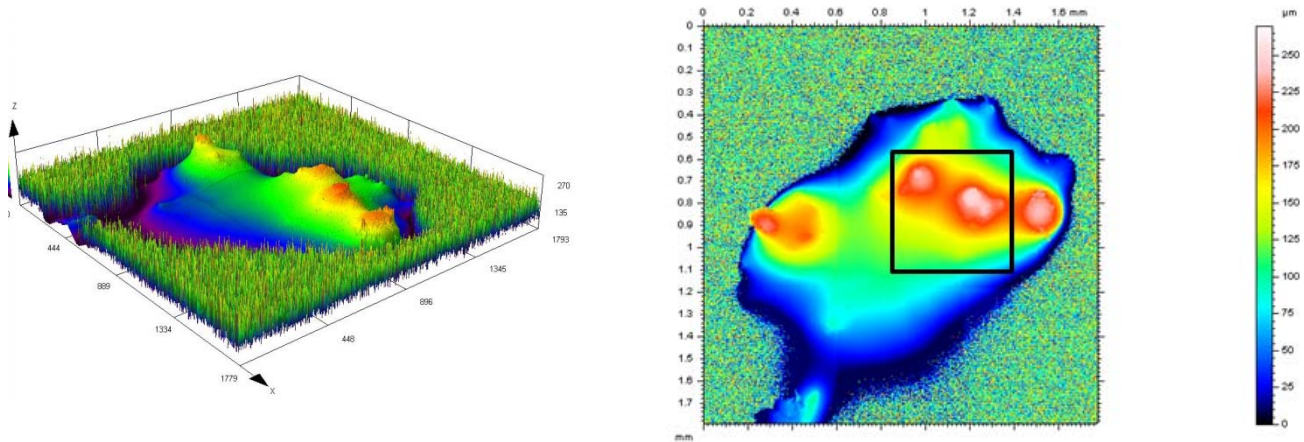


Figure 20: LDN A572 screenshot from Olympus measurement (left) and imported into Mountains™ with high point identified (right).

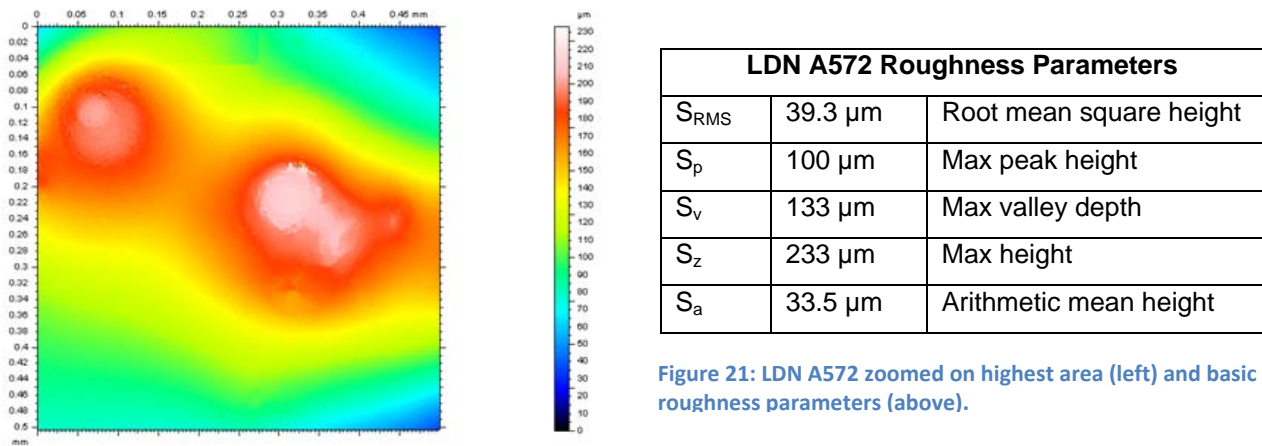


Figure 21: LDN A572 zoomed on highest area (left) and basic roughness parameters (above).

Roughness parameters S_a and S_z for all samples before and after wear testing are summarized below in table 7. The parameter S_a is the arithmetic mean height and S_z is the maximum peak to valley height of the surface. The post wear measurements were not completed on the PNS since the surface was gone after the initial wear test and the TNS A36 data was not saved properly and lost. The data shows that the basic roughness parameters of TNS and LDN are similar, yet the LDN post-wear measurements do not drop as significantly as the TNS measurements, however, a larger set of samples and measurements are needed to establish trends.

Table 8: Summary of Selected Pre and Post Wear Roughness Parameters

Basic Roughness Parameters				
Material	Pre-Wear S_a (μm)	Pre-Wear S_z (μm)	Post-Wear S_a (μm)	Post-Wear S_z (μm)
PNS A36	17.4	202	N/A	N/A
PNS A572	17.3	149	N/A	N/A
PNS 5086	16.5	138	N/A	N/A
PNS 5456	17.6	139	N/A	N/A
TNS A572	35.8	316	6.07	168
LDN A36	35.7	186	10.2	212
LDN A572	33.5	233	18.2	234
LDN 5086	24.8	581	6.47	55.1
LDN 5456	17.1	470	8.93	273

4.4.1 Area-Scale Analysis

In Sfrax™ an area-scale fractal analysis was performed comparing relative area and scale pre-wear and post wear. The analysis was performed with a slope filter of 80 degrees and without a filter. The filter eliminated some steep points on the samples and appeared to have the most impact on the aluminum samples. It was important to choose appropriate filters to produce good results (Berglund et al. 2010).

Figure 22 shows the mean relative area as a function of scale for selected non-skid materials (unfiltered) before and after wear testing. The area scale plots of the samples are distinct with some overlap of the pre-wear LDN 5086 and the post wear LDN 5456. The overlap is realistic since the LDN 5456 was only worn to 50 cycles while the LDN 5086 was worn to 500 cycles. Otherwise the difference between pre and post wear samples is clear.

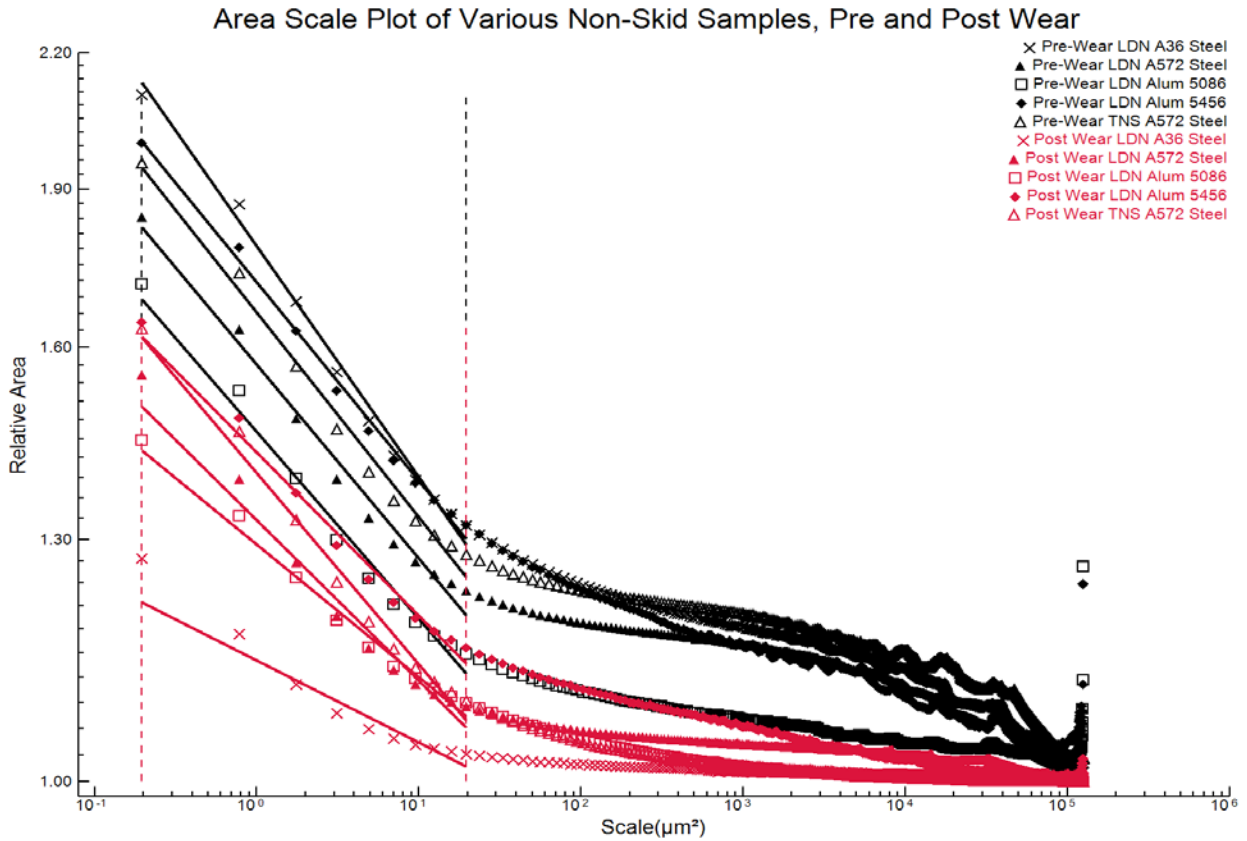


Figure 22: Mean relative area as a function of scale for selected non-skid materials.

4.4.2 Discrimination of Samples

F-tests of significance are used to compare the ability of the measurement parameters to differentiate among the samples. The mean square ratio (MSR) is calculated and is used to determine a confidence level that the two sets of measurements can be differentiated by the parameters (Brown 2006). The plot showing F-test significance comparing pre-wear parameters with post-wear parameters with 99% confidence is shown below. The plot shows that the samples are differentiable below scales of $10^5 \mu\text{m}$.

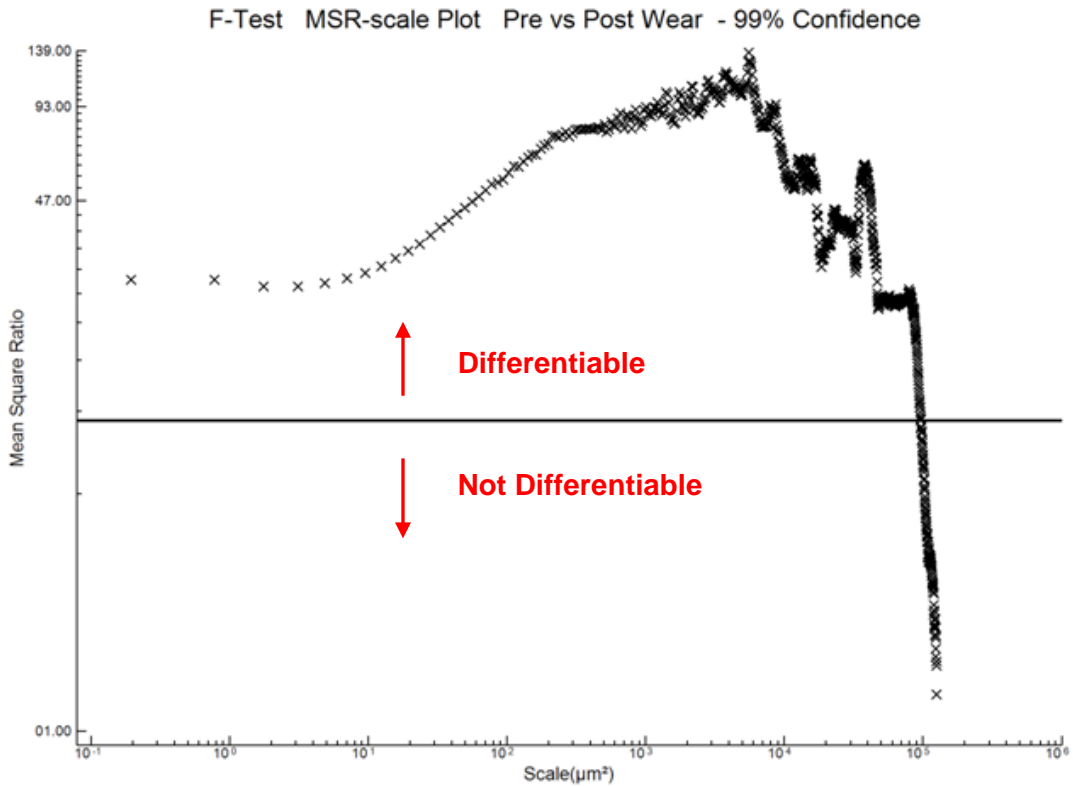


Figure 23: MSR-scale plot from F-test of significance analysis with 99% confidence.

4.4.3 Functional Correlations

Since friction is an important parameter in the design and performance of non-skid, the COF was one of the functional properties examined in this research. Since contamination issues were experienced and the COF values are questionable, an analysis was run to correlate the calculated mass loss of non-skid to relative area. An area-scale plot was created for the non-skid samples that were worn to 500 cycles (TNS A572, LDN A36, LDN A572, and LDN 5086). Neither the friction parameter nor the wear mass loss parameter correlated well with relative area. It is possible that good correlations exist at different scales or for specific roughness parameters, such as the inclination on the surface (Berglund, et al. 2010). The correlation plots between relative area and friction and relative area and wear mass loss at 804 scales are shown below.

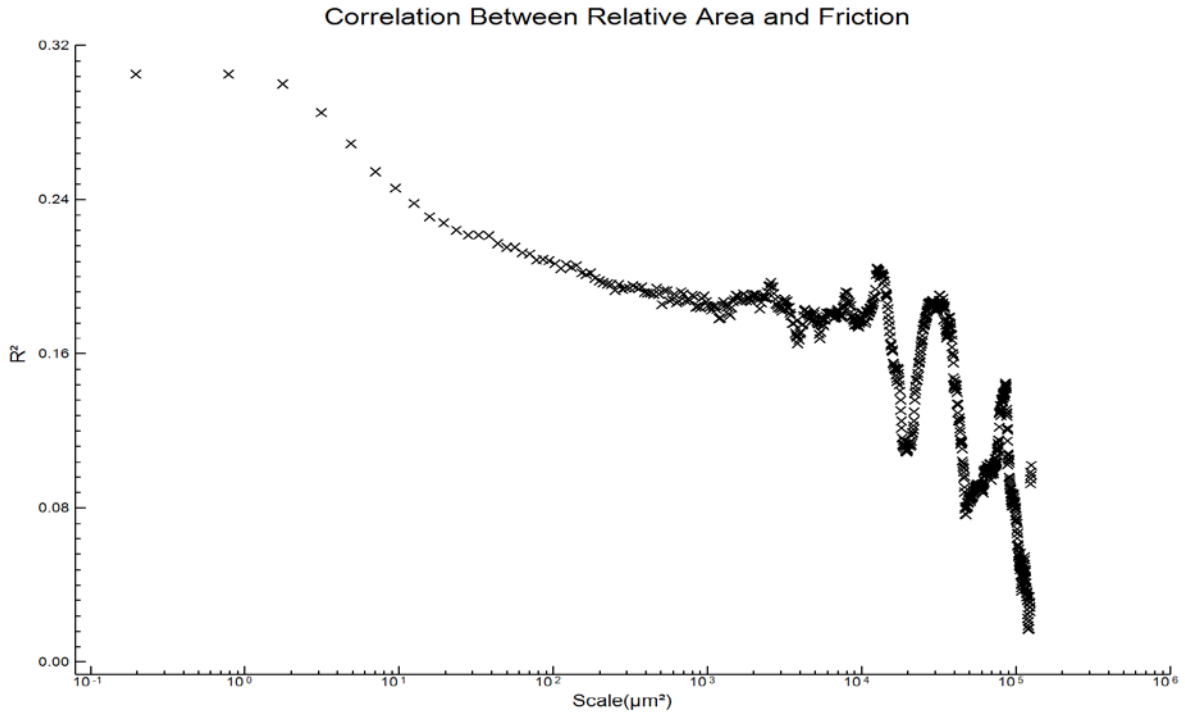


Figure 24: Correlation coefficient, R^2 , for the correlation between relative area and friction at 804 scales.

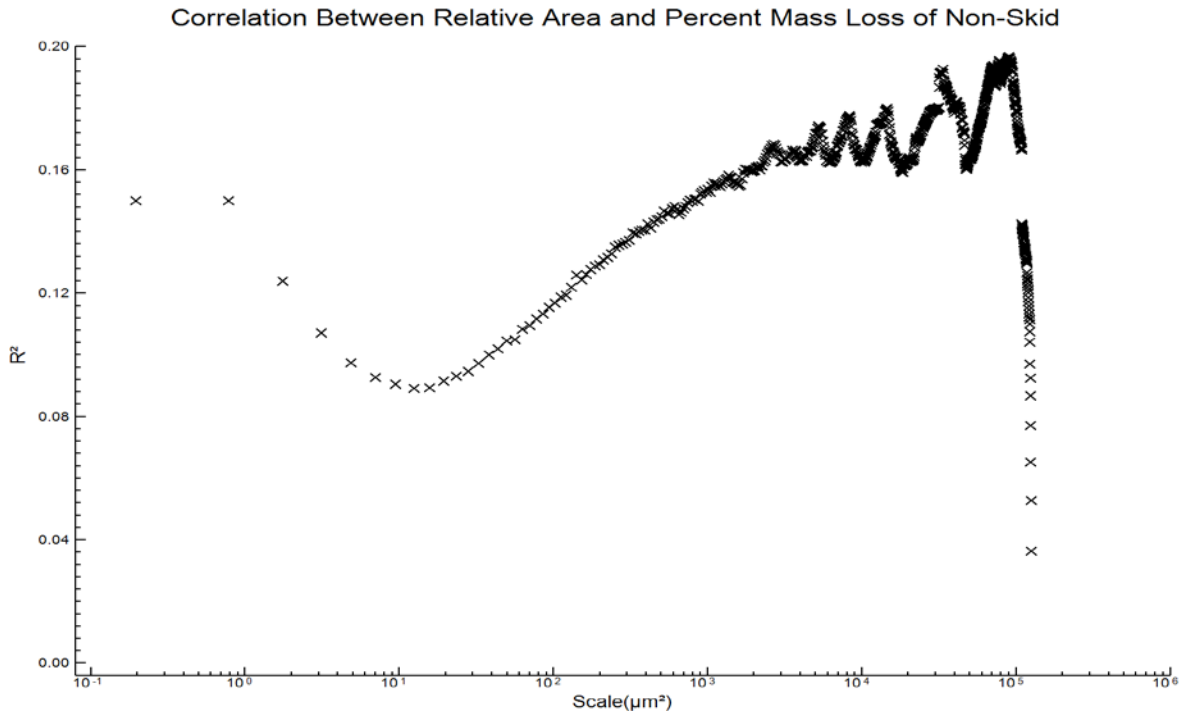


Figure 25: Correlation coefficient, R^2 , for the correlation between relative area and mass loss at 804 scales.

4.5 Cost Metrics

The cost of the non-skid materials varies from \$3.10 per square foot up to \$10 per square foot. Skilled labor is required to install TNS and LDN material while the PNS may be installed by the ship’s crew with basic tools. The cost of the PNS depends on if uncut sheets of material are purchased or if a kit is purchased which contains pre-cut pieces according to the deck arrangements of specific ships and boats. The cost of the LDN depends on the specific base metal and the spacing of the deposited “bumps.” The cost information for the LDN was provided by Barry Appolin with the Coast Guard and Andy Jones at Ross Technology. Cost data for the TNS was found on the C. G. Edwards & Co. Inc. website. Cost data for the PNS non-skid was found on the Louisiana Association for the Blind website with additional data in the PowerPoint by Dave Zilber at 3M. Table 9 shows a summary of material cost, service life, installation requirements, and experimental results. Details of the cost analysis are included in Appendix 8.

Table 9: Summary of non-skid characteristics.

Non-Skid Cost Metrics					
Material	Cost/Ft ²	Life Expectancy	Installation Considerations	Corrosion	Wear
TNS	\$3.30	2-3 years	- Skilled Labor - Curing Time - Difficult to Repair - Flight Deck Approved	Poor	Fair
PNS	\$4.50 to \$7.50 *	2 -3 years	- Ship’s Force - Immediate Use - Easy to Repair	Poor	Poor
LDN					
Steel	\$8 to \$10	Unknown	- Skilled Labor - Requires Painting - Unknown Maintenance Issues	Good	Good
Aluminum	\$8 to \$10 **	Unknown	- Skilled Labor	Excellent	Poor

* Cost per square foot for a pre-cut pieces in a kit to fit specific boat decks. Uncut sheets of material are \$4.50 per square foot.

** Cost to prototype a 41’ UTB deck was \$2,495 or \$8.19 per square foot. Price varies according to specific material and spacing of the depositions.

5 Conclusions and Recommendations

5.1 Conclusions

- Salt fog testing was more corrosive than the actual operational environment.
- The LDN steel samples experienced the least corrosion and the aluminum samples showed no signs of corrosion in either test batch.
- The principal method of corrosion on the PNS non-skid was by undercutting due to the water intrusion under the edges of the material.
- The principal method of corrosion on the TNS non-skid was by through corrosion where water penetrated the non-skid material.
- Proper surface preparation and quality control of the non-skid material influence the resistance to corrosion and wear.
- The LDN steel samples exhibited the best resistance to wear and the PNS (aluminum and steel) and LDN aluminum samples showed the worst resistance to wear.
- The result of the area-scale analysis seems appropriate for the intent of the non-skid material: larger relative area at lower scales.
- The pre-wear and post wear samples are differentiable below scales of $10^5 \mu\text{m}$.
- The relative area did not correlate well with friction or wear mass loss.
- The cost analysis is complicated by the somewhat unpredictable lifecycle of each material. More data are needed to compare all three of the evaluated non-skid materials.

5.2 Recommendations

- It is recommended that LDN on steel deck may be suitable for use as non-skid on ships, but some issues need further investigation:
 - Maintenance issues: As the paint is worn off the steel, can it be re-painted while maintaining the non-skid surface?
 - Stress cracking: Could the “bumps” serve as crack initiation sites?

- LDN non-skid on aluminum appears suitable for use as deck material on Coast Guard small boats. Although the wear tests resulted in significant mass loss of the non-skid, the test seems overly aggressive for the uses of lifeboats, surf boats, and utility boats. Further research should be done to determine the appropriate spacing of the “bumps” for COF optimization and cost minimization. The actual lifecycle of the prototyped 41’ UTB will be important information in comparing the overall value of the LDN to the other non-skid materials.
- The MIL-PRF-2667 specification is based on the daily operations and missions of the U. S. Navy and in many instances the test standards are more aggressive than required for the unique needs of the Coast Guard. It is recommended that the Coast Guard develop its own standard for non-skid material applied to non-flight deck areas.

5.3 Future Work

- Investigate the relationship of stress corrosion cracking in the LDN. Determine the effect of the “bumps” as possible crack initiation sites.
- Determine optimum spacing of the “bumps” for maximizing COF retention and minimizing cost.
- Innovate new surfaces for non-skid by finding functional correlations with friction, wear, and corrosion by optimizing specific roughness parameters.
- Develop Coast Guard specific testing standards and methodologies to optimize non-skid performance and service life while minimizing cost.

6 References

- 3M Technical Data Sheet. (2003). *Safety-Walk™ Slip Resistant Materials* [Brochure]. St. Paul, Minnesota: 3M Commercial Care Division.
- ASTM (2009). A36/A36M – 08: *Standard Specification for Carbon Structural Steel*. Annual Book of ASTM Standards 01.04 (pp. 109-111): ASTM.
- ASTM (2009) A572/A572M – 07: *Standard Specification for High-Strength Low-Alloy Columbium-Vanadium Structural Steel*. Annual Book of ASTM Standards 01.04 (pp. 313-316): ASTM.
- ASTM (2009) B 117 – 07a: *Standard Practice for Operating Salt Spray (Fog) Apparatus*. Annual Book of ASTM Standards 03.02 (pp. 1-10): ASTM.
- ASTM (2009) B928/B928M – 07: *Standard Specification for High Magnesium Aluminum-Alloy Sheet and Plate for Marine Service and Similar Environments*. Annual Book of ASTM Standards 02.02 (pp. 684-694): ASTM.
- ASTM (2009) D610 – 08: *Standard Practice for Evaluating Degree of Rusting on Painted Steel Surfaces*. Annual Book of ASTM Standards 06.02 (pp. 14-18): ASTM.
- ASTM (2009) D1654 – 05: *Standard Test Method for Evaluation of Painted or Coated Specimens Subjected to Corrosive Environments*. Annual Book of ASTM Standards 06.01 (pp. 215-218): ASTM.
- Baboian, Robert. (1995). *Corrosion Tests and Standards*. Philadelphia: ASTM.
- Bayer, Raymond G. (2004). *Mechanical Wear Fundamentals and Testing* (2nd Ed.). New York: Marcel Dekker, Inc.
- Berglund, John, Brown, Christopher A., Rosen, B.-G., and Bay, Niels. (2010). *Milled die steel surface roughness correlation with steel sheet friction*. Unpublished draft. Annals of the CIRP, 1. 18).
- Brown, Christopher A. (2010, spring semester). *Surface Metrology ME 5841*. [Class Lecture and Materials]. Worcester Polytechnic Institute.
- Cherry, Timothy. (2007) *Navy Preservation Cost/Technical Working Group* [PowerPoint slides]. Retrieved January 6, 2010 from <http://www.nstcenter.com/docs/PDFs/MR2007/MR2007-Tuesday-FCSMR2007-12-TCherry.pdf>
- Digital Surf. (2010). *Mountains* [computer software]. Besançon, France: Digital Surf.
- Dust, Mark. (2008). *U.S. Coast Guard Coatings and Corrosion Control* [PowerPoint slides]. Retrieved September 10, 2009 from: <http://www.nstcenter.com/.../Wed-1JointServices-4-MR2008-03-MDust.pdf>.

Dust, Mark. (2007). *U. S. Coast Guard Coating Status* [PowerPoint slides]. Retrieved September 16, 2009 from: <http://www.nstcenter.com/docs/PDFs/.../MR2007-Wed-JSS-MR2007-04-MDust.pdf>.

Herzberg, Eric F., Ambrogio, Erica D., Barker, Clark L., Harleston, Evelyn F., Haver, William M., O'Meara, Norman T., Marafioti, Ronald J., Stimatze, Gregg L., Timko, Andrew and Tran, James C. (2006). *The Annual Cost of Corrosion for Army Ground Vehicles and Navy Ships*. Report SKT50T1. LMI Government Consulting. Retrieved from: http://www.corrdefense.org/corrdefense_magazine/summer_2007/top_story3.htm

Herzberg, Eric. (2008). Agency Completes Cost of Corrosion Study for Coast Guard Aviation and Vessels. Retrieved from: http://web.lmi.org/CDmagazine/corrdefense_2ummer_2008/top_story3_sidebar.asp

Inspector General, United States Department of Defense. (2007). *Non-Skid Materials Used on Navy Ships* (Report Number TAD-2008-001). Washington, DC: U.S. Government Printing Office. Retrieved from <http://www.dodig.mil/Inspections/NSM%20Final%20Report%20TAD-2008-001.pdf>.

Johnsen, William A. (1997). *Advances in the Design of Pavement Surfaces*. (Doctoral dissertation, Worcester Polytechnic Institute, 1997). Retrieved from <http://www.me.wpi.edu/Images/CMS/ME-MFE-SurfMet/johnsen.pdf>.

Jordan, S. E., and Brown, C. A. (2006). *Comparing texture characterization parameters on their ability to differentiate ground polyethylene ski bases*. *Wear*, 261, 398-409.

Kato, K. (2002). *Classification of wear mechanisms/models*. Proceedings of the Institution of Mechanical Engineer, Journal of Engineering Tribology, Part J 216, 349-355.

Kramer, Stephen D., and Covino Jr., Bernard S. (2003). *ASM Handbook Volume 13A, Corrosion: Fundamentals, Testing, and Protection*. Materials Park, Ohio: ASM International.

Linton, Eric. (2009). *Coast Guard Surface Fleet Corrosion Prevention and Control Program*. [PowerPoint slides]. Retrieved March 3, 2010 from: www.nstcenter.com/docs/PDFs/.../Proceedings_MR2009-21-ELinton.pdf.

Naval Sea Systems Command, Department of the Navy. (2008). *Performance Specification: Coating System, Non-Skid, For Roll, Spray, or Self-Adhering Application* (Military Performance Specification MIL-PRF-24667C). Washington, DC: Navy Yard. Retrieved from <http://www.nstcenter.com/milspecs.aspx?milspec=24667>.

PPG Protective and Marine Coatings, Coatings for the United States Coast Guard. (2009). Retrieved April 12, 2010 from C.G. Edwards & Co. Inc. website: <http://www.cgedwards.com/ameron/uscg.html>.

Perryman, Jon. (2007). *Corrosion Resistance of Aluminum*. (Crane Materials International, A CMI Technical Paper). Retrieved April 12, 2010 from:
http://engineer.cmimarine.com/whitepapers/aluminum_corrosion.pdf.

Rabinowicz, Ernest. (1995). *Friction and Wear of Materials* (2nd ed.). New York: John Wiley & Sons, Inc.

Revie, R. Winston and Herbert H. Uhlig. (2008). *Corrosion and Corrosion Control* (4th ed). Hoboken, New Jersey: John Wiley & Sons, Inc.

“Rusting of Iron by water droplet” No date. Online image. Electrical Cells and Batteries. Retrieved 12 April 2010. www.splung.com/content/sid/3/page/batteries.

Rust Chemistry. (n.d.). Retrieved April 12, 2010 from Corrosion Doctors. website:
<http://www.corrosion-doctors.org/Experiments/rust-chemistry.htm>.

Safety-Walk™ USCG 110 Kit. (n.d.). Retrieved April 10, 2010 from the Louisiana Association for the Blind website: <http://www.lablind.com/ttstore/prod.asp?itemtype=18>.

Sisson, Richard D. (2007). *Hydrogen Embrittlement of Spring Steel*. Wire Forming Technology International/Fall 2007, 20-22.

Skillingberg, Michael. (2004). *New Temper Definitions for the Marine Market*. Retrieved March 20, 2010 from The Aluminum Association website:
<http://www.aluminum.org/Content/NavigationMenu/TheIndustry/IndustryStandards/default.htm>

Surfract Inc. (2007). *Sfrax*. (Version 1.0) [computer software]. Available from
<http://www.surfract.com>.

Tricou, Charles. (n.d.). *Development and Qualification of FLEXOLITH 2000Ga Mil-PRF-24667C Type V (Extended Durability) Nonskid Coating* [PowerPoint slides]. Retrieved September 18, 2009 from:
http://techcon.ncms.org/Symposium2009/presentations/Wednesday_Advanced_Materials/0930%20NonSkid%20Type%20V%20NRL.pdf.

Tricou, C. S. and M. J. Kelly. (2008). *Final Report, Lab Performance of Flexolith 2000G to MIL-PRF-24667B Type 5 (Extended Durability Nonskid Coating), Formulation G*. Technical Memorandum File No 08-038. State College, Pennsylvania: ARL.

Zilber, Dave. (2009). *Peel & Stick Nonskid Program: Building and Sustaining the Navy’s Fleet*. [Powerpoint slides]. Retrieved March 10, 2010 from:
http://www.nstcenter.com/docs/PDFs/.../Proceedings_MR2009-32-DZilber.pdf.

Appendix 1: Images Before and After Corrosion

Salt Fog Testing

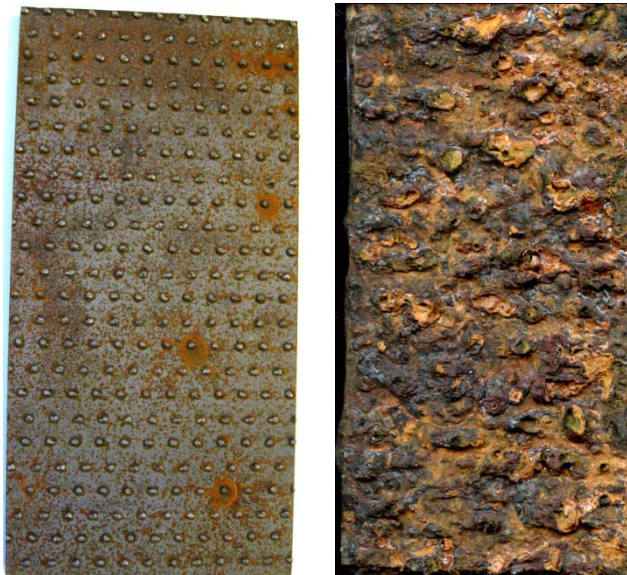
1) TNS A36:



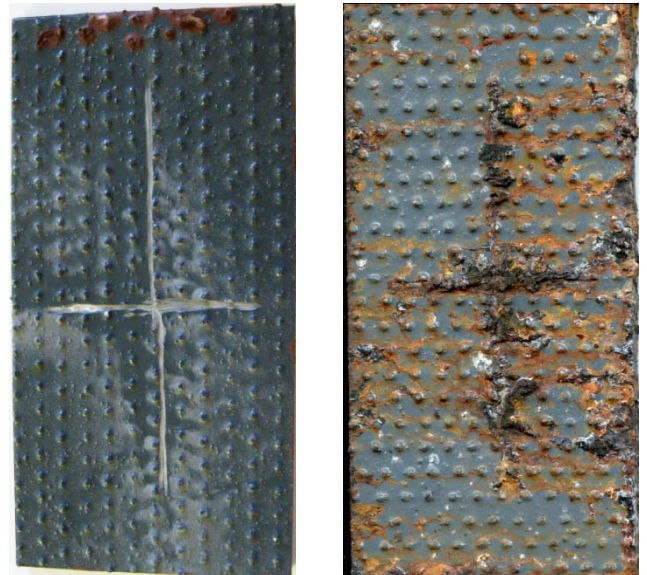
2) PNS A36:



3) LDN A36, Unpainted:



4) LDN A36, Painted:



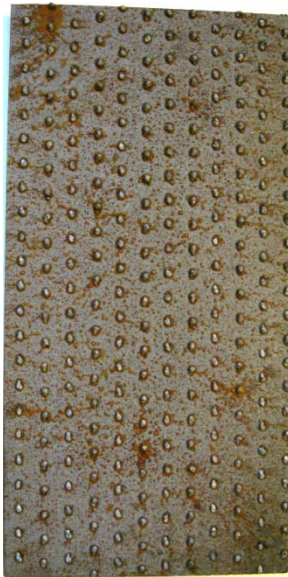
5) TNS A572:



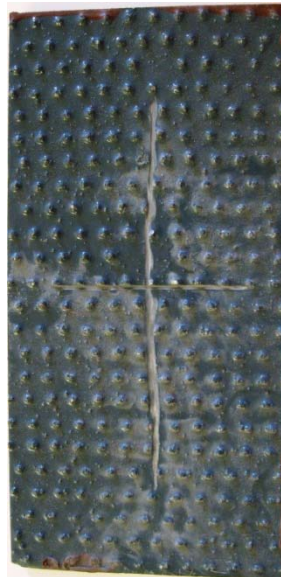
6) PNS A572:



7) LDN A572, Unpainted:



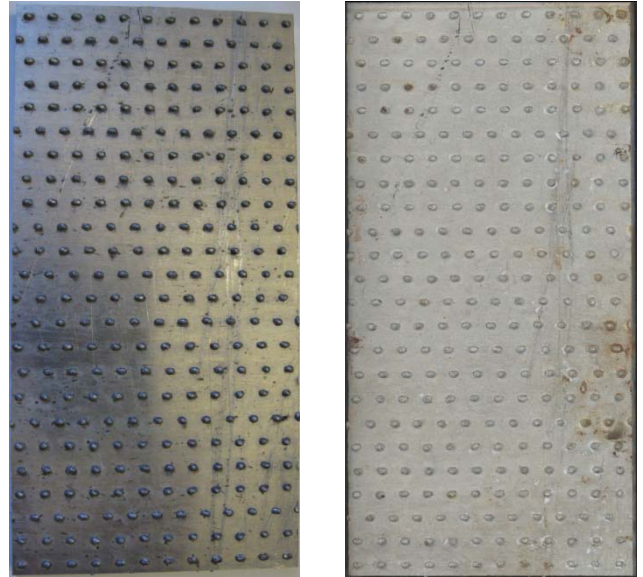
8) LDN A572, Painted:



9) PNS 5086:



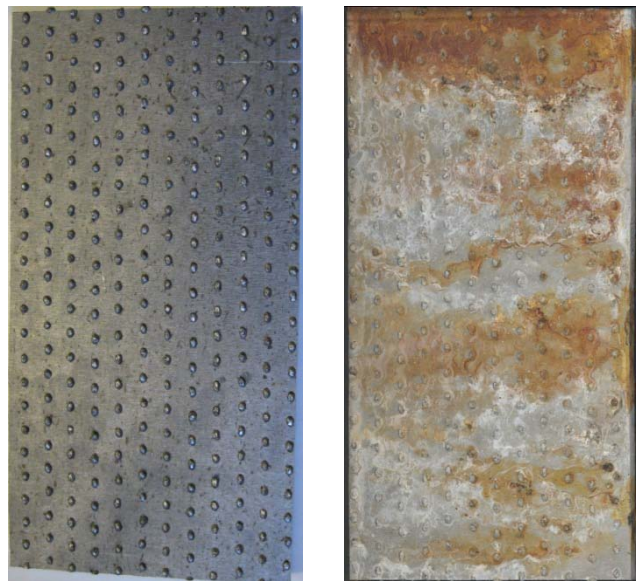
10) LDN 5086:



11) PNS 5456:



12) LDN 5456:

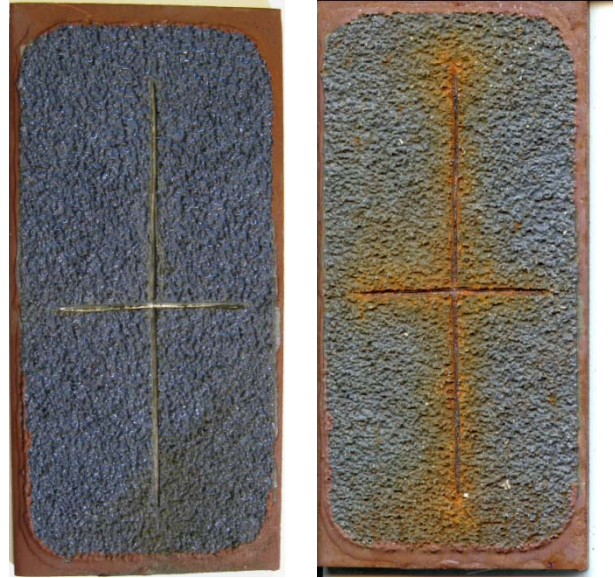


Environmental Testing: 110' Patrol Boat

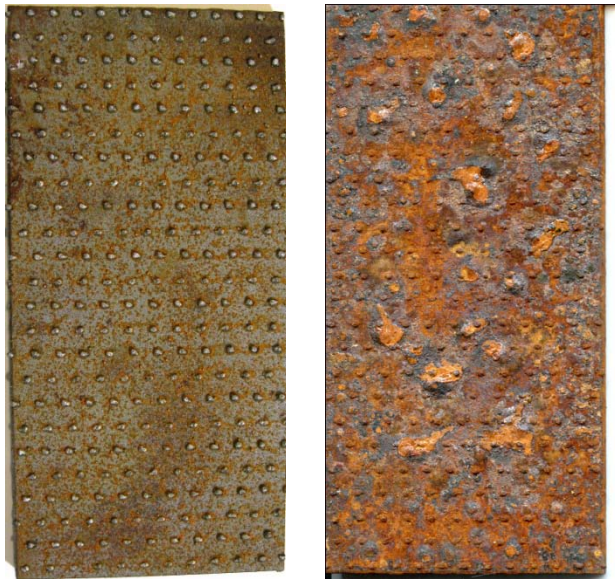
1) TNS A36:



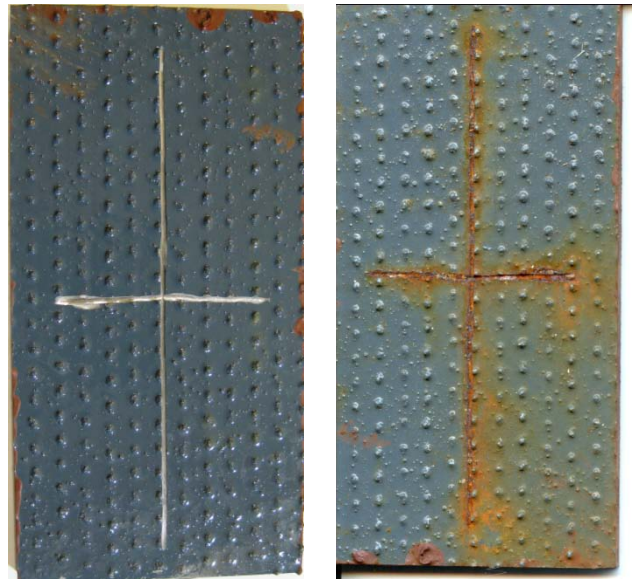
2) PNS A36:



3) LDN A36, Unpainted:



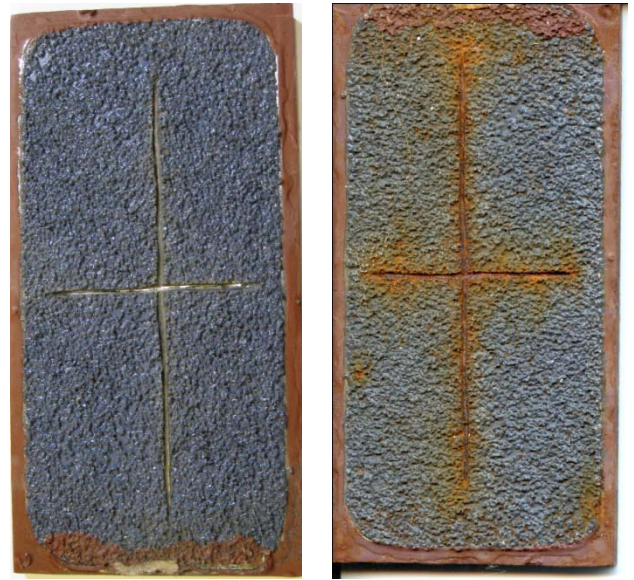
4) LDN A36, Painted:



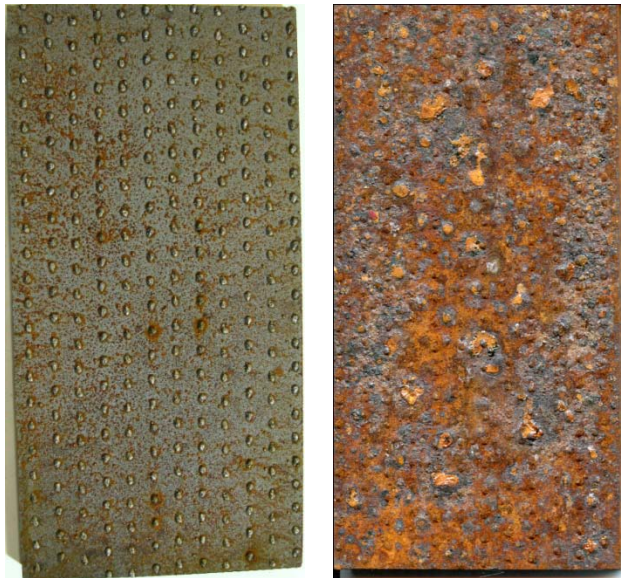
5) TNS A572:



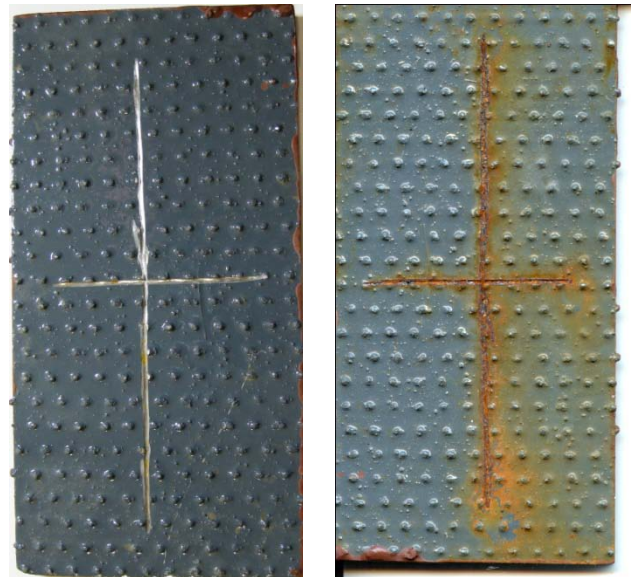
6) PNS A572:



7) LDN A572, Unpainted:



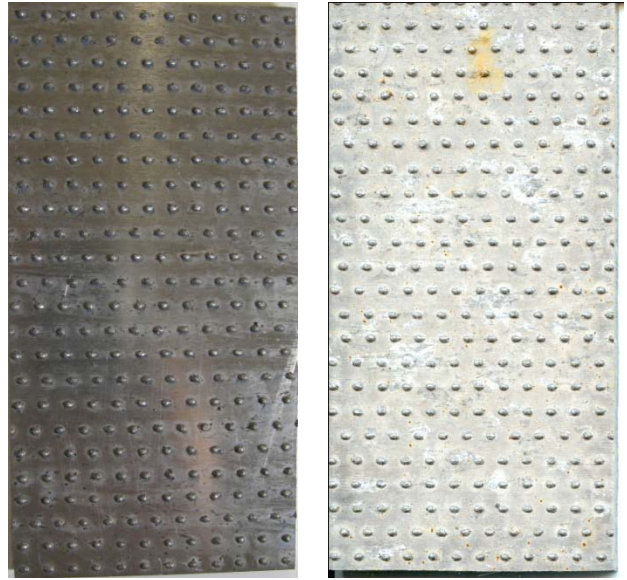
8) LDN A572, Painted:



9) PNS 5086:



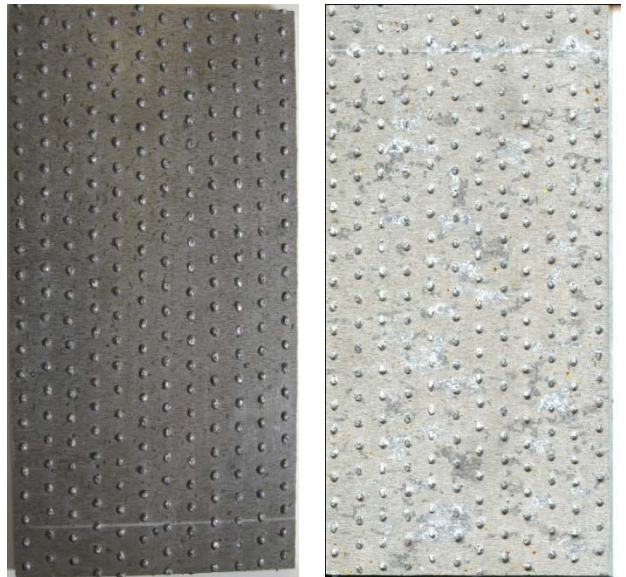
10) LDN 5086:



11) PNS 5456:



12) LDN 5456:

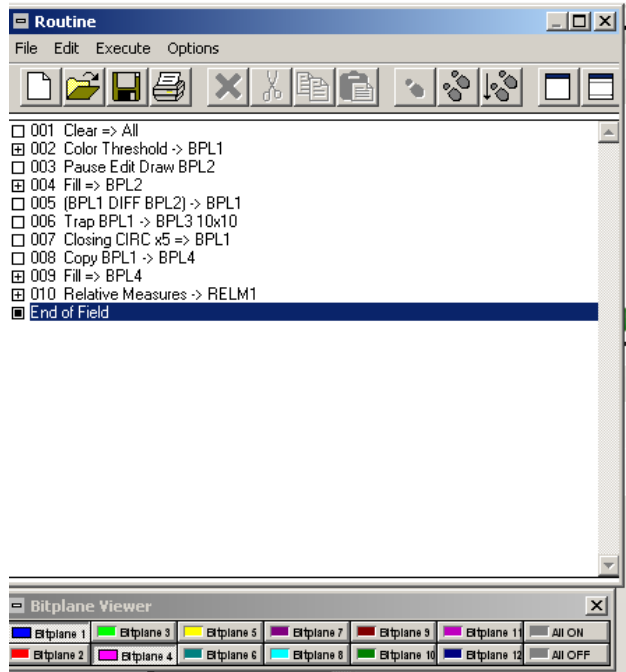


Appendix 2: Clemex™ Image Analysis

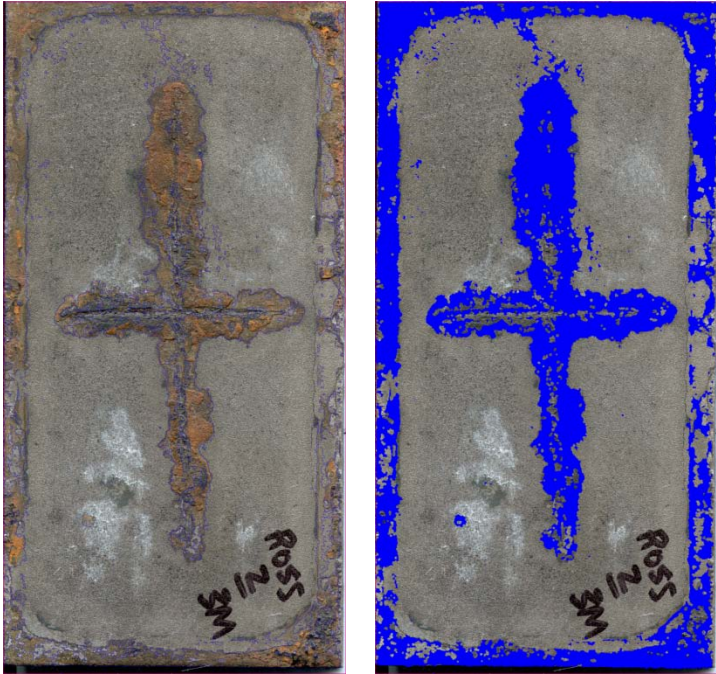
Methodology:

1. Import image into Clemex™ software
2. Create routine to:
 - a. Create a bitplane in a chosen color and threshold it to capture the corrosion
 - b. Create additional bitplanes if necessary to capture additional corrosion not captured in the first bitplane
 - c. Fill the areas of corrosion
 - d. Determine the total area of the image and the relative area of corrosion
3. Run the routine for each sample and export the calculated area measurements
4. Repeat the process for each sample

Step 1 and Step 2:



Step 2a:



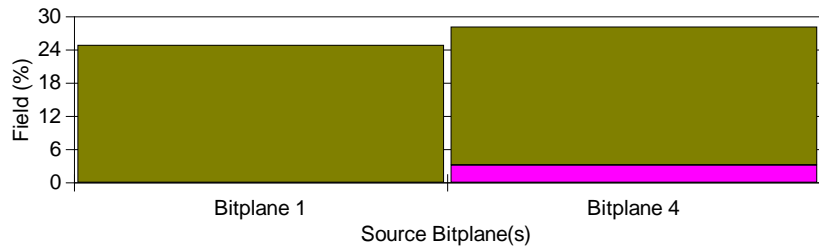
Step 2b:



Step 3:



Salt Fog Testing: PNS A36

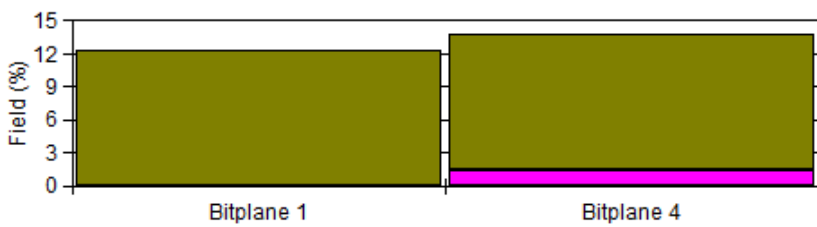
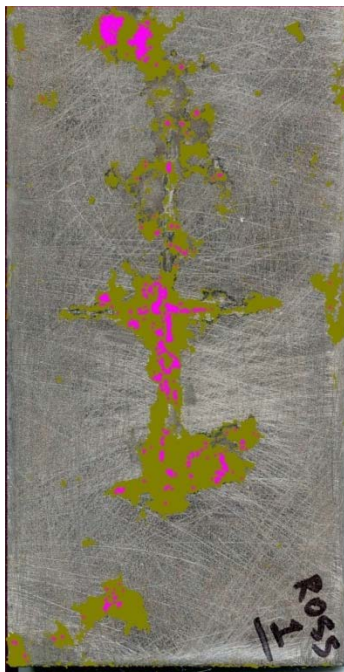


S. Bitplane(s)	Field (%)
Bitplane 1	25.0 (0)
Bitplane 4	28.2 (3.2)

Field Count: 1
 Field Area: 11.7e+09 μm^2
 Total Area: 11.7e+09 μm^2
Statistics

Salt Fog Testing Sample Analysis:

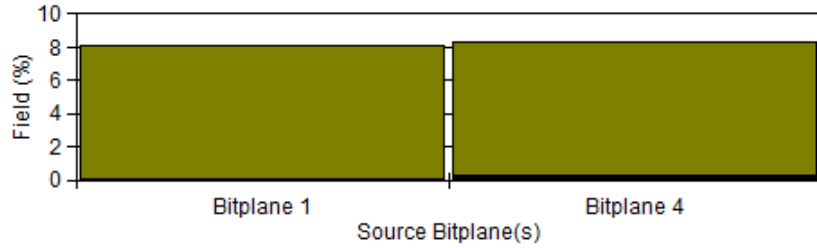
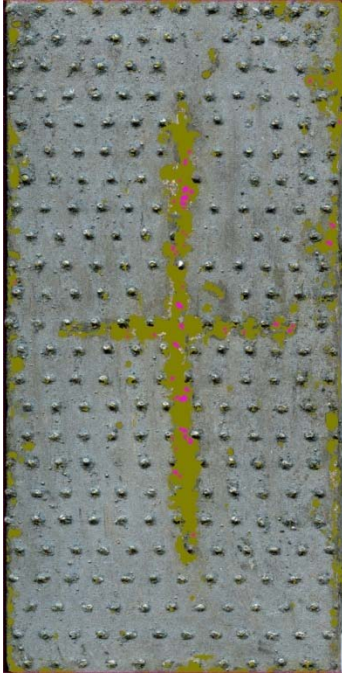
TNS A36:



S. Bitplane(s)	Field (%)
Bitplane 1	12.3 (0)
Bitplane 4	13.8 (1.5)

Field Count: 1
 Field Area: 11.7e+09 μm^2
 Total Area: 11.7e+09 μm^2
Statistics

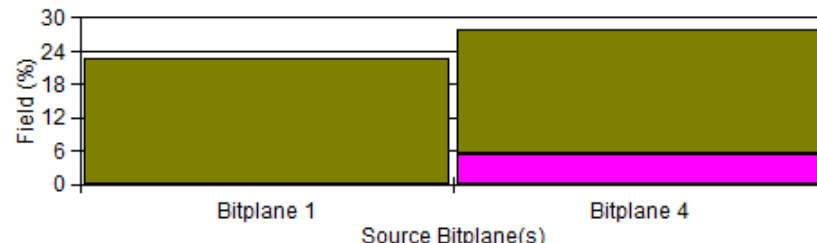
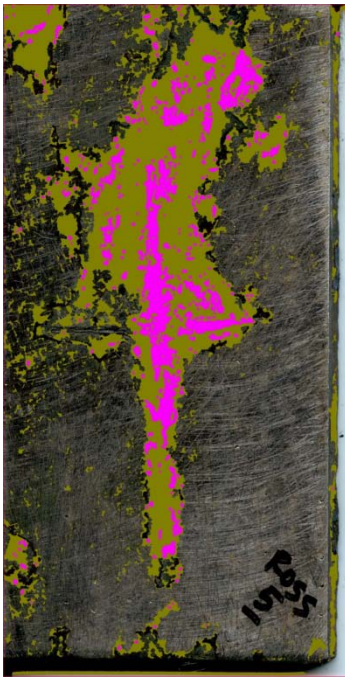
LDN A36:



S. Bitplane(s)	Field (%)
Bitplane 1	8.1 (0)
Bitplane 4	8.3 (0.2)

Field Count: 1
 Field Area: 11.7e+09 μm^2
 Total Area: 11.7e+09 μm^2
 Statistics

TNS A572:



S. Bitplane(s)	Field (%)
Bitplane 1	22.7 (0)
Bitplane 4	28.0 (5.3)

Field Count: 1
 Field Area: 11.9e+09 μm^2
 Total Area: 11.9e+09 μm^2
 Statistics

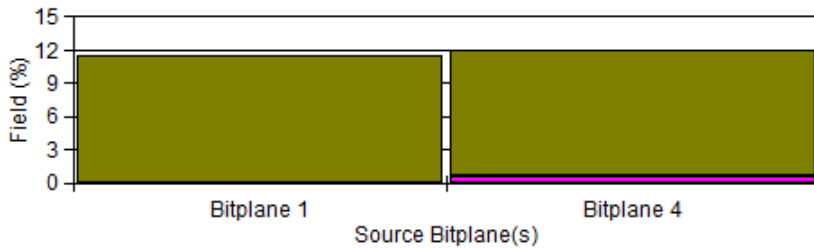
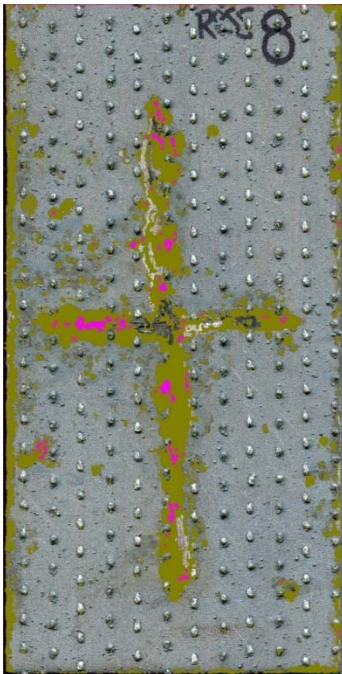
PNS A572:



S. Bitplane(s)	Field (%)
Bitplane 1	36.0 (0)
Bitplane 4	41.7 (5.7)

Field Count: 1
 Field Area: 11.7e+09 μm^2
 Total Area: 11.7e+09 μm^2
Statistics

LDN A572:



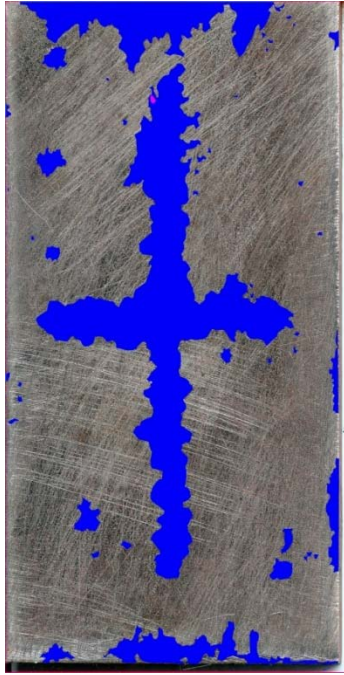
S. Bitplane(s)	Field (%)
Bitplane 1	11.4 (0)
Bitplane 4	12.0 (0.6)

Field Count: 1
 Field Area: 11.7e+09 μm^2
 Total Area: 11.7e+09 μm^2
Statistics

Environmental (CGC KODIAK ISLAND) Sample Analysis:

TNS A36:

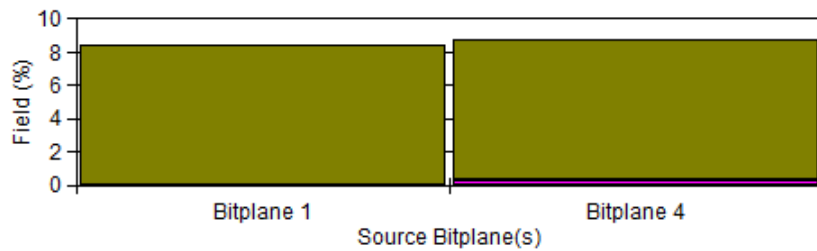
Note: This sample needed additional work in Photoshop to select and capture the corrosion.



S. Bitplane(s)	Field (%)
Bitplane 1	18.7 (0)
Bitplane 4	18.8 (12.5e-03)

Field Count: 1
 Field Area: 11.7e+09 μm^2
 Total Area: 11.7e+09 μm^2
 Statistics

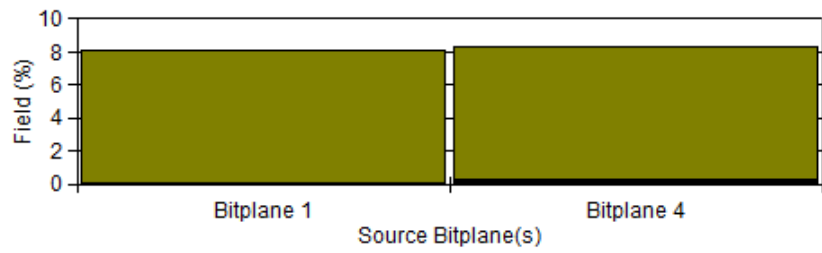
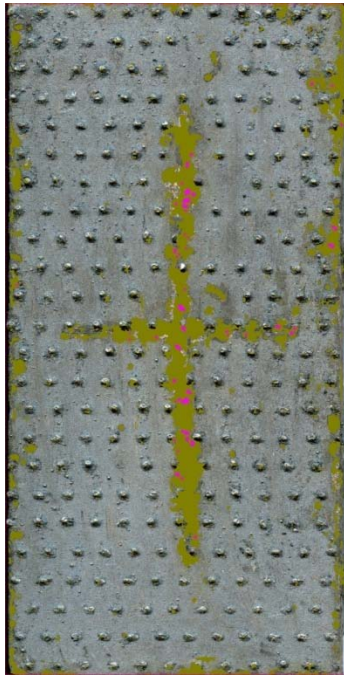
PNS A36:



S. Bitplane(s)	Field (%)
Bitplane 1	8.5 (0)
Bitplane 4	8.7 (0.2)

Field Count: 1
 Field Area: 11.7e+09 μm^2
 Total Area: 11.7e+09 μm^2
 Statistics

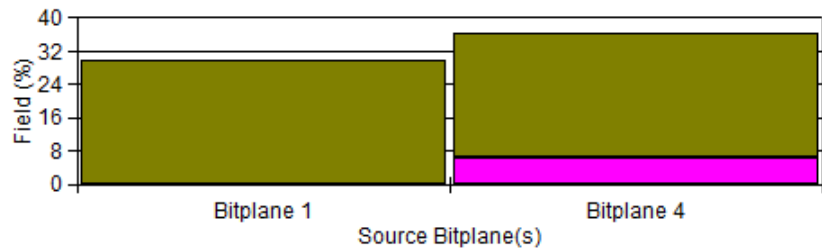
LDN A36:



S. Bitplane(s)	Field (%)
Bitplane 1	8.1 (0)
Bitplane 4	8.3 (0.2)

Field Count: 1
 Field Area: 11.7e+09 μm^2
 Total Area: 11.7e+09 μm^2
Statistics

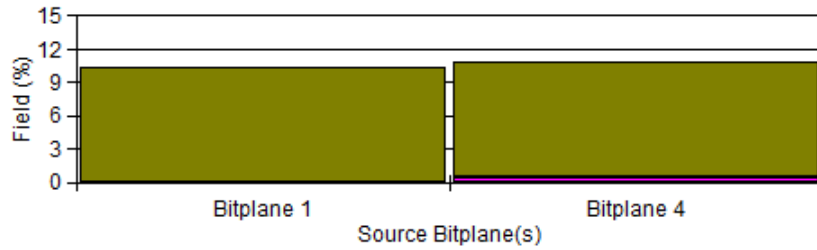
TNS A572:



S. Bitplane(s)	Field (%)
Bitplane 1	29.8 (0)
Bitplane 4	36.2 (6.4)

Field Count: 1
 Field Area: 11.7e+09 μm^2
 Total Area: 11.7e+09 μm^2
Statistics

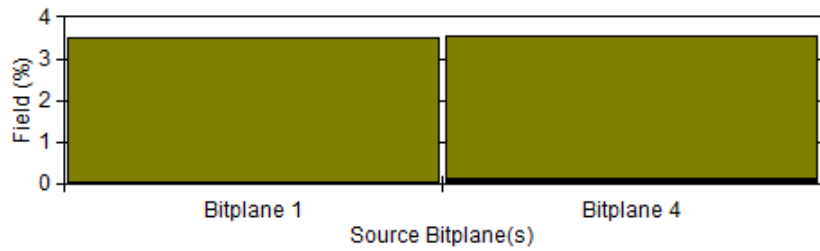
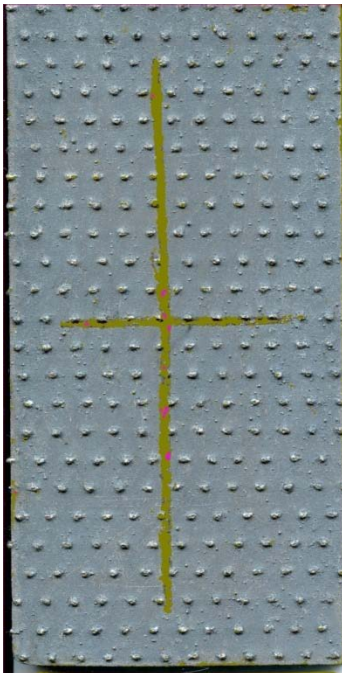
PNS A572:



S. Bitplane(s)	Field (%)
Bitplane 1	10.3 (0)
Bitplane 4	10.8 (0.5)

Field Count: 1
 Field Area: 11.7e+09 μm^2
 Total Area: 11.7e+09 μm^2
Statistics

LDN A572:



S. Bitplane(s)	Field (%)
Bitplane 1	3.5 (0)
Bitplane 4	3.6 (54.7e-03)

Field Count: 1
 Field Area: 11.7e+09 μm^2
 Total Area: 11.7e+09 μm^2
Statistics

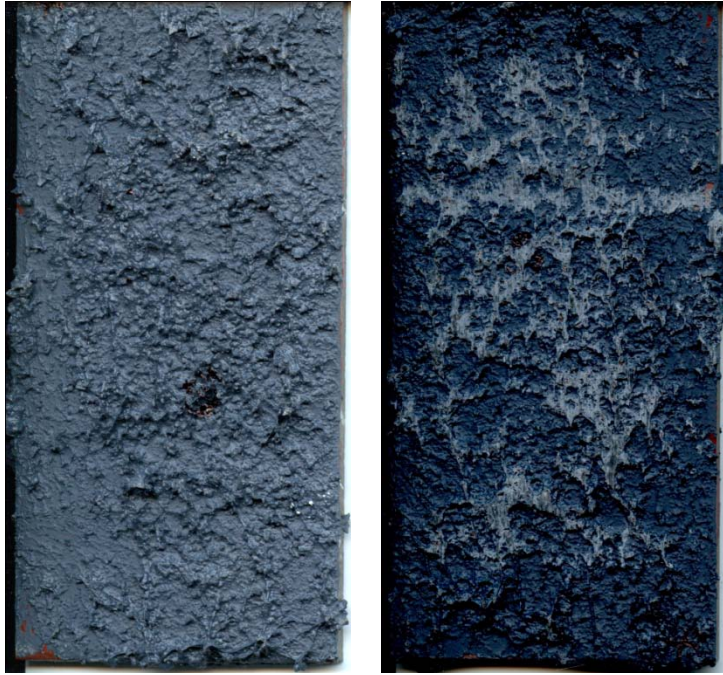
Appendix 3: Corrosion Mass Loss Data and Corrosion Rate Calculations

Corrosion Data													
Mass Changes: Salt Fog Testing						Mass Changes: Environmental, CGC KODIAK ISLAND							
Sample	Material	Mass Before Corrosion (g)	Mass After Corrosion (g)	% Area Corroded	Mass, Corrosion Removed (g)	Sample	Material	Mass Before Corrosion (g)	Mass After Corrosion (g)	% Area Corroded	Mass, Corrosion Removed (g)		
1	TNS A36	619	624	13.8	578	1	TNS A36	608	608	18.8	582		
2	PNS A36	604	608	28.2	579	2	PNS A36	570	572	8.7	556		
3	LDN A36 (Unpainted)	581	604	100	578	*	3	LDN A36 (Unpainted)	558	565	100	562	*
4	LDN A36 (Painted)	580	585	8.3	566		4	LDN A36 (Painted)	578	579	6.5	574	
5	TNS A572	637	640	28	587		5	TNS A572	622	622	36.2	578	
6	PNS A572	622	629	41.7	594		6	PNS A572	616	617	10.8	600	
7	LDN A572 (Unpainted)	612	636	100	603		7	LDN A572 (Unpainted)	611	618	100	613	*
8	LDN A572 (Painted)	616	623	12	599	*	8	LDN A572 (Painted)	601	602	3.6	598	
9	PNS 5086	201	201	0	201		9	PNS 5086	209	209	0	209	
10	LDN 5086	197	198	0	198		10	LDN 5086	196	196	0	196	
11	PNS 5456	207	207	0	207		11	PNS 5456	208	207	0	208	
12	LDN 5456	198	198	0	198		12	LDN 5456	202	201	0	201	

* Raw (unpainted) samples had very thick rust and all of it couldn't be removed

Appendix 4: Images of Samples Before and After Wear

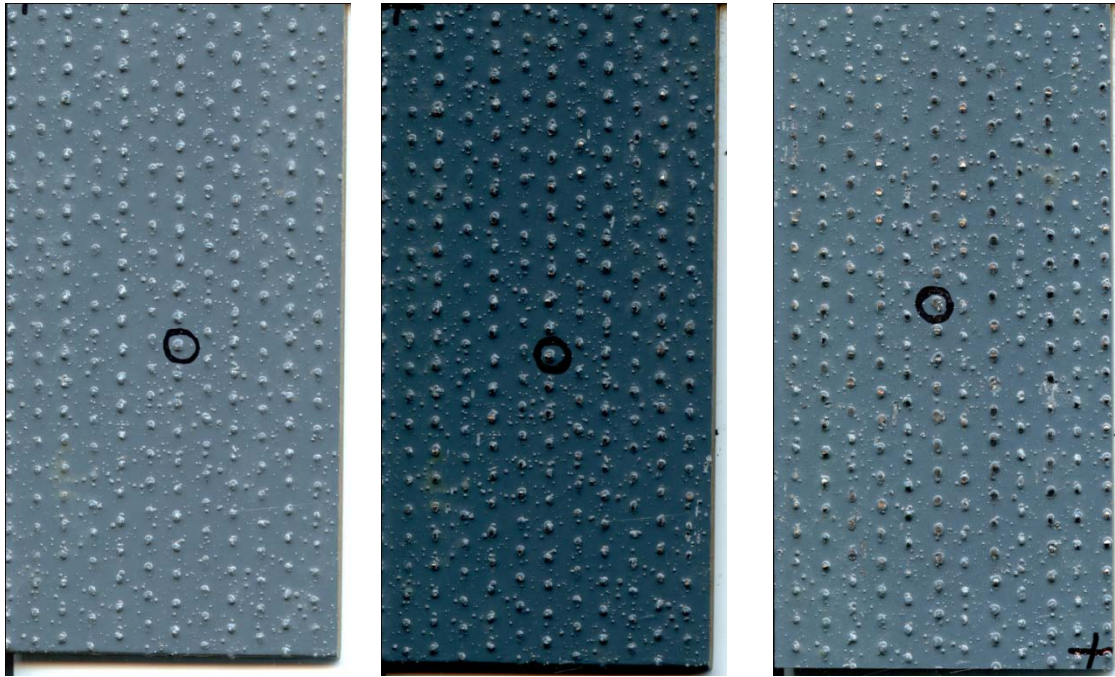
TNS A36: Pre-Wear, 50 Cycles of Wear



TNS A572: Pre-Wear, 50 Cycles of Wear, 500 Cycles of Wear



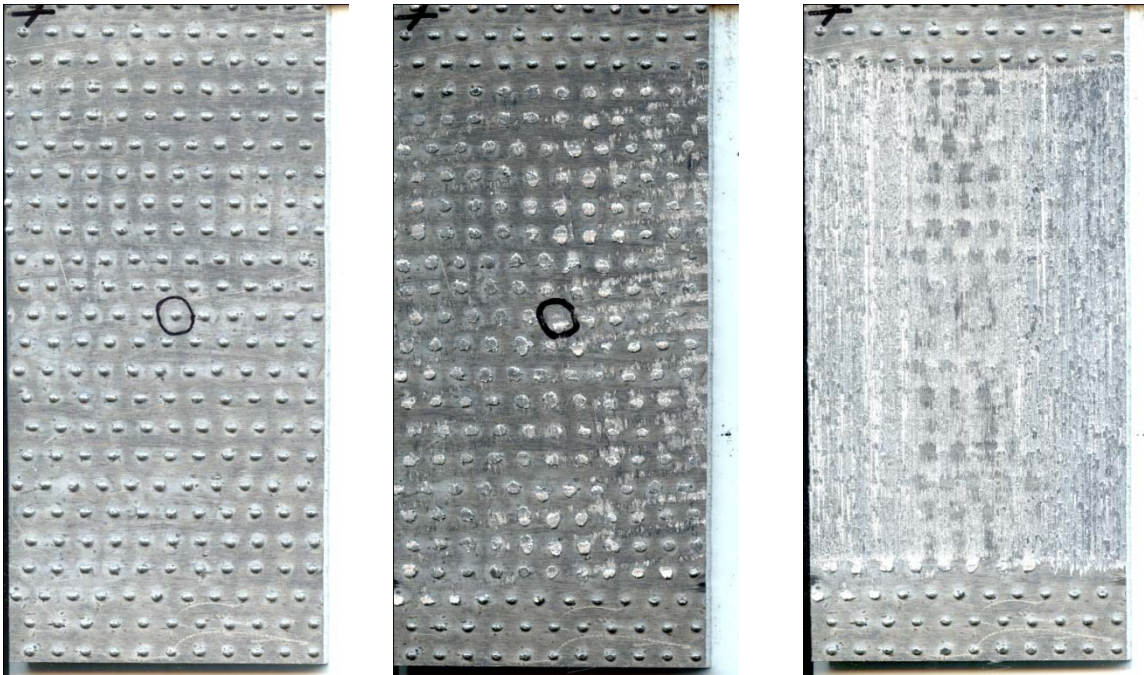
LDN A36: Pre-Wear, 50 Cycles of Wear, 500 Cycles of Wear



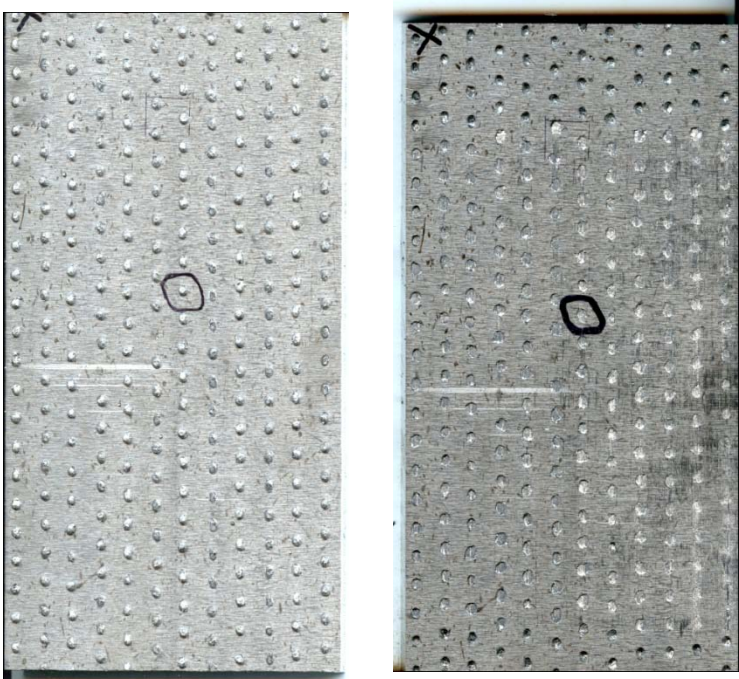
LDN A572: Pre-Wear, 50 Cycles of Wear, 500 Cycles of Wear



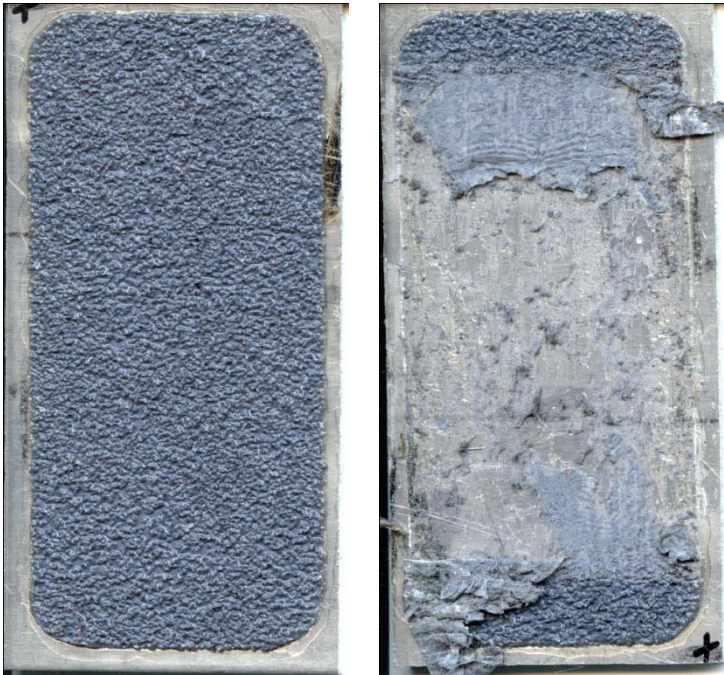
LDN 5086: Pre-Wear, 50 Cycles of Wear, 500 Cycles of Wear



LDN 5456: Pre-Wear, 50 Cycles of Wear



PNS 5456: Pre-Wear, 50 Cycles of Wear



Appendix 5: Wear Mass Loss Calculations and Data

Non-Skid Material Percent Mass Loss Calculation Data										
Material	*Area of Sample (cm ²)	Thickness of Base Metal (cm)	Volume of Base Metal (cm ³)	Density of Base Material (g/cm ³)	M1: Calculated Mass of Base Metal (g)	Pre-Wear Mass, 0 Cycles (g)	Mass of Non-Skid Material (g)	M2: Mass After 50 Cycles (g)	M3: Mass, 500 Cycles (g)	Non Skid % Mass Loss
TNS A36	110.66	0.635	70.27	7.85	552	610	59	607	605	3.25
PNS A36	114.19	0.635	72.51	7.85	569	604	35	N/A	N/A	N/A
LDN A36 (Painted)	115.05	0.635	73.06	7.85	573	583	9	583	583	1.09
TNS A572	112.40	0.635	71.37	7.85	560	628	68	626	624	2.45
PNS A572	113.39	0.635	72.00	7.85	565	616	51	608	N/A	N/A
LDN A572 (Painted)	112.00	0.635	71.12	7.85	558	608	50	607	606	1.86
PNS 5086	113.73	0.635	72.22	2.66	192	209	17	N/A	N/A	N/A
LDN 5086	107.11	0.635	68.01	2.66	181	184	3	183	182	56.44
PNS 5456	112.75	0.635	71.60	2.66	190	208	18	199	N/A	N/A
LDN 5456	114.19	0.635	72.51	2.66	193	201	8	200	**N/A	**N/A

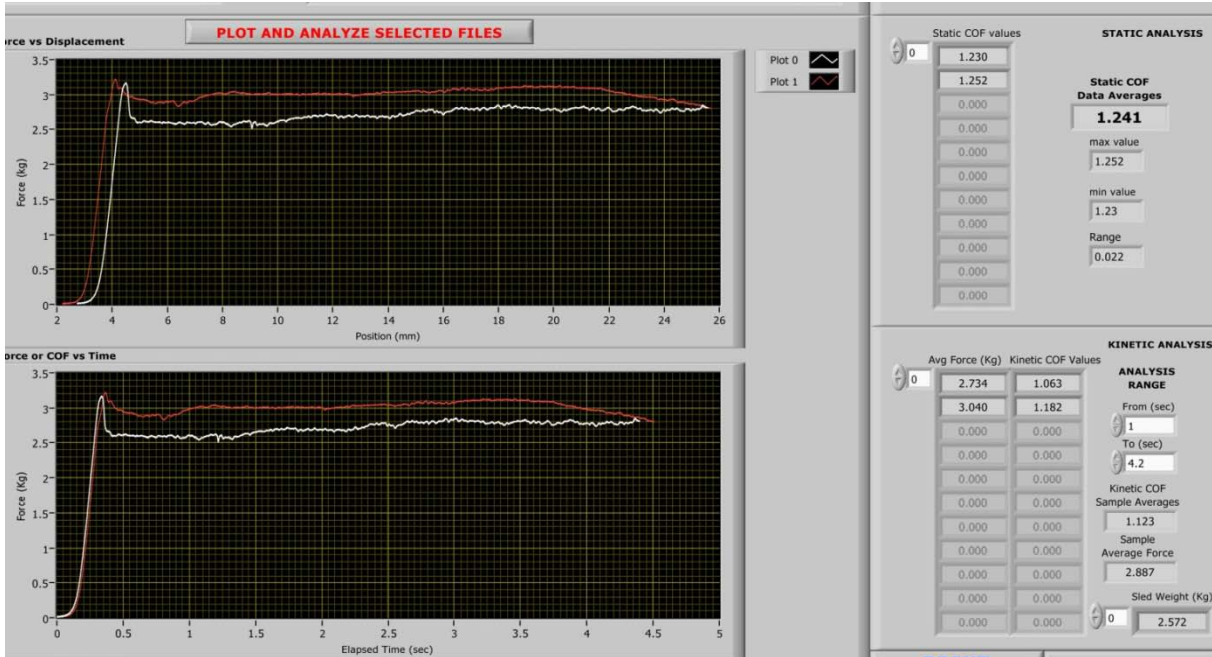
*Area - Imported into CAD to measure area of sample

PNS non-skid material was destroyed after 20-30 wear cycles and led to glue contamination on the drag sled. Further wear testing to 500 cycles was abandoned.

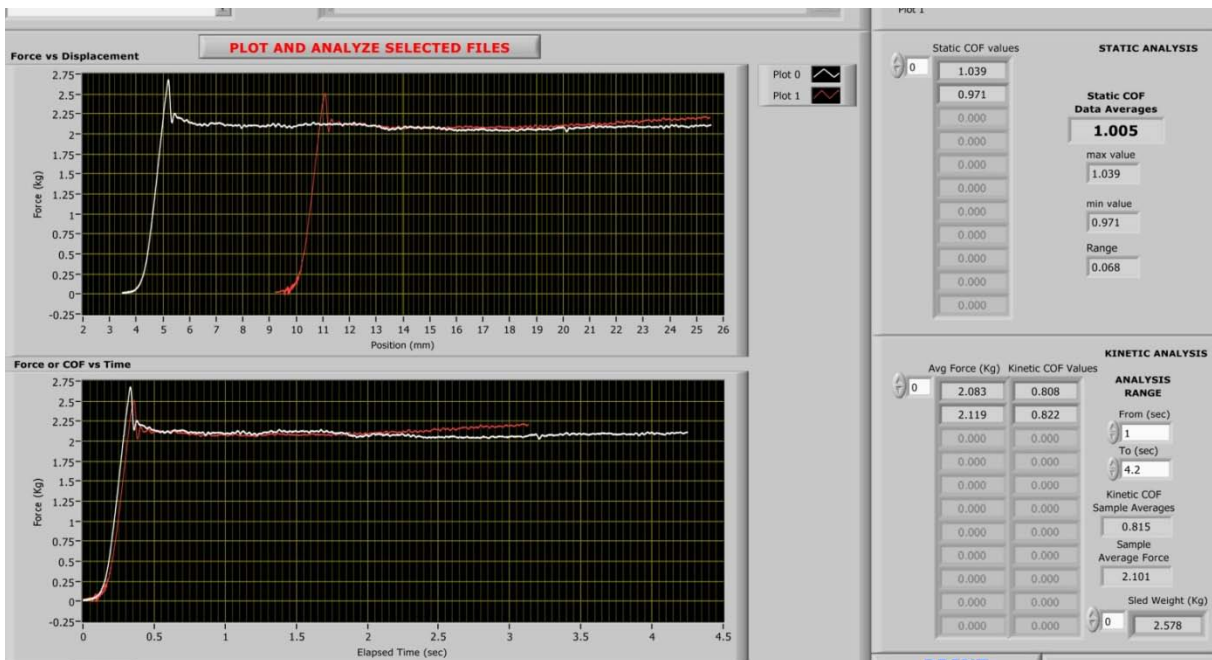
**The LDN 5086 aluminum surface was destroyed (gone) after 500 cycles. Further testing of the LDN 5456 was abandoned so

Appendix 6: Coefficient of Friction Measurements

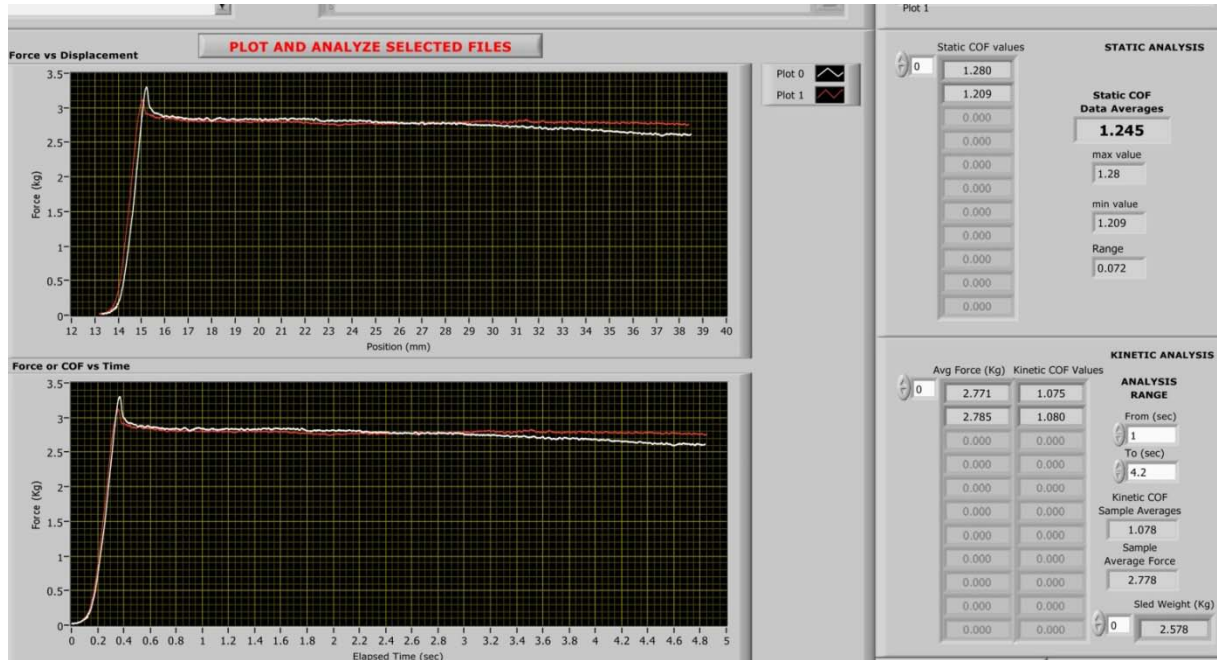
TNS A36: Dry COF, 50 Cycles



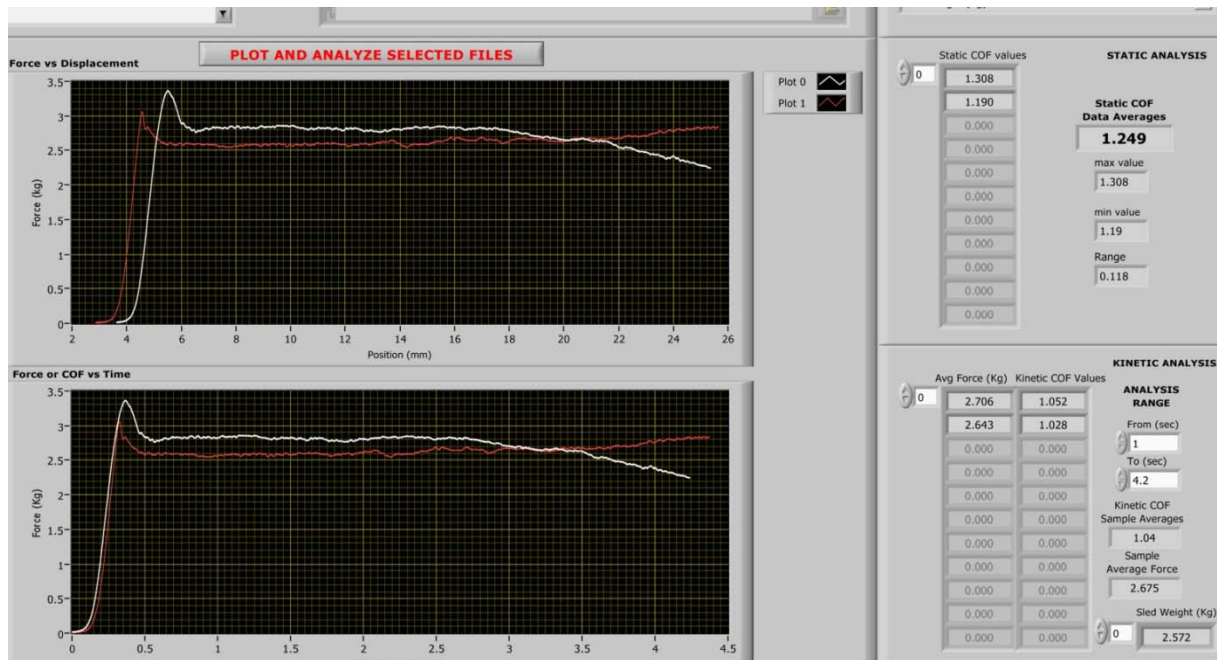
TNS A36: Dry COF, 500 Cycles



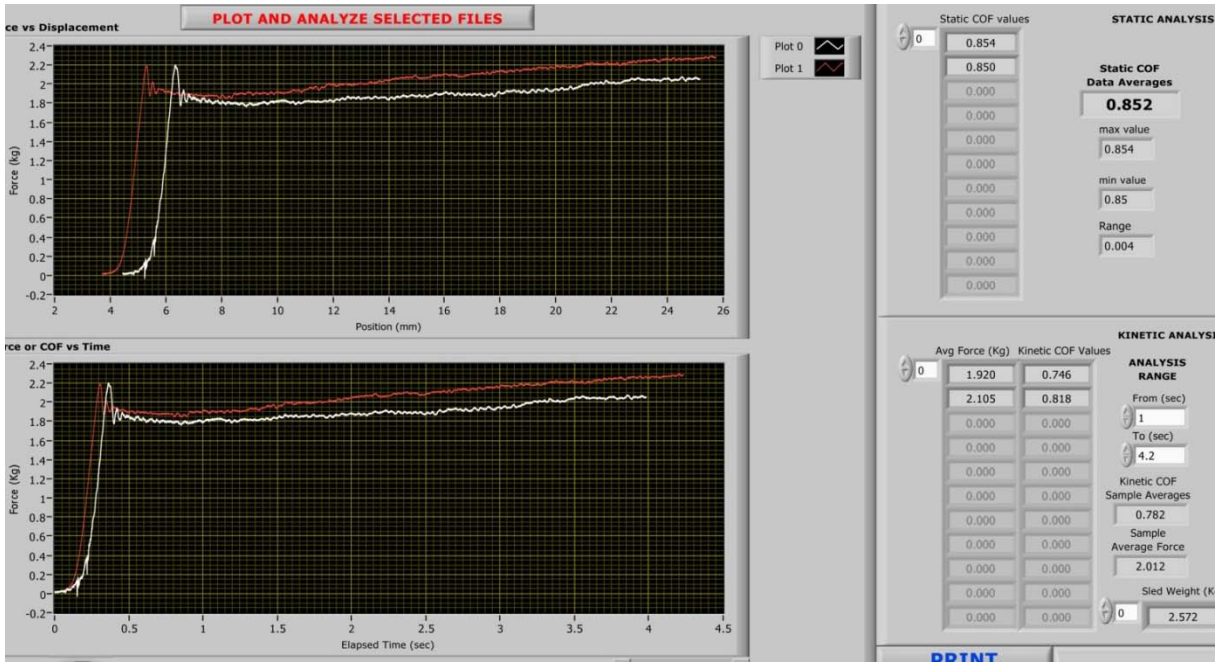
TNS A36: Wet COF, 500 Cycles



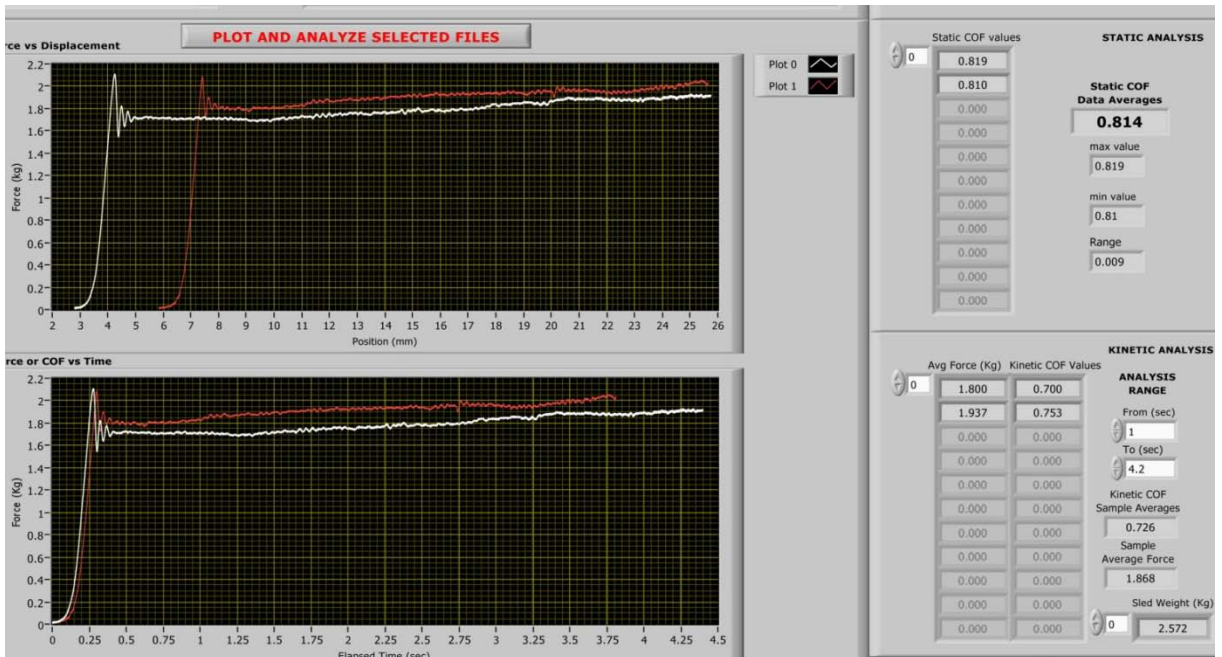
LDN A36: Dry COF, 50 Cycles



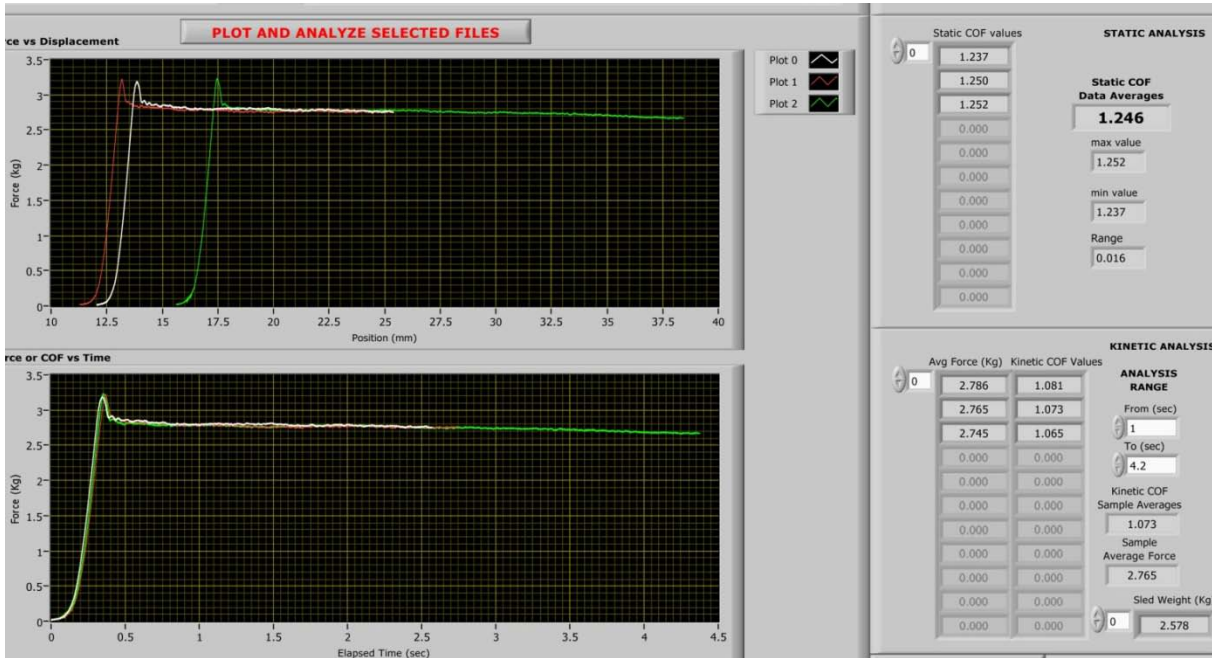
TNS A572: Dry COF, 50 Cycles



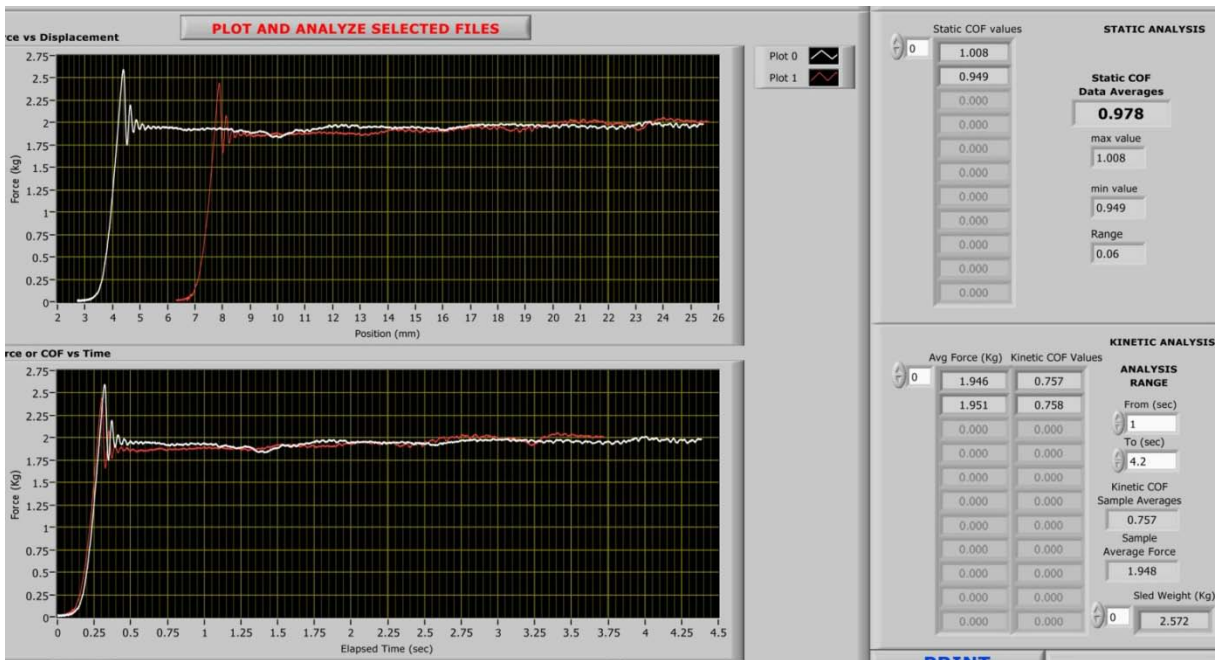
TNS A572: Dry COF, 500 Cycles



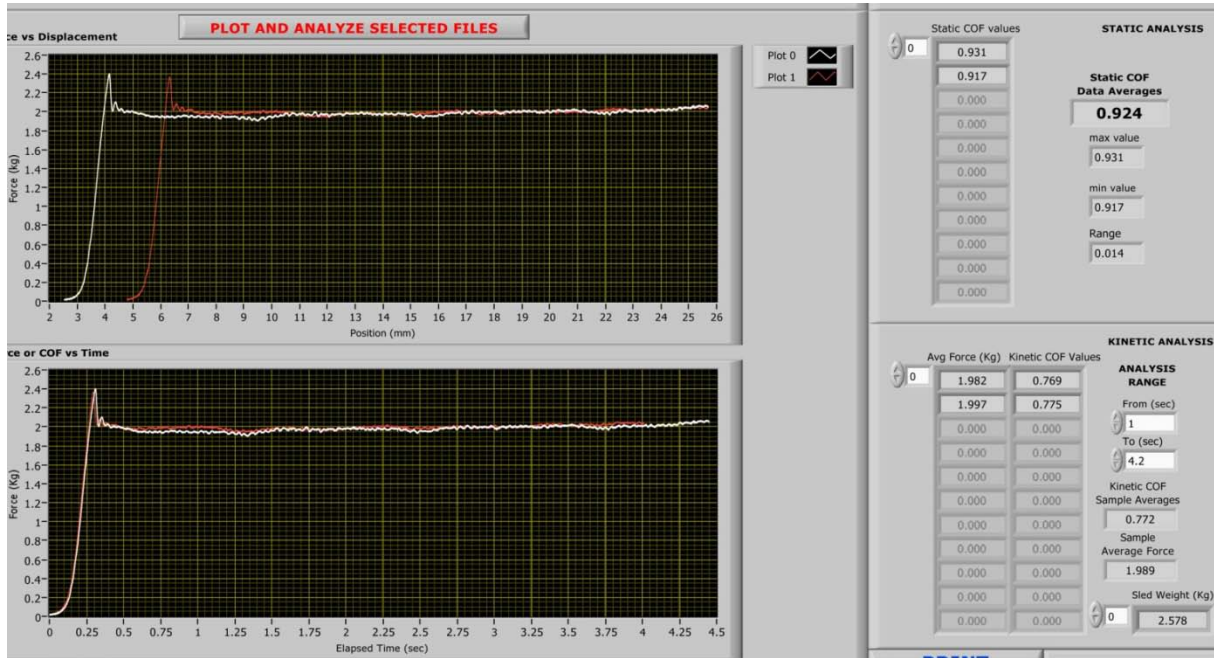
TNS A572: Wet COF, 500 Cycles



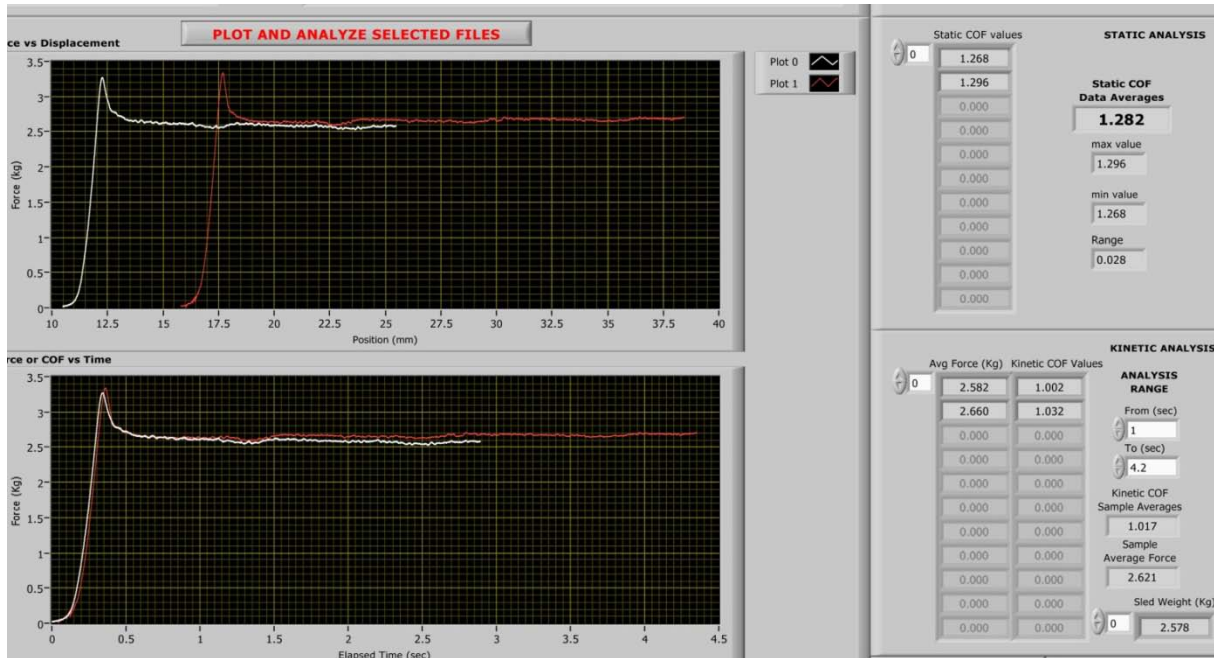
LDN A572: Dry COF, 50 Cycles



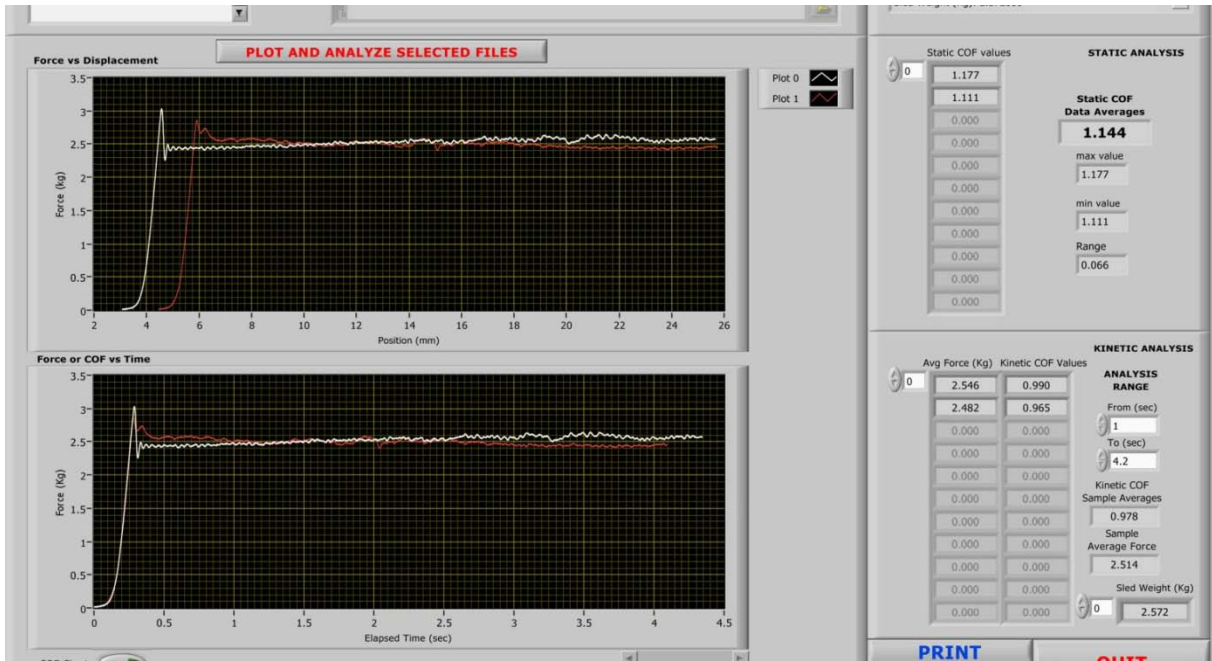
LDN A572: Dry COF, 500 Cycles



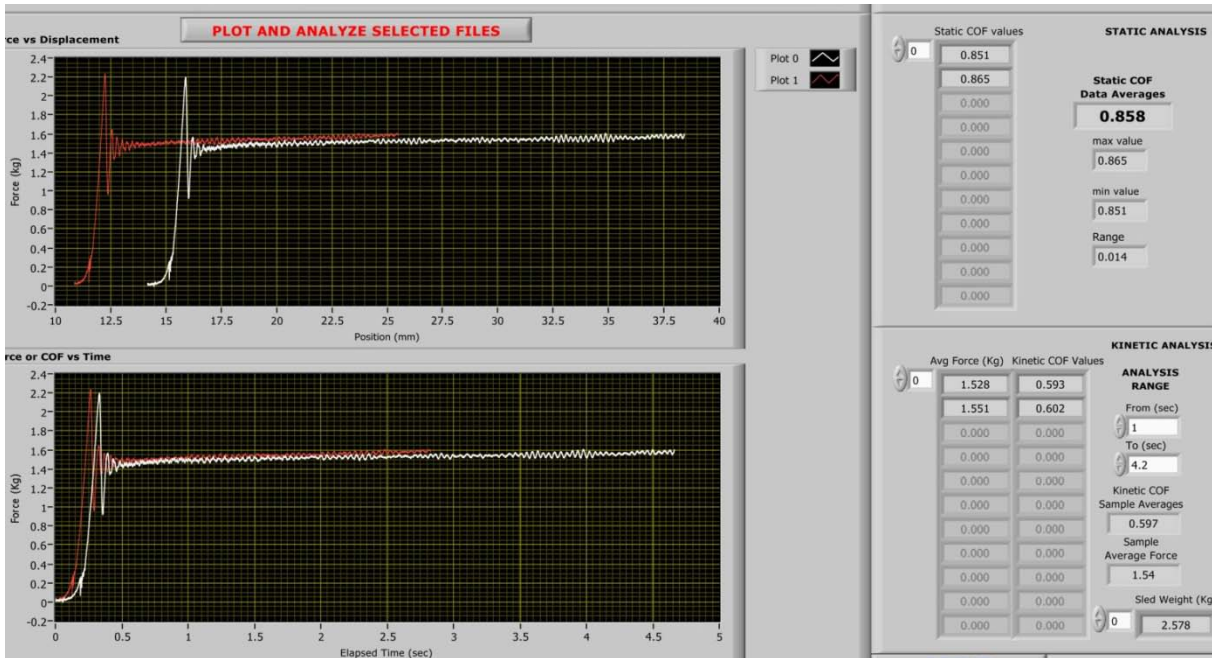
LDN A572: Wet COF, 500 Cycles



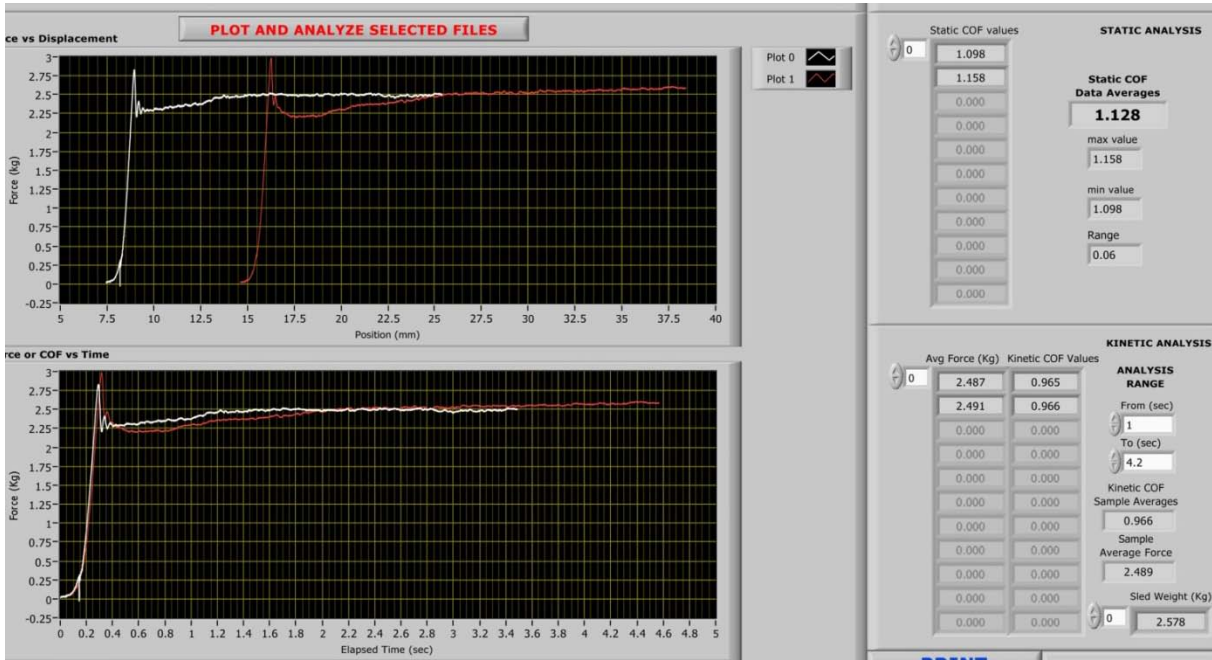
LDN 5086: Dry COF, 50 Cycles



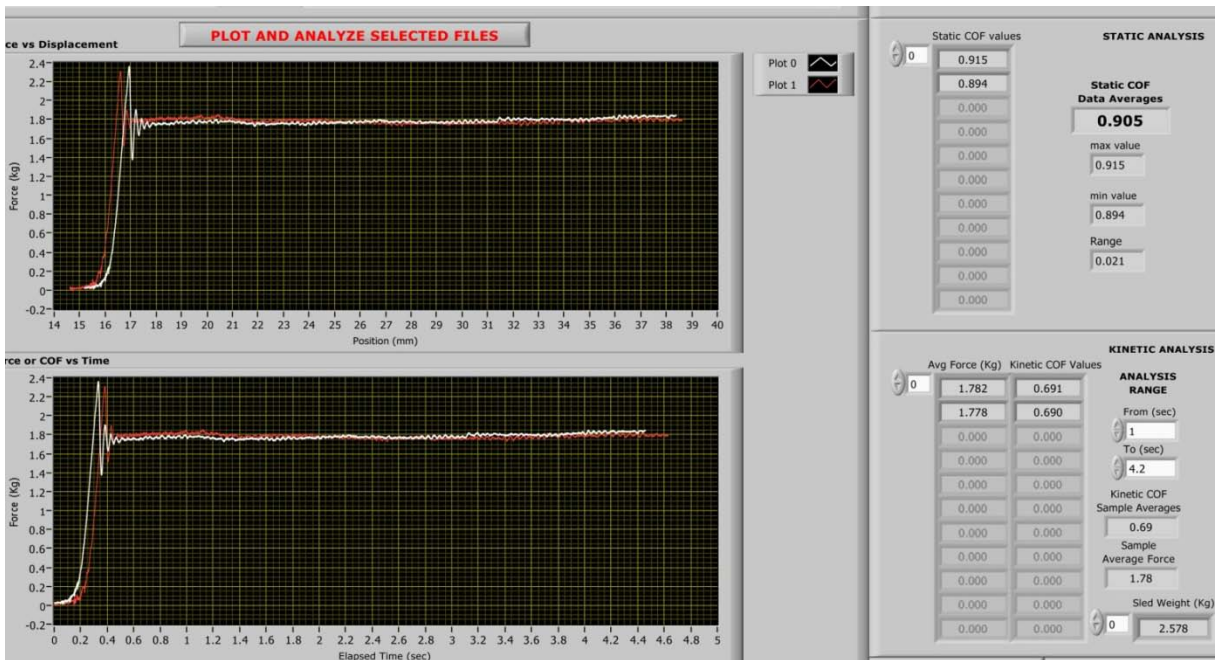
LDN 5086: Dry COF, 500 Cycles



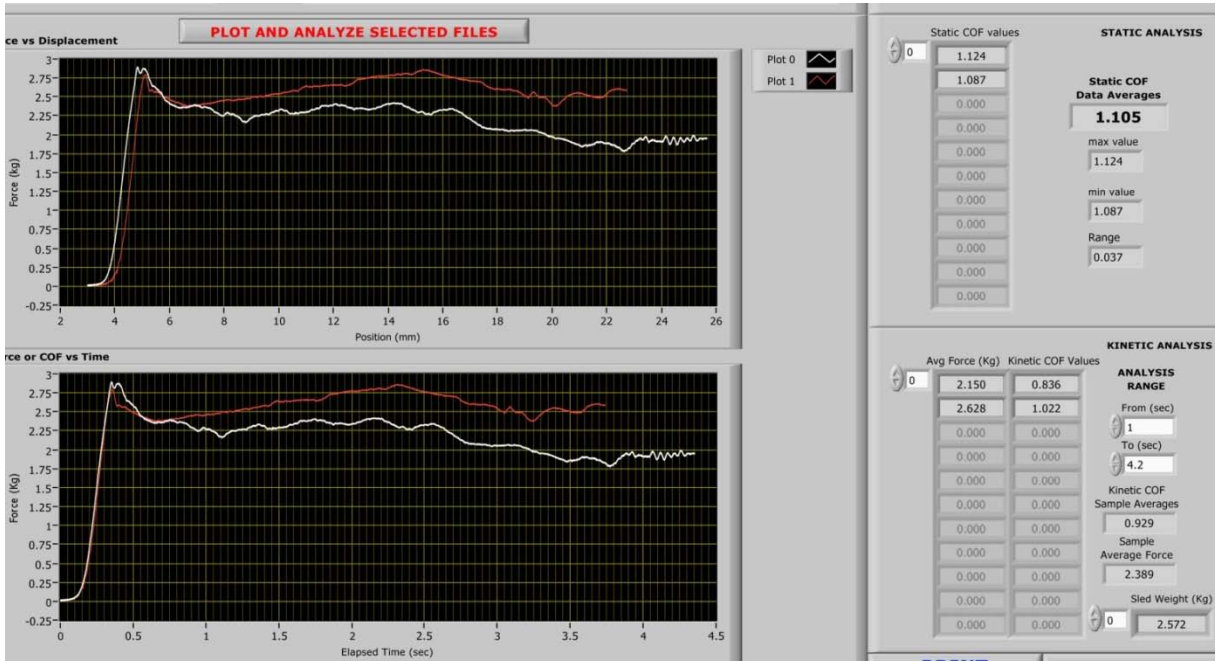
LDN 5086: Wet COF, 500 Cycles



LDN 5486: Dry COF, 50 Cycles



PNS 5456: Dry COF, 50 Cycles



Appendix 7: Surface Characterization Images

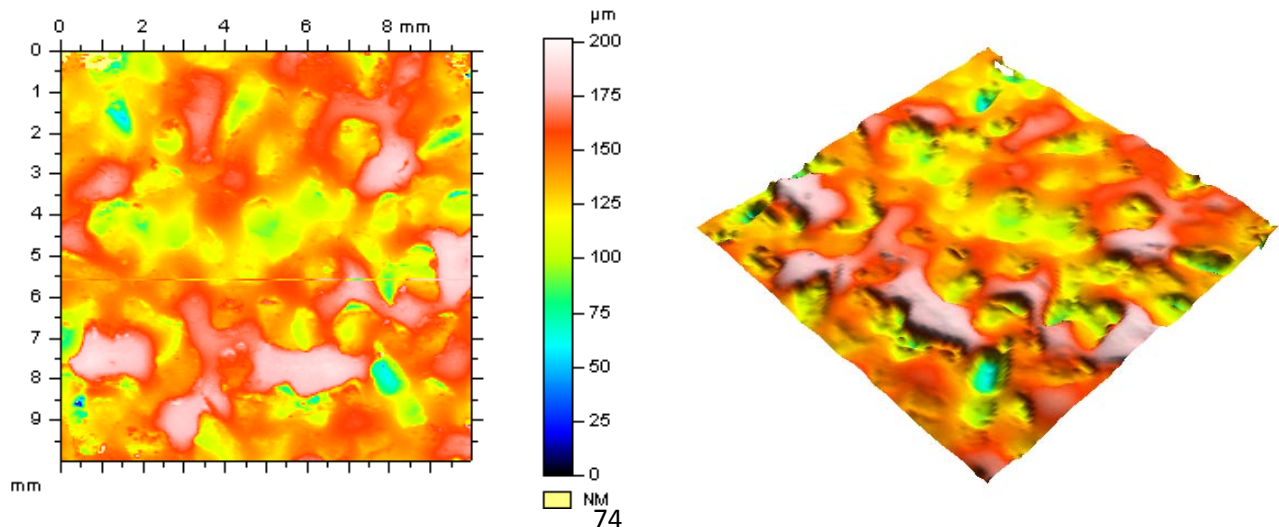
UBM

PNS Samples were measured on the UBM Scanning Laser Profiler and Triangulation Sensor.

Methodology:

- Fixed sample
- Unplug sensor, move the z-axis (sensor) up until the output reads “far” then move it until the sensor reads “low” and write down the value
- Marked the point on the sample with a permanent marker, set the origin
- In the x direction, entered 10 (mm), move, marked the point on the sample
- In the y direction, entered 10 (mm), move, marked the point on the sample
- In the x direction entered 0, and move
- Move back to the origin, but to account for backlash in the y direction, move to -5 and then to 0
 - The area of measurement was set for 10mm x 10mm
- Set the measurement parameters
 - Traverse 10 mm
 - Point, or Sampling Interval 10 μm
 - Speed 1 mm/second
 - Measure rate 100 points/second
- Save the file and start the measurement
- Import the files into MountainsMap™
 - Threshold the images to remove noise
 - Run a study – “Parameters Table” to output basic roughness parameters
- The measurement took approximately 3 ½ hours per sample

PNS A36:

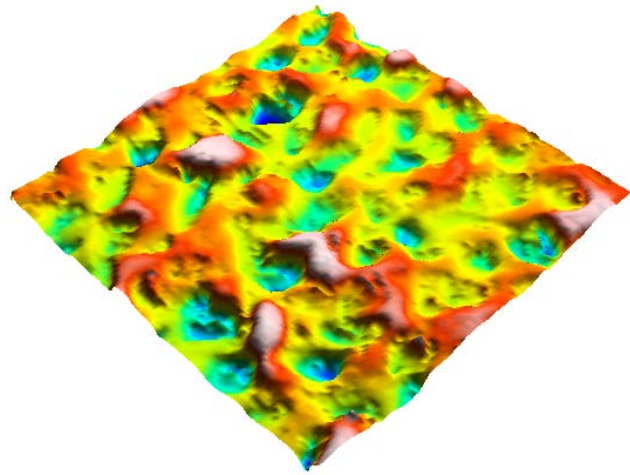
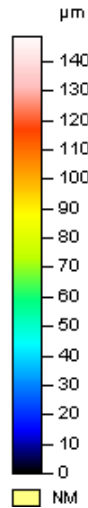
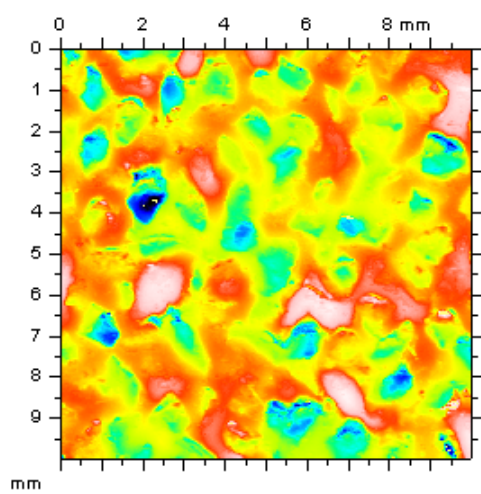


Height Parameters

Sq	22.1
Ssk	-0.282
Sku	3.32
Sp	59.5
Sv	142
Sz	202
Sa	17.4

μm	Root mean square height
	Skewness
	Kurtosis
μm	Maximum peak height
μm	Maximum pit height
μm	Maximum height
μm	Arithmetic mean height

PNS A572:

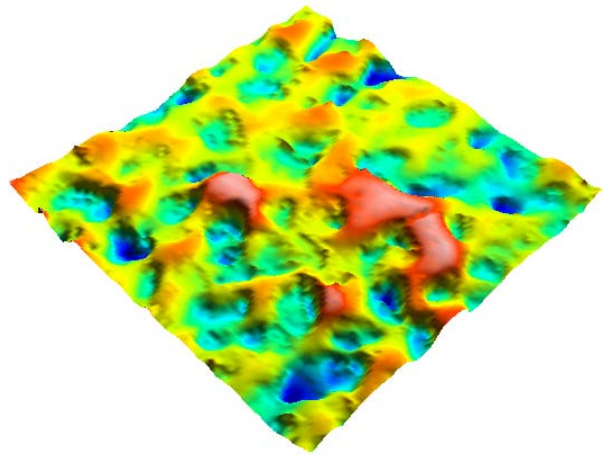
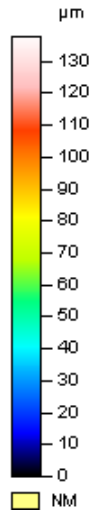
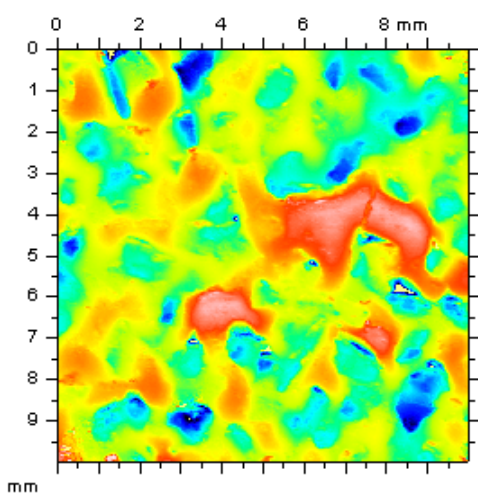


Height Parameters

Sq	22.3
Ssk	-0.373
Sku	3.47
Sp	56.9
Sv	91.6
Sz	149
Sa	17.3

μm	Root mean square height
	Skewness
	Kurtosis
μm	Maximum peak height
μm	Maximum pit height
μm	Maximum height
μm	Arithmetic mean height

PNS 5086:

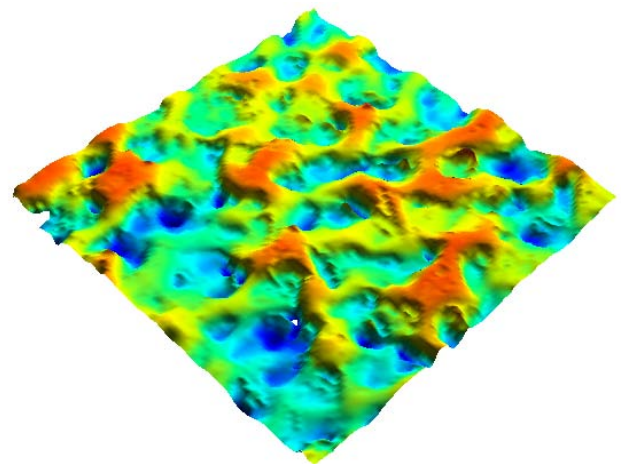
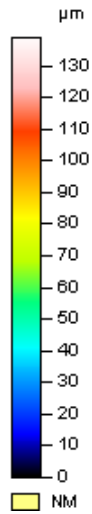
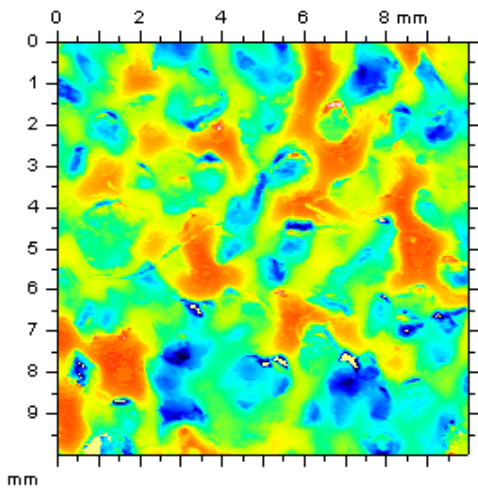


Height Parameters

Sq	21.6
Ssk	0.0314
Sku	2.48
Sp	74.8
Sv	64.1
Sz	139
Sa	17.6

- μm Root mean square height
- Skewness
- Kurtosis
- μm Maximum peak height
- μm Maximum pit height
- μm Maximum height
- μm Arithmetic mean height

PNS 5456:



Height Parameters

Sq	21.6
Ssk	0.0314
Sku	2.48
Sp	74.8
Sv	64.1
Sz	139
Sa	17.6

- μm Root mean square height
- Skewness
- Kurtosis
- μm Maximum peak height
- μm Maximum pit height
- μm Maximum height
- μm Arithmetic mean height

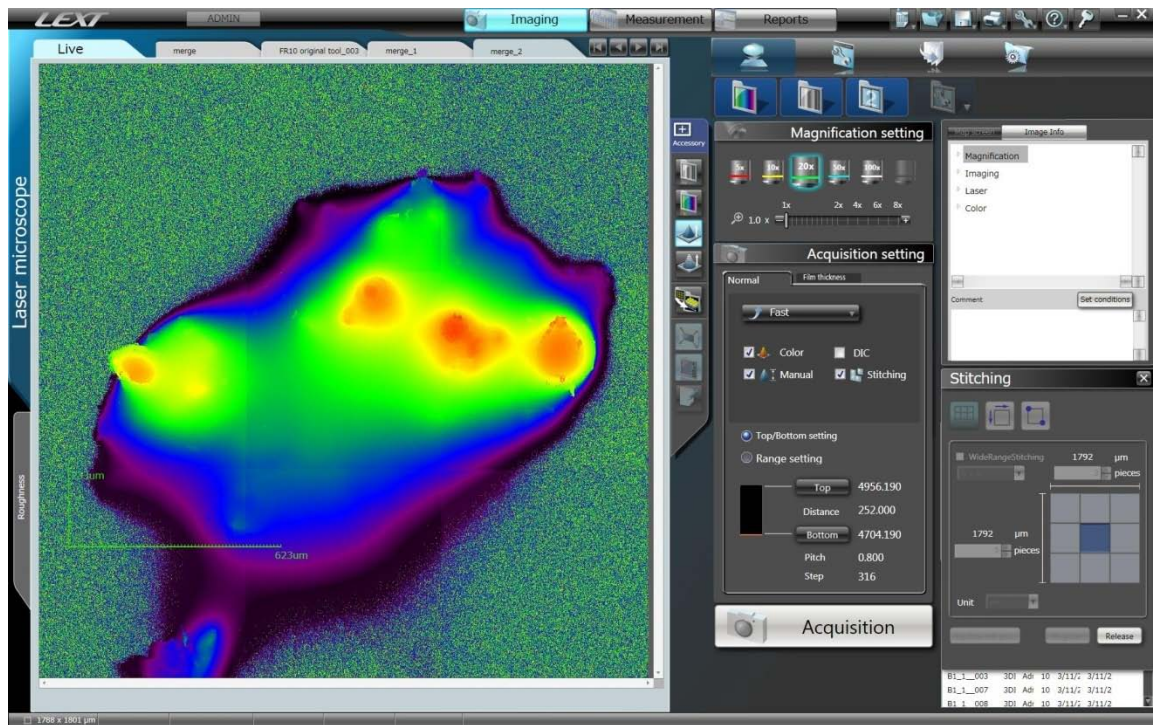
Olympus 4000 Confocal Microscope

TNS and LDN Samples were measured with the LEXT Olympus 3D Measuring Laser Microscope OLS4000 before and after the wear testing. A peak of the each TNS sample and a bump on each LDN sample was selected for measurement.

Methodology:

- Identified a high point on each sample for measurement and circled the area on the sample with a permanent marker
- Placed sample on the stage and moved it to the origin
- Centered the “bump” under the light with the joystick
- Using the 5X lens, focused on the “bump” and took a picture
- Switched to the 20X lens and focused on the sample
- Enabled stitching and selected 3 x 3 stitching pattern centered around the “bump”
- Changed to laser setting, adjusted brightness
- Set the bottom by using the fine adjustment to scroll down, adjusting intensity as needed
- Set the top in the same manner
- Checked each square of the stitching pattern to ensure the top and bottom were selected correctly
- Set the acquisition to fast and ensured stitching was enabled
- Data acquisition took approximately 1 hour per sample
- The file was saved, screenshots were taken and then the files were imported into MountainMaps and Sfrax for data acquisition and analysis

Screenshot of LDN A572 Measurement Acquisition:



Data Acquisition and Analysis

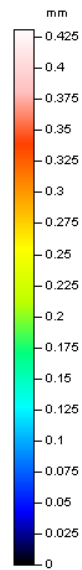
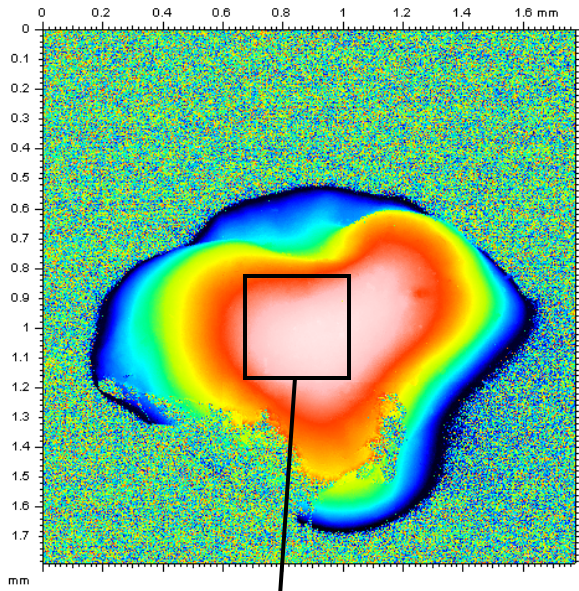
Methodology:

- Open .sur file in MountainsMap (all pre-wear and post wear files)
- Use thresholding operator to find the highest spot on the “bump”
- Run a study – “Parameters Table” to output basic roughness parameters
 - Create table of basic parameters
- Using the zoom operator, zoom in on the high spot in an area of 0.5 mm x 0.5 mm
- Run a study – “Parameters Table” to output basic roughness parameters
 - Create table of basic parameters
- Save all images

- Import the zoomed images into Sfrax
 - Create Zoom PreWear Group (unfiltered)
 - Create Zoom PreWear Group (with 80° slope filter)
 - Create Zoom PostWear Group (unfiltered)
 - Create Zoom PostWear Group (filtered)
- Run analysis for Area-scale for both groups, using the method “4 corners and full overlap”
- Create log-log results plot of Area-scale for pre wear and post wear
 - Change title
 - Label samples in legend
 - Turn on regression line
- Ran an F-Test analysis comparing pre-wear and post wear samples
 - Used Area-scale results
 - Examined relative area
 - Created plots for 90%, 95%, and 99% confidence levels
- Ran analysis for variable correlation
 - Created surface properties
 - Entered COF measurements and percent mass loss data
 - Ran linear regression analysis to correlate:
 - Relative area and friction
 - Relative area and percent mass loss
 - Created and saved plots of functional variable correlations

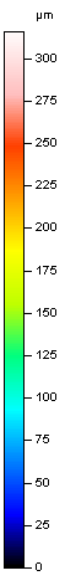
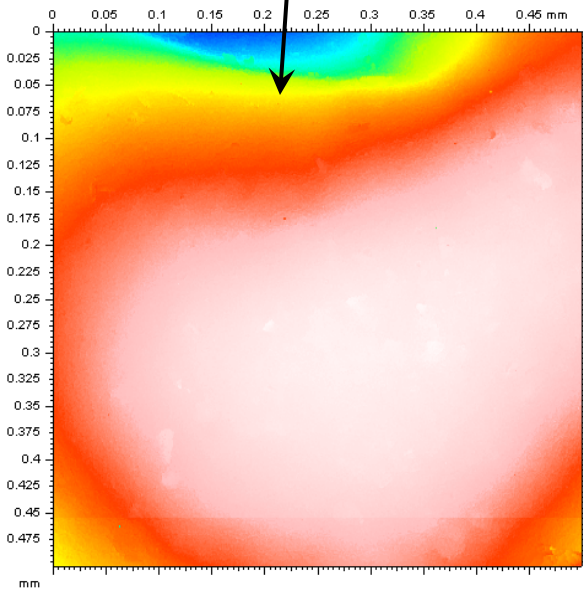
TNS A36: The working file was not saved properly and the data was lost for this sample.

TNS A572: Pre-Wear



Height Parameters

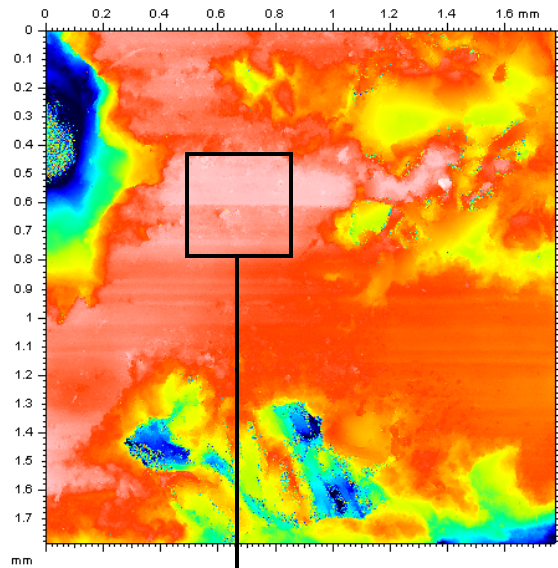
Sq	0.106	mm	Root mean square height
Ssk	0.264		Skewness
Sku	2.05		Kurtosis
Sp	0.239	mm	Maximum peak height
Sv	0.193	mm	Maximum pit height
Sz	0.431	mm	Maximum height
Sa	0.0894	mm	Arithmetic mean height



Height Parameters

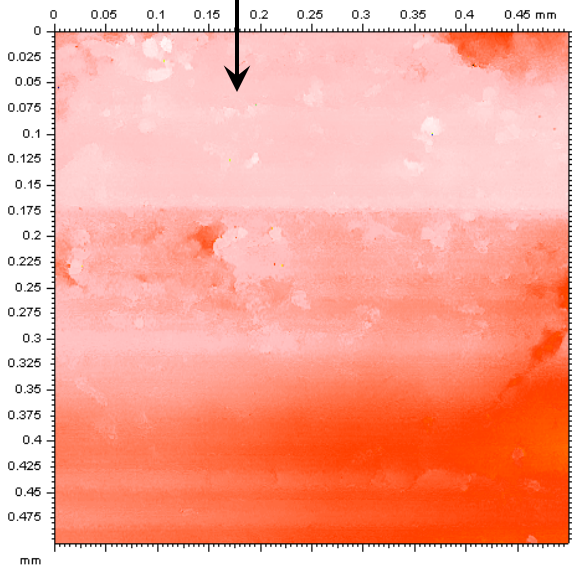
Sq	49.4	μm	Root mean square height
Ssk	-1.85		Skewness
Sku	6.57		Kurtosis
Sp	54.2	μm	Maximum peak height
Sv	262	μm	Maximum pit height
Sz	316	μm	Maximum height
Sa	35.8	μm	Arithmetic mean height

TNS A572: Post Wear



Height Parameters

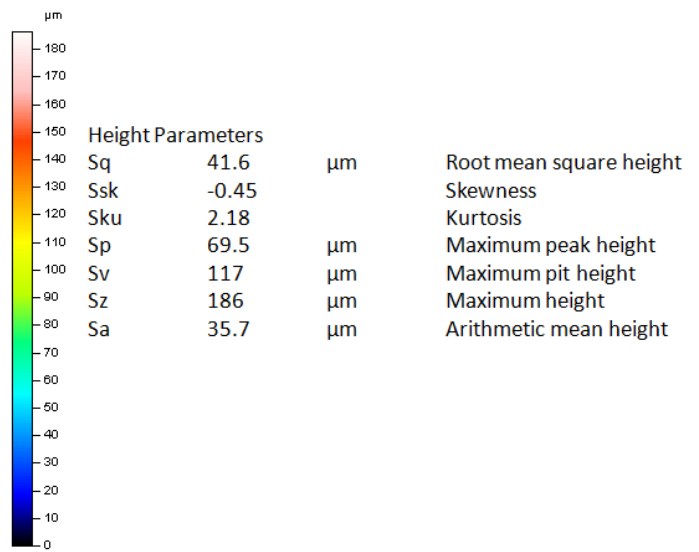
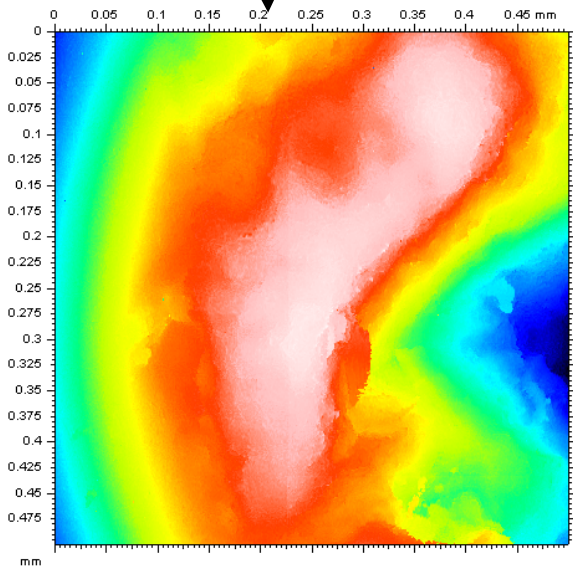
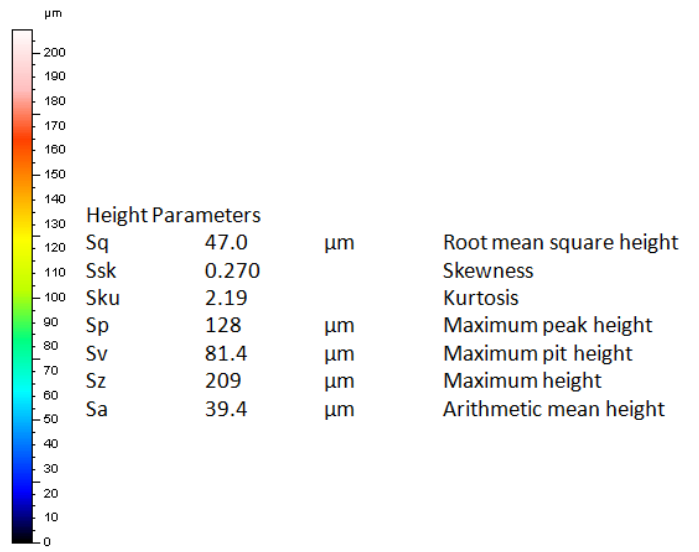
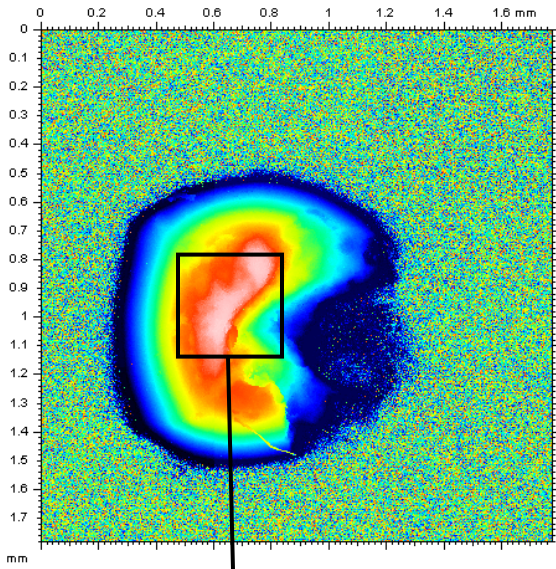
Sq	38.2	μm	Root mean square height
Ssk	-1.85		Skewness
Sku	6.41		Kurtosis
Sp	65.4	μm	Maximum peak height
Sv	152	μm	Maximum pit height
Sz	218	μm	Maximum height
Sa	27.5	μm	Arithmetic mean height



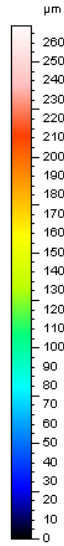
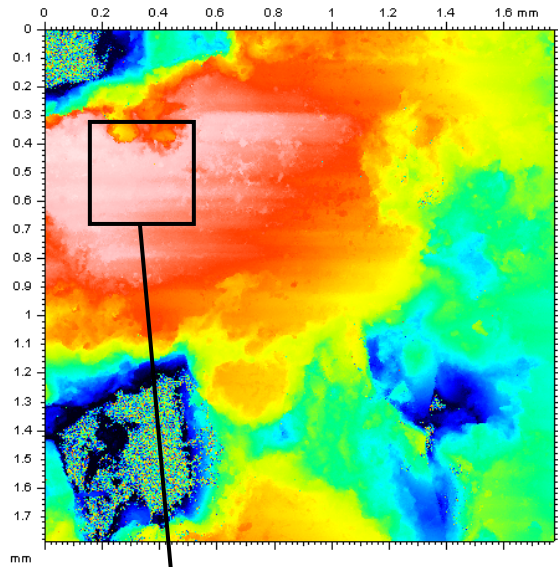
Height Parameters

Sq	7.30	μm	Root mean square height
Ssk	-0.465		Skewness
Sku	4.35		Kurtosis
Sp	22.8	μm	Maximum peak height
Sv	146	μm	Maximum pit height
Sz	168	μm	Maximum height
Sa	6.07	μm	Arithmetic mean height

LDN A36: Pre-Wear

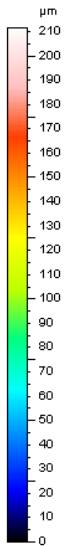
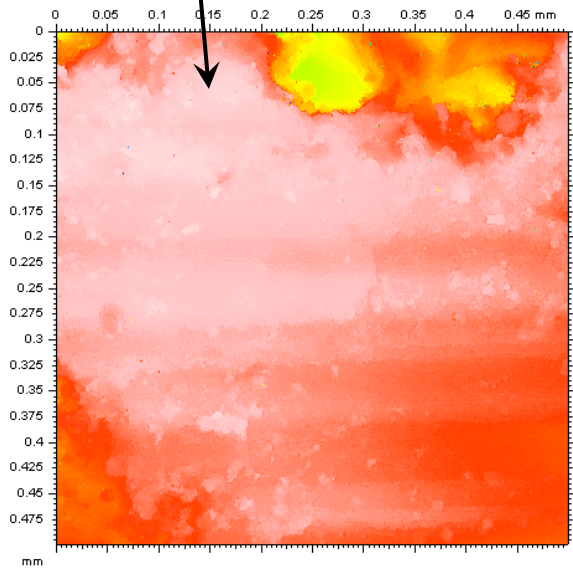


LDN A36: Post Wear



Height Parameters

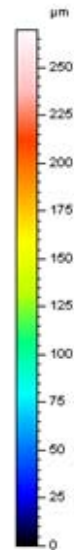
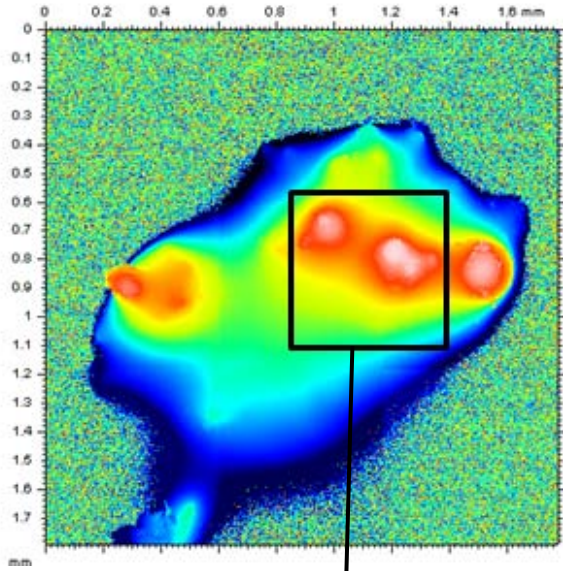
Sq	62.3	μm	Root mean square height
Ssk	-0.257		Skewness
Sku	2.24		Kurtosis
Sp	124	μm	Maximum peak height
Sv	145	μm	Maximum pit height
Sz	269	μm	Maximum height
Sa	52.7	μm	Arithmetic mean height



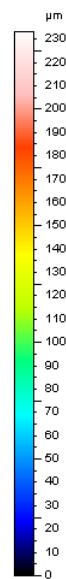
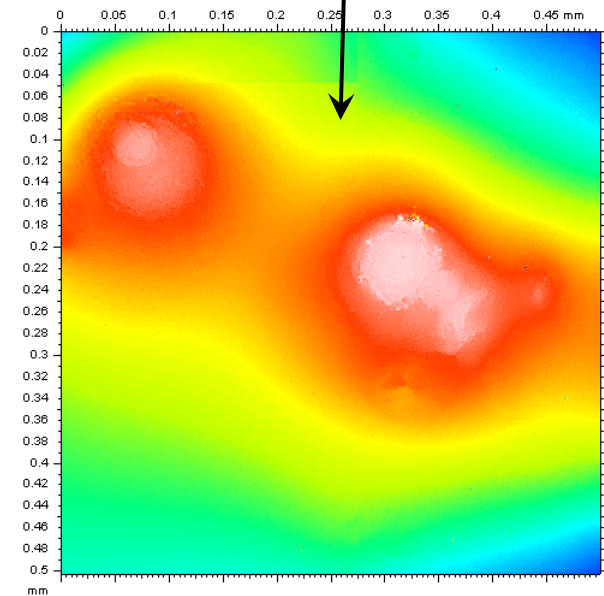
Height Parameters

Sq	14.3	μm	Root mean square height
Ssk	-1.92		Skewness
Sku	8.42		Kurtosis
Sp	33.4	μm	Maximum peak height
Sv	178	μm	Maximum pit height
Sz	212	μm	Maximum height
Sa	10.2	μm	Arithmetic mean height

LDN A572: Pre-Wear

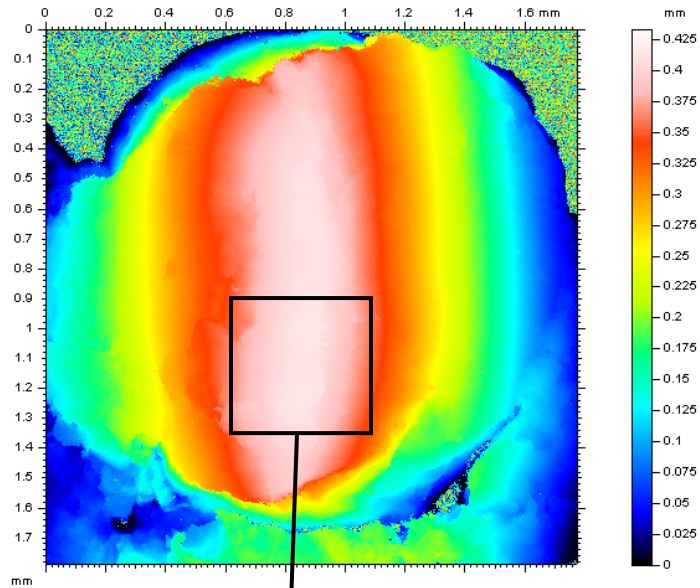


Height Parameters			
Sq	58.7	μm	Root mean square height
Ssk	0.328		Skewness
Sku	2.26		Kurtosis
Sp	169	μm	Maximum peak height
Sv	101	μm	Maximum pit height
Sz	270	μm	Maximum height
Sa	48.9	μm	Arithmetic mean height



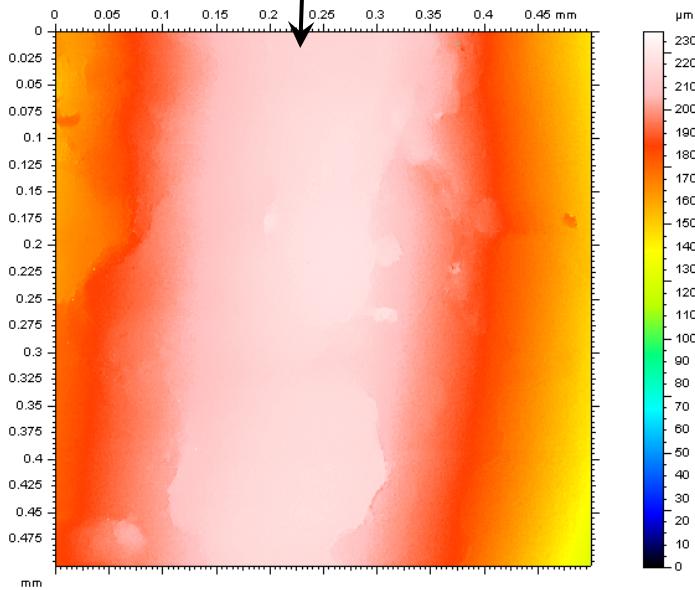
Height Parameters			
Sq	39.3	μm	Root mean square height
Ssk	-0.0297		Skewness
Sku	2.09		Kurtosis
Sp	100	μm	Maximum peak height
Sv	133	μm	Maximum pit height
Sz	233	μm	Maximum height
Sa	33.5	μm	Arithmetic mean height

LDN A572: Post Wear



Height Parameters

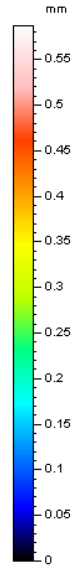
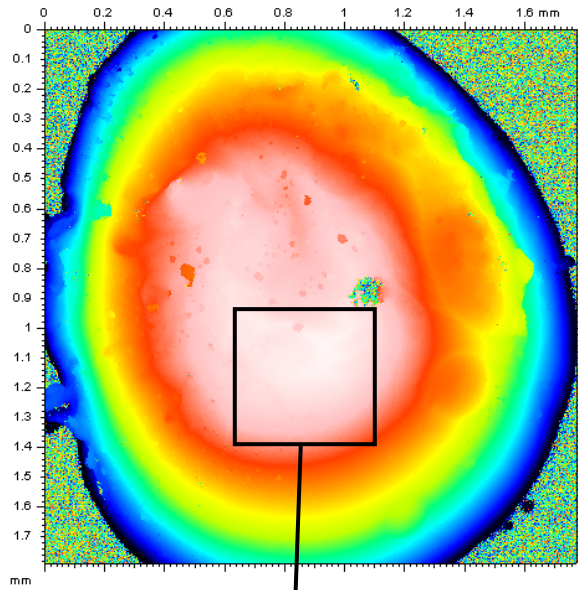
Sq	0.117	mm	Root mean square height
Ssk	0.000124		Skewness
Sku	1.74		Kurtosis
Sp	0.205	mm	Maximum peak height
Sv	0.227	mm	Maximum pit height
Sz	0.433	mm	Maximum height
Sa	0.103	mm	Arithmetic mean height



Height Parameters

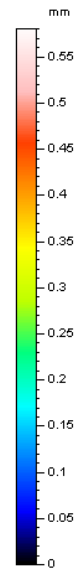
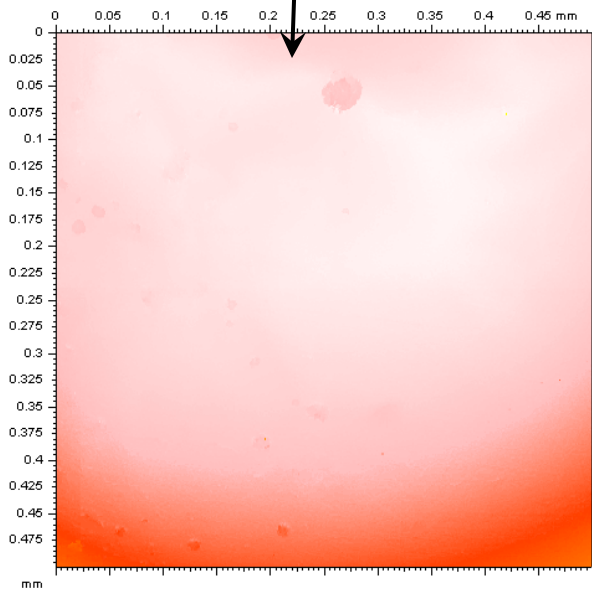
Sq	21.5	μm	Root mean square height
Ssk	-0.616		Skewness
Sku	2.38		Kurtosis
Sp	38.6	μm	Maximum peak height
Sv	196	μm	Maximum pit height
Sz	234	μm	Maximum height
Sa	18.2	μm	Arithmetic mean height

LDN 5086: Pre-Wear



Height Parameters

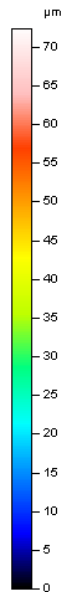
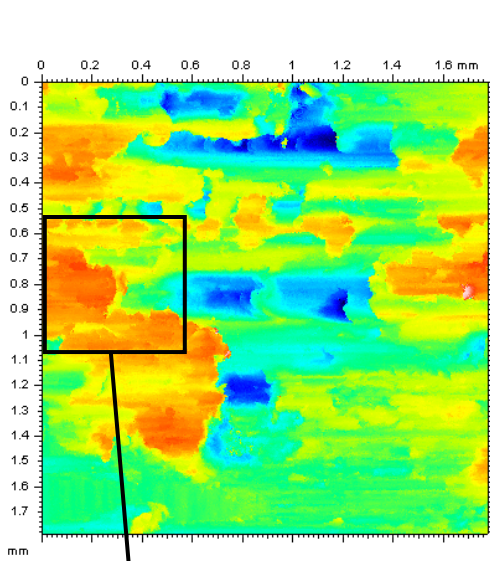
Sq	0.158	mm	Root mean square height
Ssk	-0.36		Skewness
Sku	1.99		Kurtosis
Sp	0.250	mm	Maximum peak height
Sv	0.337	mm	Maximum pit height
Sz	0.587	mm	Maximum height
Sa	0.136	mm	Arithmetic mean height



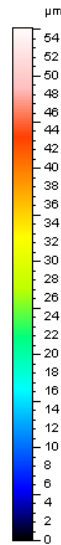
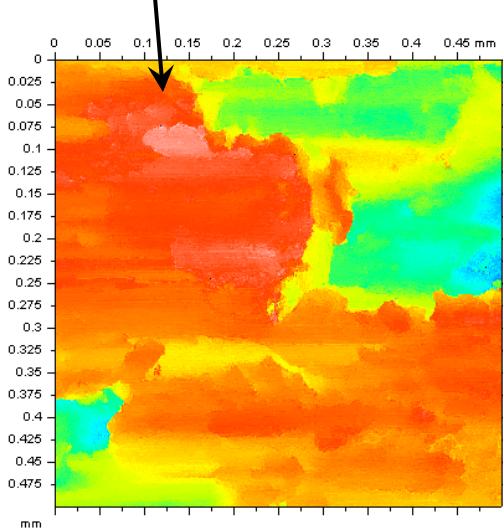
Height Parameters

Sq	0.0305	mm	Root mean square height
Ssk	-1.04		Skewness
Sku	3.42		Kurtosis
Sp	0.0458	mm	Maximum peak height
Sv	0.535	mm	Maximum pit height
Sz	0.581	mm	Maximum height
Sa	0.0248	mm	Arithmetic mean height

LDN 5086: Post Wear (500 cycles)

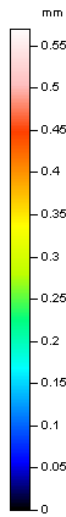
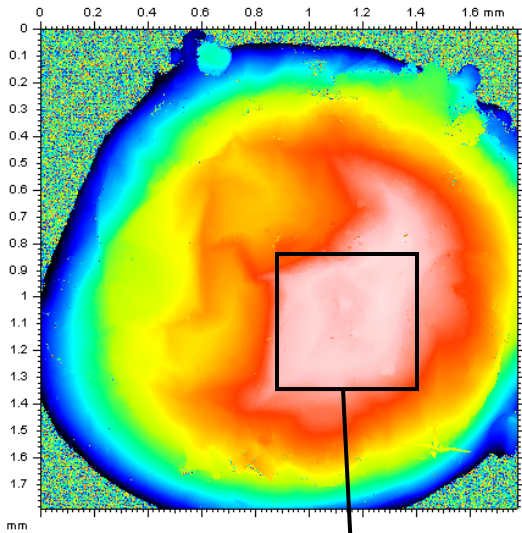


Height Parameters				
Sq	9.97	μm	Root mean square height	
Ssk	-0.0478		Skewness	
Sku	2.79		Kurtosis	
Sp	38.0	μm	Maximum peak height	
Sv	34.3	μm	Maximum pit height	
Sz	72.4	μm	Maximum height	
Sa	7.93	μm	Arithmetic mean height	



Height Parameters				
Sq	7.75	μm	Root mean square height	
Ssk	-0.88		Skewness	
Sku	2.63		Kurtosis	
Sp	19.3	μm	Maximum peak height	
Sv	35.8	μm	Maximum pit height	
Sz	55.1	μm	Maximum height	
Sa	6.47	μm	Arithmetic mean height	

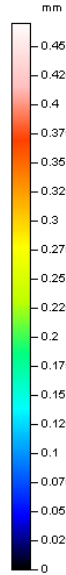
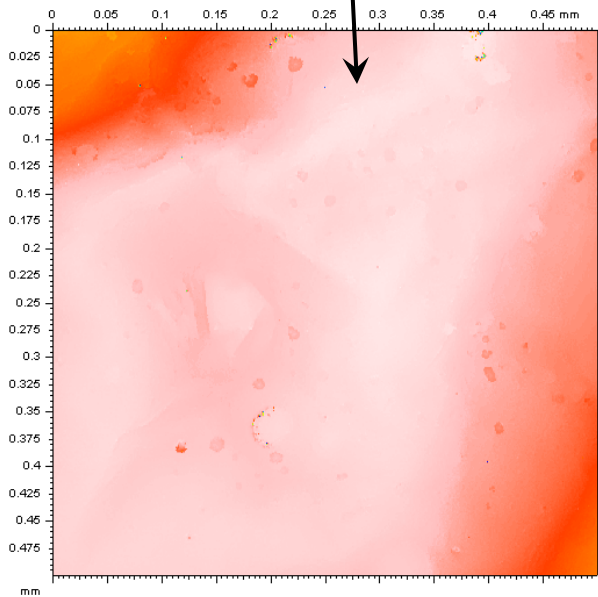
LDN 5456: Pre-Wear



Height Parameters

Sq	0.140	mm
Ssk	-0.344	
Sku	2.10	
Sp	0.260	mm
Sv	0.310	mm
Sz	0.570	mm
Sa	0.119	mm

Root mean square height
 Skewness
 Kurtosis
 Maximum peak height
 Maximum pit height
 Maximum height
 Arithmetic mean height

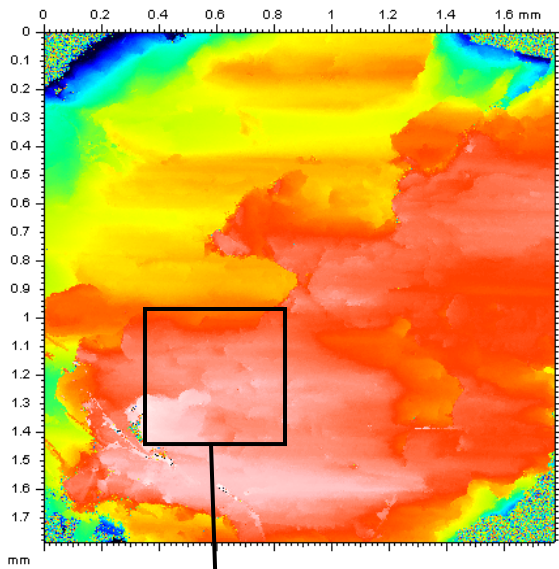


Height Parameters

Sq	0.0229	mm
Ssk	-1.79	
Sku	9.16	
Sp	0.0483	mm
Sv	0.421	mm
Sz	0.470	mm
Sa	0.0171	mm

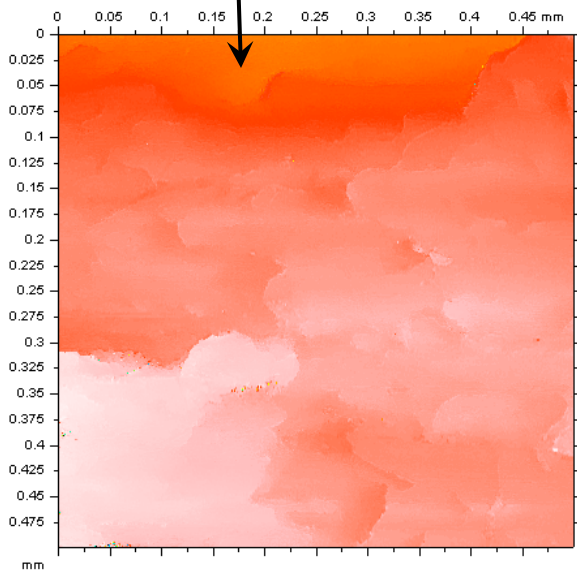
Root mean square height
 Skewness
 Kurtosis
 Maximum peak height
 Maximum pit height
 Maximum height
 Arithmetic mean height

LDN 5456: Post Wear (50 cycles)



Height Parameters

Sq	45.5	μm	Root mean square height
Ssk	-1.35		Skewness
Sku	4.90		Kurtosis
Sp	82.5	μm	Maximum peak height
Sv	191	μm	Maximum pit height
Sz	273	μm	Maximum height
Sa	35.8	μm	Arithmetic mean height



Height Parameters

Sq	12.7	μm	Root mean square height
Ssk	-0.577		Skewness
Sku	6.41		Kurtosis
Sp	41.7	μm	Maximum peak height
Sv	231	μm	Maximum pit height
Sz	273	μm	Maximum height
Sa	8.93	μm	Arithmetic mean height

Appendix 8: Cost Analysis Data

Traditional Non-Skid

From: C.G. Edwards & Co. Inc. website:

<http://www.cgedwards.com/ameron/uscg.html>

- Amercoat 138HR, Heavy Duty Epoxy Non-Skid Coating
 - 5 gal kit: \$329.95
 - Covers 150 ft²
 - \$2.20 per square foot

- Amercoat 137 Primer, Epoxy Primer for Non-Skid
 - 5 gal kit: \$269.95
 - Covers 1075 ft² per gallon at 1 mil thickness
 - Assume a 4 mil coat (2-6 mils recommended)
 - Covers 268 ft² per gallon at 4 mil thickness
 - \$1.00 per square foot

Total cost of material: \$3.20 per square foot

Peel and Stick Non-Skid (3M Safety Walk 700 Series, 770 Gray)

From: PowerPoint by Dave Zilber at 3M and the Louisiana Association for the Blind website:

<http://www.lablind.com/ttstore/prod.asp?itemtype=18>

- 41' UTB Kit
 - \$2,281.49
 - Covers approximately 305 ft²
 - \$7.48 per square foot

- Uncut sheets of 3M SafetyWalk material
 - \$4.50 per square foot

Laser Deposited Non-Skid

From: Barry Appolin with the U. S. Coast Guard and Andy Jones at Ross Technology

- 41' UTB Prototyped with Aluminum LDN
 - Actual cost of \$2,495
 - Covers approximately 305 ft²
 - \$8.18 per square foot

- Cost of material is \$8-10 per square foot
 - Depends on substrate material (aluminum, carbon steel, or stainless steel)
 - Depends on the spacing of the deposits